Resonances in Dispersive Wave Systems

by

David Embury Amundsen

B.Sc., Mathematics and Physics
University of British Columbia, 1994

Submitted to the Department of Mathematics
in partial fulfillment of the requirements for the degree of

DOCTOR OF PHILOSOPHY

AT THE

MASSACHUSETTS INSTITUTE OF TECHNOLOGY

JUNE 1999

Author . . . . . .
Department of Mathematics
April 26, 1999

Certified by . . . . . .
David J. Benney
Chairman, Department of Mathematics
Thesis Supervisor

Accepted by . . . . . .
Michael Sipser
Chairman, Applied Mathematics Committee

Accepted by . . . . . .
Richard B. Melrose
Chairman, Department Committee on Graduate Students

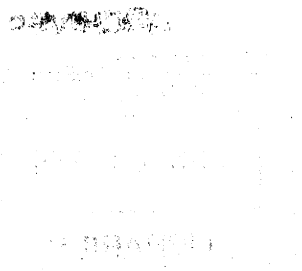

Resonances in Dispersive Wave Systems

by

David Embury Amundsen

Submitted to the Department of Mathematics
on April 26, 1999, in partial fulfillment of the
requirements for the degree of
DOCTOR OF PHILOSOPHY

Abstract

The focus of this thesis is to investigate the differences that arise in weakly nonlinear wave interactions under the assumption of a discrete or continuous spectrum. In particular the latter is investigated in detail for the case of three wave interactions. It is known that an extra condition on the group velocities is required for resonant growth. Such so called double resonances can be shown to occur in a variety of physical regimes.

A direct multiple scale analysis of the spectral representation of a model equation containing arbitrary linear dispersion and weak quadratic nonlinearity was conducted. Consequently a system of "three wave" equations analogous to those for simple resonances was derived for the double resonance case. Key distinctions include an asymmetry between the temporal evolution of the modes and a longer time scale of $O(\epsilon\sqrt{t})$ as opposed to $O(\epsilon t)$ for the case of a discrete simple triad resonance. A number of numerical simulations were then conducted for a variety of dispersions and nonlinearities in order to verify and extend the analytic results.

Furthermore, a generalized version of the discrete three wave equations containing higher order dispersive terms was investigated with the intention of providing a link between the continuous and discrete three wave cases. Both analytic and numerical studies were conducted for a number of parameter regimes. In particular for the case analogous to the double resonance, energy propagation and transfer at the group velocity predicted by the continuous theory was seen. But differences also persisted in the time scales which reinforced the subtle, yet significant, distinction between the continuous and discrete points of view.

Finally, a discussion of double resonances and their effect on statistical treatments of turbulent flows was given. The existence of double resonances appeared to effect the hierarchy of the perturbation expansions, and subsequent closures, in a significant fashion. A modified closure was proposed containing terms arising from both simple and double resonances.

Thesis Supervisor: David J. Benney
Title: Chairman, Department of Mathematics

Acknowledgments

There were many people who played an important role in the development of this dissertation.

First and foremost I wish to thank my advisor, Prof. David J. Benney, whose patient guidance throughout the course of this research was invaluable. I cannot convey how appreciative I am of his unwavering willingness to discuss ideas, answer questions, and share his vast knowledge of the field.

Furthermore I would like to thank Prof. Fabian Waleffe who was instrumental in setting me on to this project and provided valuable input during the early stages. I'd also like to thank Prof. R. Ruben Rosales with whom I had many helpful discussions providing insight at critical moments during this study.

I would also like to thank my fellow graduate students for providing assistance, support, and at times a necessary diversion. Specifically I'd like to thank Mats Nigam who was always willing to share his knowledge of fluids, Lior Pachter for showing me that skill and wisdom are sometimes mitigated by good fortune, Radica Sipcic for helpful discussions and fortuitous introductions, John Weatherwax for getting me on the program, and Boris Schlittgen and Jing Li for many enlightening lunchtime conversations.

And finally I would like to thank my family and the many people throughout my life who have helped to foster my love of mathematics. In particular my parents, Camilla and Harald, for always allowing me the freedom to make my own choices and unconditional support in them. My sister Ellen for her strength and my Grandfather, Maurice Embury, who besides always being willing to assist on any technical problems arising during the course of this work, also taught me through his inspiring example the value of hard work and the joy of life.

Contents

List of Figures

List of Tables

Chapter 1

Introduction

Waves occur in an astonishingly diverse range of physical, chemical and biological systems. In a mathematical sense, such systems may often be described by partial differential equations containing the two essential effects of nonlinearity and dispersion. The former typically causes an initial waveform to steepen and often results in shock type structures or other singularities. Dispersion serves to balance this by causing a waveform to spread out, smoothing any sharp transitions. One typically can scale the equations in order to emphasize either effect, but often the case of most interest arises when the two effects are taken in balance. The Korteweg-de Vries equation, for example, represents the result of such a balance for long waves on shallow water.

Nonlinear evolution equations have been the focus of much study over the past decades. They are typically derived by a multiple scale argument which separates the fast time and space oscillations, isolating the longer scale variations in amplitude and frequency. Although the form of the equations depends on the particular physical system and regime under consideration, many of the resulting evolution equations possess similar characteristics. These include a class of so-called solitary wave solutions which manifest the balance between the spreading caused by dispersion and steepening caused by the nonlinearity. Solitary wave solutions were both derived and shown experimentally by Korteweg and de Vries [17] and subsequently Gardner *et al.* [13] found more complicated multiple soliton solutions for the Korteweg-de Vries

Equation. Their Inverse Scattering Transform technique was then generalized allowing for a much wider class of nonlinear evolution equations in one space dimension to be solved. A comprehensive review of this technique and its implications is given by Ablowtiz and Clarkson [1].

Another intrinsic characteristic brought about by the nonlinearity is that it provides a mechanism for multiple wave interactions. The nonlinear term facilitates energy exchange between modes. This leads to the possibility of a resonance when the nonlinear interaction of two modes force a third mode which is also naturally admitted by the system. Historically, though, a detailed theory for four wave interactions was actually developed prior to that for three wave interactions. This was due mainly to the fact that initial investigations, such as that by Phillips [19], involved gravity waves, a regime where no three wave resonances exist meaning that the effect of the nonlinearity first comes from cubic rather than quadratic interactions. More mathematical treatments then followed by Benney [4] and Zakharov and Karpman [24] resulting in a system of four equations for the slow time evolution of the modal amplitudes. A similar investigation of three wave systems was conducted by Bloembergen [7] in the field of nonlinear optics, resulting in an analogous system of three equations. Spatially independent solutions were then found independently by Jurkus & Robson [15], Armstrong *et al.* [2] and Bretherton [8], while Kaup *et al.* [16] used the Inverse Scattering Transform technique to give a comprehensive treatment of the spatially dependent case.

Typically for these systems it is assumed *a priori* that the spectrum of modes is discrete and limited to the modes involved in the resonance. But if one considers this problem from the perspective of an initial value problem where the initial spectrum is arbitrary and continuously distributed in wavenumber space then the resulting evolution can change dramatically. In fact an added resonance condition, namely that the group velocities of two of the three modes in the triad be equal, is required for there to be any long term growth. This is borne out by the fact that the previously known spatially dependent solutions for the discrete three wave equations [16] are valid only for modes whose group velocities are distinct. These solutions encounter a

singularity when two of the group velocities are equal. Examples of physical regimes where double resonances can occur include, for instance, internal wave systems and Wilton ripples in surface gravity-capillary waves.

The distinct nature of these so called "double resonances" was first recognized by Benney and Saffman [6] in their discussion of random waves in a dispersive media. In this problem a continuous spectral distribution is taken but the arguments depend crucially on the dispersion relation not admitting any double resonances. Fields such as wave turbulence, as described by Zakharov *et al.* [23] build upon this argument and thus stand to benefit from a better understanding of the effect double resonances have on the spectral evolution. The focus of this dissertation will be to investigate this added resonance condition and more generally the subtle distinctions between considering continuous or discrete spectra.

To begin the discussion of the effects of double resonances, a derivation of the evolution equations for a specific physical regime will be given. Using this example as a guide, a more general model equation will be proposed and studied.

1.1 Multiple Scale analysis for Capillary-Gravity waves

Surface waves in the capillary-gravity regime provide a good starting point with which to derive a basic three-wave type system. Furthermore it will be seen that doubly resonant modes also exist in this regime. The following discussion follows that of Case and Chiu [9].

Consider surface waves on deep water where both gravitational and surface tension effects are to be considered. Furthermore assume that the flow is inviscid, irrotational, and incompressible.

By virtue of irrotationality, introduce a velocity potential $\phi(\vec{\mathbf{r}}, z, t)$ where $\nabla\phi = \vec{v}$ the velocity field of the flow, $\vec{\mathbf{r}}$ represents the horizontal coordinates (x, y) and similarly ∇_r represents the gradient over these coordinates only. By virtue of incompress-

ibility it is evident that ϕ must satisfy Laplace's Equation:

$$\nabla^2\phi = 0\ . \tag{1.1}$$

As is often the case in problems such as this, the nonlinearity arises not in the governing equation but in the boundary conditions. First there is a dynamic condition that the pressure on either side of the surface is balanced by the effects of surface tension:

$$\phi_t + \frac{1}{2}(\nabla\phi)^2 = -\frac{\gamma}{\rho}\nabla_r \cdot \left(\frac{\nabla_r(z-h)}{|\nabla_r(z-h)|}\right) - gz\ , \tag{1.2}$$

where γ is the surface tension, ρ the density, g the gravitational acceleration, and $h(x,t)$ the height of the free surface.. Secondly there is a kinematic condition relating the motion of the surface to the motion of the fluid at the surface:

$$h_t + (\nabla_r h)\cdot(\nabla_r\phi(\vec{r},h,t)) = \phi_z(\vec{r},h,t)\ . \tag{1.3}$$

Both these conditions are taken at $z = h$. For convenience, the following dimensionless variables are introduced

$$(x,y,z) \to L(x,y,z)\ ,$$

$$h \to Hh\ ,$$

$$t \to \sqrt{\frac{L}{g}}t\ ,$$

$$\phi \to H\sqrt{Lg}\phi\ ,$$

$$\rho \to \frac{\gamma}{gL^2}\rho\ ,$$

where H and L represent the vertical and horizontal length scales respectively. Then (1.1) remains unchanged while (1.2) and (1.3) become:

$$\left.\begin{aligned} \phi_t + \frac{1}{\epsilon}z + \frac{1}{\rho}\left(\frac{\nabla_r^2 h}{\sqrt{1+\epsilon(\nabla_r h)^2}}\right) &= -\epsilon\tfrac{1}{2}(\nabla\phi)^2 \ , \\ h_t - \phi_z(\vec{\mathbf{r}},z,t) &= -\epsilon(\nabla_r h)\cdot(\nabla_r\phi(\vec{\mathbf{r}},z,t)) \end{aligned}\right\} \text{ at } z = \epsilon h \ ,$$

where $\epsilon = \frac{H}{L}$ is a measure of the relative amplitude of the waves.

Now expanding around $z = 0$ and keeping terms to $O(\epsilon)$,

$$\left.\begin{aligned} \phi_t + h - \tfrac{\nabla_r^2 h}{\rho} &= -\epsilon(\phi_{zt}h + \tfrac{1}{2}(\nabla\phi)^2) + O(\epsilon^2) \\ h_t - \phi_z(\vec{\mathbf{r}},z,t) &= \epsilon(\phi_{zz}h - (\nabla_r h)\cdot(\nabla_r\phi(\vec{\mathbf{r}},z,t))) + O(\epsilon^2) \end{aligned}\right\} \text{ at } z = 0 \ . \qquad (1.4)$$

At first order ($\epsilon = 0$) the linear equations can be solved to give the well known solutions for wavenumber $\vec{\mathbf{k}}$, magnitude k,

$$h_0 = A\left[e^{i(\vec{\mathbf{k}}\cdot\vec{\mathbf{r}}-\omega t)} + c.c.\right] \qquad (1.5)$$

$$\phi_0 = A(\frac{-i\omega}{k}e^{kz})\left[e^{i(\vec{\mathbf{k}}\cdot\vec{\mathbf{r}}-\omega t)} + c.c.\right] \ , \qquad (1.6)$$

c.c. denotes the complex conjugate of the associated expression, and ω satisfies the dispersion relation

$$\omega^2 = k + \frac{k^3}{\rho} \ , \qquad (1.7)$$

which when put back into dimensionalized variables takes the more familiar form

$$\omega^2 = gk + \frac{\gamma k^3}{\rho} \ . \qquad (1.8)$$

Now suppose one builds upon these linear solutions and consider a solution composed of a superposition of these modes:

Let

$$\phi = \sum_{i=1}^{3}(\frac{i\omega_i}{k_i}e^{k_i z})\left[P_i(\mu\vec{\mathbf{r}},\mu z,\mu t)e^{i(\vec{\mathbf{k}}_i\cdot\vec{\mathbf{r}}+\omega t)} - Q_i(\mu\vec{\mathbf{r}},\mu z,\mu t)e^{i(\vec{\mathbf{k}}_i\cdot\vec{\mathbf{r}}-\omega t)}\right] + c.c.\ , \qquad (1.9)$$

$$h = \sum_{i=1}^{3}\left[P_i(\mu\vec{\mathbf{r}},0,\mu t)e^{i(\vec{\mathbf{k}}_i\cdot\vec{\mathbf{r}}+\omega t)} + Q_i(\mu\vec{\mathbf{r}},0,\mu t)e^{i(\vec{\mathbf{k}}_i\cdot\vec{r}-\omega t)}\right] + c.c.\ , \qquad (1.10)$$

where P_i and Q_i are the amplitudes of the respective modes, allowed to vary slowly subject to a small parameter μ. In some sense one can think of μ as a measure of the spread of the frequencies around the modes k_i. In other words, the width of the wave-packets as a long scale in space corresponds to a small scale in frequency space.

Now substituting (1.9) and (1.10) into (1.4) and (1.1) the resulting equations are:

$$\begin{aligned}
&\sum_{i=1}^{3}\left[\mu\frac{\partial P_i}{\partial t} - \mu\frac{i\omega_i}{k_i}\frac{\partial P_i}{\partial z}\right]e^{i(\vec{\mathbf{k}}_i\cdot\vec{r}+\omega t)} + \left[\mu\frac{\partial Q_i}{\partial t} + \mu\frac{i\omega_i}{k_i}\frac{\partial Q_i}{\partial z}\right]e^{i(\vec{\mathbf{k}}_i\cdot\vec{r}-\omega t)} + c.c.\ , \\
&= \epsilon\left(\alpha\left[P_2P_3e^{i(\vec{\mathbf{k}}_2+\vec{\mathbf{k}}_3)\cdot\vec{\mathbf{r}}+(\omega_2+\omega_3)t} + Q_2Q_3e^{i(\vec{\mathbf{k}}_2+\vec{\mathbf{k}}_3)\cdot\vec{\mathbf{r}}-(\omega_2+\omega_3)t}\right]\ldots\right) \qquad (1.11) \\
&\sum_{i=1}^{3}\left[\mu\frac{i\omega_i}{k_i}\frac{\partial P_i}{\partial t} - \frac{2\mu}{\rho}\vec{\mathbf{k}_i}\cdot\nabla_{\vec{\mathbf{r}}}P_i - \frac{\mu^2}{\rho}\nabla_r^2P_i\right]e^{i(\vec{\mathbf{k}}_i\cdot\vec{\mathbf{r}}+\omega_i t)} + \\
&\left[-\mu\frac{i\omega_i}{k_i}\frac{\partial P_i}{\partial t} - \frac{2\mu}{\rho}\vec{\mathbf{k}_i}\cdot\nabla_rQ_i - \frac{\mu^2}{\rho}\nabla_r^2Q_i\right]e^{i(\vec{\mathbf{k}}_i\cdot\vec{\mathbf{r}}-\omega_i t)} + c.c.\ , \\
&= \epsilon\left(\beta\left[P_2P_3e^{i(\vec{\mathbf{k}}_2+\vec{\mathbf{k}}_3)\cdot\vec{\mathbf{r}}+(\omega_2+\omega_3)t} + Q_2Q_3e^{i(\vec{\mathbf{k}}_2+\vec{\mathbf{k}}_3)\cdot\vec{\mathbf{r}}-(\omega_2+\omega_3)t}\right]\ldots\right)\ . \qquad (1.12)
\end{aligned}$$

Note that the terms of $O(\mu^0)$ have cancelled by virtue of the fact our solutions are based on the solutions of the linearized problem. Also, only the first of the nonlinear terms on the right is shown, with α and β being interaction coefficients in terms of k_i and $\omega_i = \omega(k_i)$. The exact form of these coefficients is not necessary for the subsequent discussion, it suffices to say that they represent the magnitude and direction of energy flow between the two interacting modes (in this case modes 2 and 3) and the resultant mode. But the reader is directed to [9], and more generally [10] for the complete description of these coefficients. All other nonlinear combinations are similarly present but for the sake of clarity have been omitted. For these terms

it is apparent that they resonate with the linear terms if the following conditions are met:

Condition 1) $k_1 = k_2 + k_3$,

Condition 2) $\omega_1 = \omega_2 + \omega_3$,

Which are the well known three wave resonance conditions, as first noted by Phillips [19], who studied this problem in the context of gravity waves in the absence of surface tension. Now each term in (1.11) and (1.12) will have oscillatory terms $e^{\pm i(\vec{\mathbf{k}}_i \cdot \vec{\mathbf{r}} \pm \omega_i t)}$, each of which can be isolated by the standard multiplication and integration operations since the equations are linear meaning each forcing term may be treated separately. Then if, for instance, one considers the terms proportional to $e^{i(\vec{\mathbf{k}}_1 \cdot \vec{\mathbf{r}} \pm \omega_1 t)}$ and eliminate P by taking α (1.12) $-\beta$ (1.11) the resultant equation takes the form:

$$\mu \frac{\partial Q_1}{\partial t} + \mu \vec{\mathbf{C}}_1 \cdot \nabla_r Q_1 + O(\mu^2) = \epsilon i \gamma_1 Q_2 Q_3 + O(\epsilon^2, \epsilon\mu) \ ,$$

and similarly the amplitudes of the other modes evolves according to:

$$\mu \frac{\partial Q_2}{\partial t} + \mu \vec{\mathbf{C}}_2 \cdot \nabla_r Q_2 + O(\mu^2) = \epsilon i \gamma_2 Q_1 Q_3^* + O(\epsilon^2, \epsilon\mu) \ ,$$

$$\mu \frac{\partial Q_3}{\partial t} + \mu \vec{\mathbf{C}}_3 \cdot \nabla_r Q_3 + O(\mu^2) = \epsilon i \gamma_3 Q_1 Q_2^* + O(\epsilon^2, \epsilon\mu) \ ,$$

where $\vec{\mathbf{C}}_i$ is the group velocity of the ith mode. This mathematically captures the coupling which occurs between the three modes, facilitating energy exchange. γ_i are the interaction coefficients (exact expressions may be found in [9]) which characterize this exchange. If a balance $\mu = O(\epsilon)$ is taken the solutions of systems of equations such as this are known and will be discussed further in the following section. As it will be shown, systems such as this can be derived from a much simpler and broader class of PDEs which account for the key effects of dispersion and weak nonlinearity.

1.2 The Model

Three wave type evolution equations arise in many more physical situations, with the essential characteristic that each mode is coupled to the others via quadratic nonlinearity. A simple 1-D model which unifies these cases and captures this effect is embodied by

$$u_t + \mathcal{L}(u) = \epsilon \mathcal{N}(u) \ , \tag{1.13}$$

where $\mathcal{L}$ is a linear differential operator, $\mathcal{N}$ is a nonlinear and for our purposes assumed quadratic, differential operator, and ϵ is a small parameter governing the weak nonlinearity. In Fourier space this corresponds to

$$A_t + i\omega(k)A = \epsilon \int H(l, k-l)A(l)A(k-l)dl \ , \tag{1.14}$$

where A is the Fourier Transform of u, ω corresponds to the linear dispersion relation given by $\mathcal{L}$, and H is an interaction coefficient. The modes naturally admitted by the linearized system are given by the linear dispersion relation $\omega(k)$, and one assumes that it is purely dispersive, and odd in k so that the complex conjugate of the linear solution is also a solution. For each wavenumber k, this gives the corresponding linearized frequency ω. Then by expressing the amplitude in a perturbation expansion in ϵ one then obtains a hierarchy of integro-differential equations. In this case it is known, and will be shown in detail in Chapter 2, that conditions 1 and 2 are not sufficient to generate secularity. i.e. for modes $\bar{k}, \bar{l}, \bar{m}$

Condition 1) $\bar{l} + \bar{m} = \bar{k}$,

Condition 2) $\omega(\bar{l}) + \omega(\bar{m}) = \omega(\bar{k})$,

But if one makes a further stipulation that the group velocities of the two interacting waves, be equal:

Condition 3) $\omega'(\bar{l}) = \omega'(\bar{m})$

stationary phase analysis predicts a dramatic increase in amplitude for modes whose wavenumbers are near the so called "doubly resonant" mode $\bar{k}$. This suggests that the

evolution of any system containing such resonances will be dominated by these doubly resonant modes. Double resonances exist in a variety of systems, including internal gravity waves and surface waves in the gravity-capillary regime, yet surprisingly there has been very little prior work done investigating this. It can be easily seen, for example, that the dispersion relation for capillary-gravity waves (1.8) has a double resonance at $\bar{k} = \sqrt{\frac{2g\rho}{\alpha}}$, $\bar{l} = \bar{m} = \frac{\bar{k}}{2}$, commonly referred to as Wilton's ripples[21]. Furthermore Figure (1-1) shows the double resonances for internal waves where a

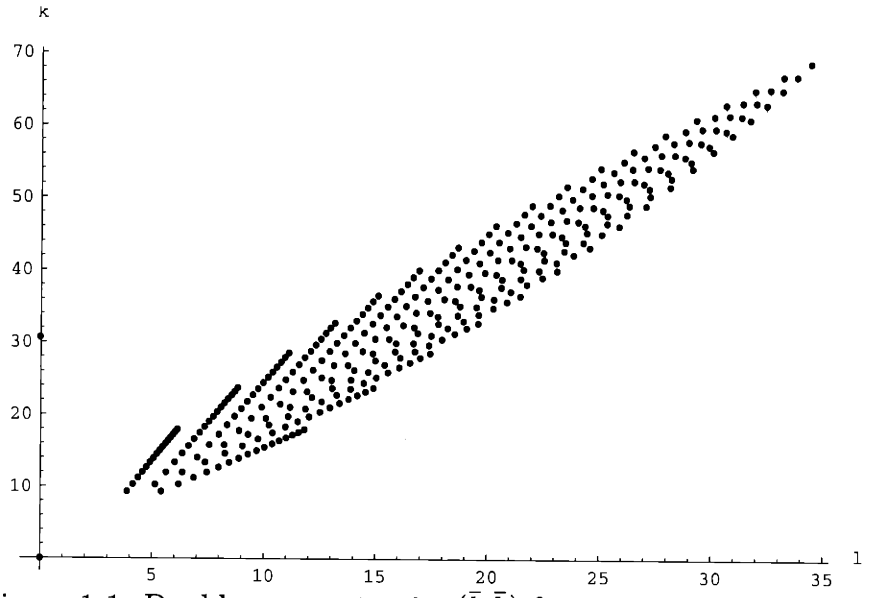

Figure 1-1: Double resonant pairs $(\bar{l}, \bar{k})$ for internal waves

simple form for the dispersion relation [12] is

$$\omega = \frac{Nk}{\sqrt{k^2 + \frac{n^2\pi^2}{h_0^2} + \frac{N^2}{4g^2}}},$$

where N is the Brunt-Väisälä frequency characterizing the stratification, h_0 the height of the layer, and n an integral parameter corresponding to the particular vertical mode. In general for arbitrary dispersion the usual construction for simple triad resonances (conditions 1 and 2) involves taking the curve $\omega(k)$ and overlaying a second

plot of the curve with the origin shifted to an arbitrary point on the first curve. A slight modification of this is shown in Figure 1-2 gives a pictorial interpretation of

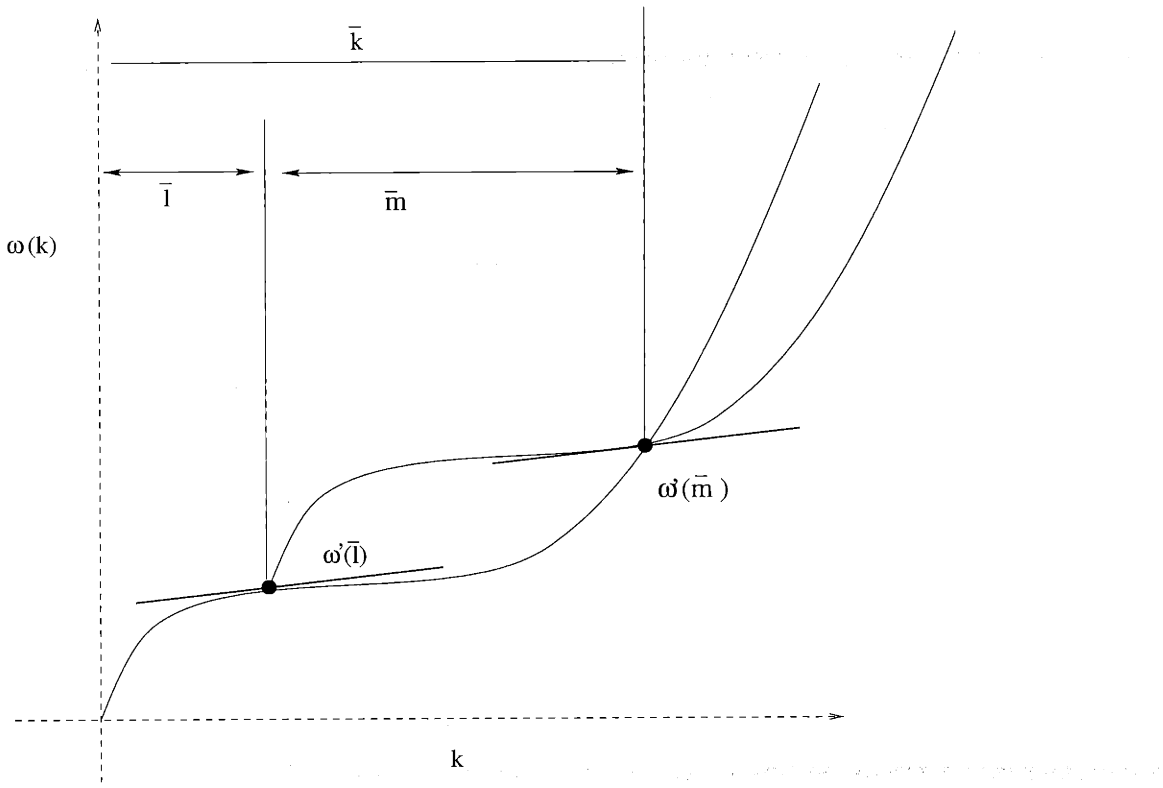

Figure 1-2: Construction of doubly resonant triad $\bar{k}, \bar{l}, \bar{m}$ for an arbitrary dispersion relation.Constants N, h_0 are taken to be 1, and n varies from 1 to 20

the added condition. This also illustrates a key distinction between simple resonances and double resonances. The added condition implies that while a typical dispersion relation may contain a continuum of possible simple resonances, there will be merely a single or at most discrete set of double resonances in the one dimensional case. Mathematically this is borne out by the fact one goes from 2 (nonlinear) equations in 3 unknowns to 3 equations in 3 unknowns. Therefore in the simple resonance case there is likely a continuum of triples of wavenumbers which satisfy the two conditions whereas in the double resonance case there are only discrete triples which satisfy the three conditions. In other words if one of the wavenumbers in a doubly resonant triad is changed slightly, one or more of the conditions will no longer be satisfiable for any choice of second and third modes. Thus there is a somewhat paradoxical twist

that when the spectrum is considered continuous, a discrete set of modes can exhibit resonant behavior. It will be seen that this paradox is resolved by realizing that it is in fact not only the modes precisely at resonance but an asymptotically decreasing band of wavenumbers around each mode which exhibit growth. Or alternatively, modes which closely, but not exactly, satisfy the resonance conditions will exhibit growth for a time related to how close to resonance they are. Only in the infinite time limit do the resonant modes really become a discrete set. This study of the effect of the continuous spectrum and the added resonance condition will be the focus of Chapter 2.

In order to draw a more complete contrast and comparison with the continuous spectrum approach, this problem was also considered under the assumption of a discrete spectrum. The relevant system of equations turns out, not surprisingly, to be similar to the classical three wave equations. It can be readily seen that if one restricts the spectrum to three discrete modes such that

$$u(x,t) = A(\mu x, \mu t)e^{i(kx-\omega(k)t)} + B(\mu x, \mu t)e^{i(lx-\omega(l)t)} + C(\mu x, \mu t)e^{i(mx-\omega(m)t)} + c.c.\ ,$$

where $\bar{k}, \bar{l}, \bar{m}$ satisfy Conditions 1 and 2, then (1.13) reduces to:

$$\left.\begin{aligned} \mu A_T + \mu c_g(\bar{k})A_X - i\tfrac{\mu^2}{2}\tfrac{d^2\omega(\bar{k})}{dk^2}A_{XX} + O(\mu^3) &= \epsilon\gamma_{BC}BC + O(\epsilon^2, \epsilon\mu)\ , \\ \mu B_T + \mu c_g(\bar{l})B_X - i\tfrac{\mu^2}{2}\tfrac{d^2\omega(\bar{l})}{dk^2}B_{XX} + O(\mu^3) &= \epsilon\gamma_{AC}AC^* + O(\epsilon^2, \epsilon\mu)\ , \\ \mu C_T + \mu c_g(\bar{m})C_X - i\tfrac{\mu^2}{2}\tfrac{d^2\omega(\bar{m})}{dk^2}C_{XX} + O(\mu^3) &= \epsilon\gamma_{BC}AB^* + O(\epsilon^2, \epsilon\mu)\ , \end{aligned}\right\} \quad (1.15)$$

This approach will be the focus of Chapter 3. As noted earlier, typically a balance is chosen such that $\mu = O(\epsilon) \ll 1$, and the second order derivatives ignored. This then reduces to the usual three wave system discussed in [16]. But one limitation of these solutions lies in the fact that it is assumed that the group velocities are all distinct. In fact, as noted earlier, the solutions obtained via Inverse Scattering Techniques are singular for the case when two or more of the group velocities are equal. This suggests that there may be a discrete analogy to the continuous case discussed in

Chapter 2. But if a Galilean transformation is made such that one moves in a frame moving at the common group velocity then two of the three equations lose their spatial dependence. Thus in order to study this a new balance is chosen such that $\epsilon = O(\mu^2)$ so that the higher order spatial derivatives play a role in the evolution. There were some qualitative similarities between the continuous and discrete approaches, but in the final analysis it seems apparent that the effects seen in the earlier analysis rely very much on having a continuous spectrum in order to obtain the contribution from the stationary phase integrals. Physically this can be interpreted as suggesting that sideband modes near k, l, m play an important role in the evolution.

Chapter 2

The Three Wave Problem: Continuous Spectrum

Typically the three wave problem is taken from a point of view where the solution is considered to be composed of a discrete set of three modes and then evolution equations are derived in the spirit of equation (1.15). But it is also interesting to consider solutions composed of a fully continuous spectrum of modes. This would be the case, for example, if one considers an initial value type problem where the solution evolves from an initially prescribed spectral distribution on an infinite, or very large, domain where boundary conditions do not put restrictions on the spectrum. As will be seen in the discussion that follows, dramatic differences arise due mainly to the contribution, or interference, by modes sufficiently close to the resonant modes. Or from a mathematical point of view, arising from the differences between the asymptotic behavior of a Fourier integral involving continuous functions versus Dirac delta functions.

2.1 Perturbation Expansion

As introduced earlier, consider a model PDE of the form:

$$u_t + \mathcal{L}(u) = \epsilon \mathcal{N}(u), \tag{2.1}$$

where $\mathcal{L}$ is a linear differential operator, $\mathcal{N}$ is a nonlinear (quadratic) differential operator. In Fourier space this corresponds to:

$$A_t + i\omega(k)A = \epsilon \int H(l, k-l)A(l)A(k-l)dl, \tag{2.2}$$

where ω corresponds to the linear dispersion relation given by $\mathcal{L}$, H corresponds to the derivatives in $\mathcal{N}$. It is assumed that ω is odd in k, and that the system is purely dispersive. Equivalently,

$$a_t = \epsilon \int H(l, k-l)a(l)a(k-l)e^{-i\Delta\omega(k,l)t}dl \ , \tag{2.3}$$

where $A(k,t) = a(k,t)e^{-i\omega(k)t}$ and $\Delta w(k,l) = \omega(l) + \omega(k-l) - \omega(k)$. So now if one considers a perturbation series

$$a = a_0 + \epsilon a_1 + \epsilon^2 a_2 + ...$$

then to zeroth order

$$a_{0_t}(k) = 0 \ . \tag{2.4}$$

So a_0 is simply the initial wave number distribution. To first order

$$a_{1_t}(k) = \int H(l, k-l)a_0(l)a_0(k-l)e^{-i\Delta\omega(k,l)t}dl \ , \tag{2.5}$$

which can be integrated right away to give

$$a_1(k) = \int H(l, k-l)a_0(l)a_0(k-l)\frac{e^{-i\Delta\omega(k,l)t} - 1}{-i\Delta\omega(k,l)}dl \ . \tag{2.6}$$

But a long time approximation to this can be obtained by using stationary phase on (2.5)

$$a_{1_t}(k) = \frac{\sqrt{2\pi}e^{i\frac{\pi}{4}}}{\sqrt{-(\Delta\omega_{ll}(k,\tilde{l}))}}H(\tilde{l}, k-\tilde{l})a_0(\tilde{l})\frac{e^{-i\Delta\omega(k,\tilde{l})t}}{\sqrt{t}} \ , \tag{2.7}$$

where $\tilde{l}(k)$ satisfies

$$\frac{d}{dl}\Delta\omega(k,\tilde{l}) = 0 \qquad \Rightarrow \qquad \omega'(\tilde{l}) = \omega'(k-\tilde{l}) \ , \tag{2.8}$$

and then integrating up in time gives

$$a_1(k) \approx \sum_{\tilde{l}} \frac{2\sqrt{2\pi}e^{i\frac{\pi}{4}}}{\sqrt{-(\Delta\omega_{ll}(k,\tilde{l}))}}\sqrt{t}\int_0^1 e^{-i\Delta\omega(k,\tilde{l})tv^2}dv \ , \tag{2.9}$$

where the sum is understood to be over all possible values of $\tilde{l}$ which satisfy (2.8). The merit of (2.9) as opposed to (2.6) is that the $\sqrt{t}$ growth at resonance has now been isolated, ($\Delta\omega(k,\tilde{l}) = 0$ i.e. $l = \bar{l}$, $k = \bar{k}$) along with the basic peak structure nearby which is contained in the Fresnel type integral. This form will make computation of subsequent terms in the perturbation expansion simpler as the phase will be contained in a single term.

To evaluate and verify the validity of (2.9), Figures 2-1 and 2-2 show a comparison of (2.9) to (2.6) for this case. These rather artificial dispersion relations were chosen for clarity and ease of computation, and will be discussed and analyzed further in Section 2.3, along with more physical dispersions such as that for gravity-capillary waves discussed in Section 1.1. But for the sake of completeness, Figure 2-3 shows a comparison for the gravity-capillary dispersion as well, where without loss of generality the coefficients are taken to be unity. It should be noted that strictly speaking, in order to compute (2.9), the nonlinear equation (2.8) must be solved for $\tilde{l}$. But for wavenumbers nearby $\bar{l}$ as in these plots, the following linear approximation easily suffices,

$$\tilde{l}(\bar{k}+s) = \bar{l} + \frac{\omega''(\bar{k}-\bar{l})}{\omega''(\bar{k}-\bar{l})+\omega''(\bar{l})}s \ ,$$

It is clear that the peak structure is captured by the approximation as well as the temporal growth. The error in the approximation remains $O(1)$ in magnitude and thus for longer times becomes less and less significant. It arises from the contribution of the simple resonances which are known to contribute at this level as well as the fact that the asymptotic form is valid only for long time. As will be seen for the

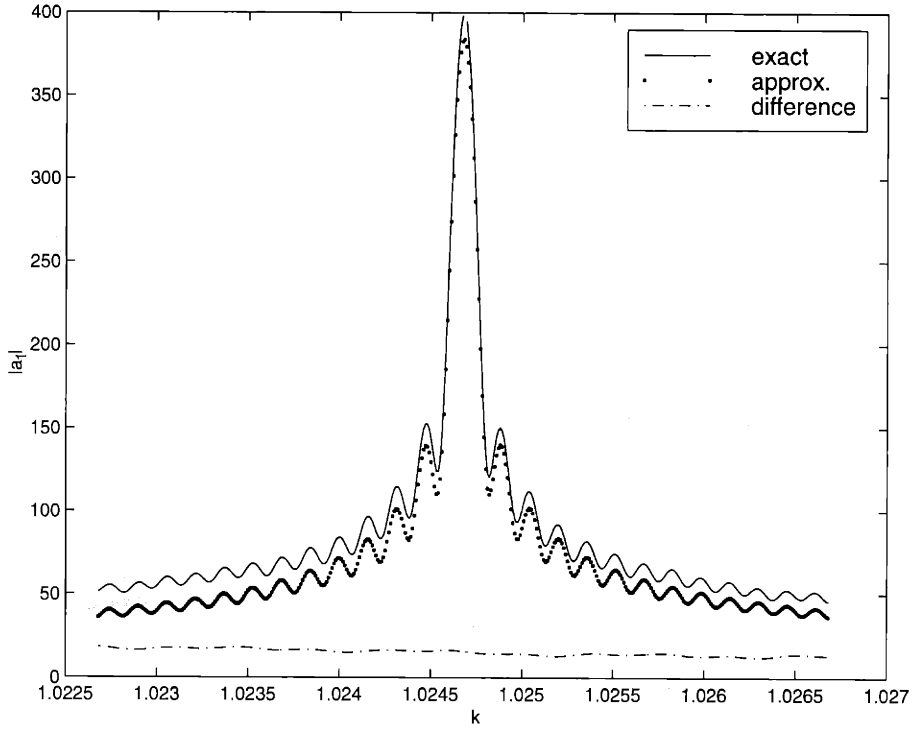

Figure 2-1: Comparison for a_1 with $\omega(k) = \tanh(.25k + 3.125k^3)$ at $t = 20000$

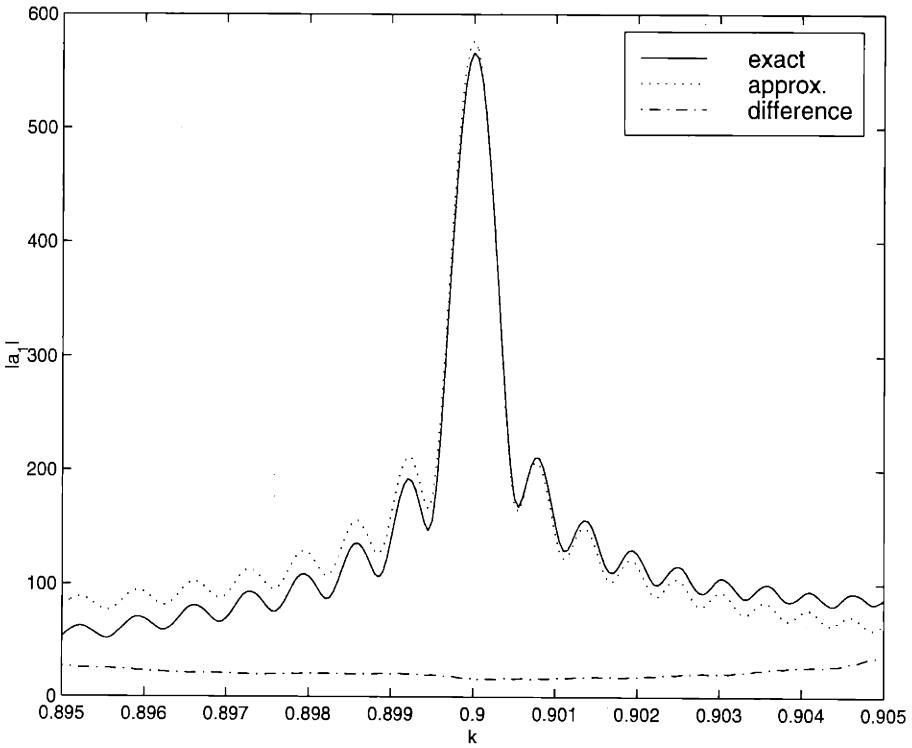

Figure 2-2: Comparison for a_1 with $\omega(k) = -\tanh(.116335k - 6.31965k^3)$ at $t = 10000$

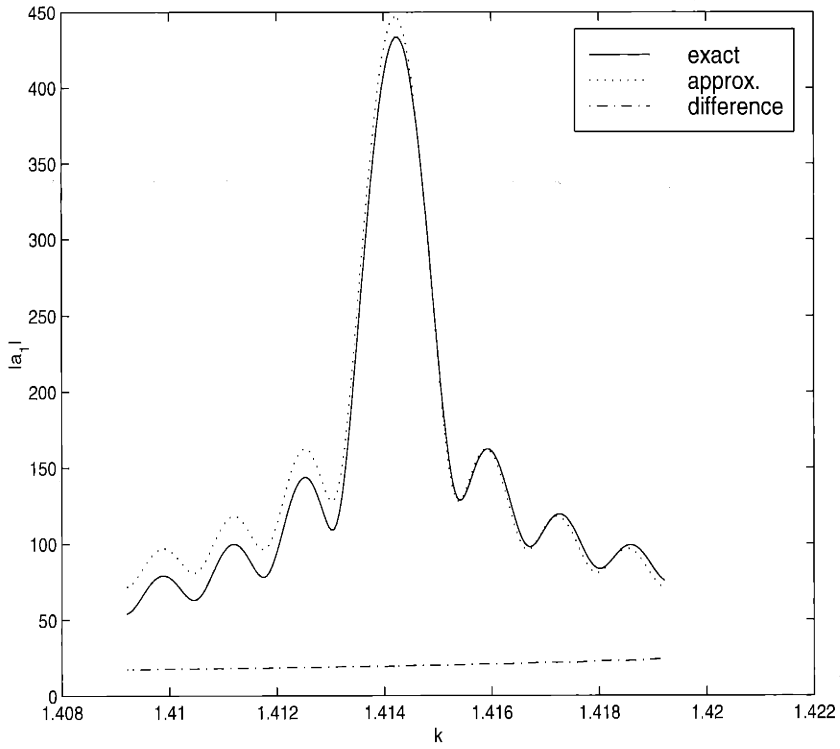

Figure 2-3: Comparison for a_1 with $\omega(k) = \sqrt{k + k^3}$ at $t = 10000$

purposes of the arguments to follow, it is only the terms which exhibit growth which are significant.

Essentially a_1 captures the main mechanism of the double resonance. It is $O(1)$ for all k except near the peak around $\bar{k}$ where it exhibits $\sqrt{t}$ growth. Moreover numerical experiments have clearly shown this structure, as will be shown later in this chapter. In order to investigate possible saturation and feedback from other modes one needs to consider higher order terms.

For a_2 it is seen that

$$a_{2_t}(k) = \int 2H(l, k-l)a_1(l,t)a_0(k-l)e^{-i\Delta\omega(k,l)t}dl \ , \tag{2.10}$$

$$= \int\int 2H(l,k-l)H(m,l-m)a_0(m)a_0(l-m)a_0(k-l)\frac{e^{-i\Delta\omega(l,m)t}-1}{-i\Delta\omega(l,m)}e^{-i\Delta\omega(k,l)t}dmdl \ ,$$

$$= \int\int 2H(l,k-l)H(m,l-m)a_0(m)a_0(l-m)a_0(k-l)\frac{e^{-i\Delta\omega(k,l,m)t}-e^{-i\Delta\omega(k,l)}}{-i\Delta\omega(l,m)}dmdl \ ,$$

where $\Delta\omega(k,l,m) = \omega(m) + \omega(l-m) + \omega(k-l) - \omega(k)$. And this also can now be integrated right away

$$a_2(k) = \int\int 2H(l,k-l)H(m,l-m)a_0(m)a_0(l-m)a_0(k-l)\frac{D(\Delta\omega(k,l,m),t) - D(\Delta\omega(k,l),t)}{-i\Delta\omega(l,m)}, \tag{2.11}$$

where $D(x,t) = \frac{e^{-ixt}-1}{-ix}$.

To gain more insight, one can use (2.9) and stationary phase to construct an approximate long time form for a_2. The use of (2.9) in (2.10) introduces a two dimensional stationary phase integral which contains two possible critical points for the phase. One represents a repetition of the interaction captured by a_1, which is ignored as is the usual procedure in order to avoid secularity. But the second is a saddle point which represents a non-trivial feedback involving the two "feeder" modes $\bar{l}$ and $\bar{k} - \bar{l}$. Standard two dimensional stationary phase analysis [22] then suggests

$$a_2(k) \approx \sum_{\bar{l}} \frac{4\pi\sqrt{2\pi}e^{i\frac{\pi}{4}}H(k-\bar{k},\bar{k})H(\bar{k}-\bar{l},\bar{l})}{\sqrt{-(\Delta\omega_{ll}(\bar{k},\bar{l}))\tilde{v}}\,|\alpha|}a_0(\bar{l})a_0(\bar{k}-\bar{l})a_0(k-\bar{k})\sqrt{t}\int_0^1 e^{-i\Delta\omega(k,\bar{k})tv^2}dv\,, \tag{2.12}$$

where the sum represents a sum over distinct feeder modes $\bar{l}$, and where

$$\alpha = \omega'(\bar{l}) - \omega'(\bar{k})\,, \tag{2.13}$$

$$\tilde{v} = \sqrt{\frac{\omega'(k-\bar{k}) - \omega'(\bar{k})}{\omega'(\bar{l}-\bar{k}) - \omega'(\bar{k})}}\,.$$

Note the similar structure to (2.9), the main difference being the $\Delta\omega(k,\bar{k})$ in the integral which means there are peaks at $\bar{l}$ and $\bar{k} - \bar{l}$. Basically this represents an interaction whereby the peak in a_1 interacts with the conjugate of one of the feeder modes to produce the other. This is presumably the basic feedback mechanism which could serve to produce a saturation, ceasing the otherwise unbounded growth at $\bar{k}$ suggested by (2.9). Figure 2-4 shows a comparison of the analytic expression for a_2, (2.11), and the stationary phase approximation (2.12). In this case the exact

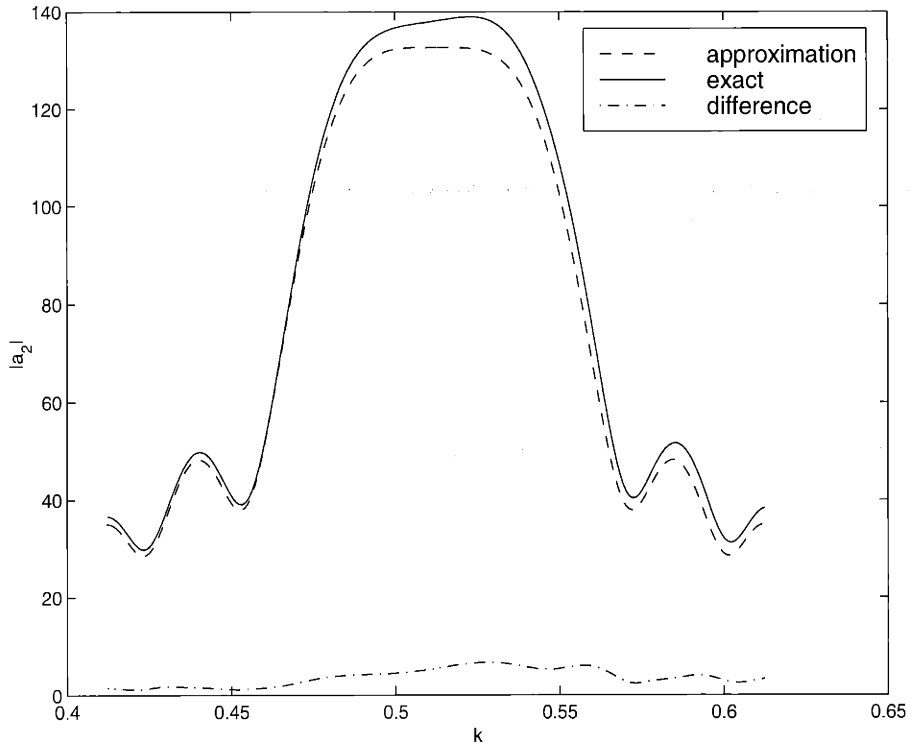

Figure 2-4: Comparison for a_2 with $\omega(k) = \tanh(.25k + 3.125k^3)$ at $t = 1000$, and $a_0 = (e^{-10(k-.6)^2} + e^{-10(k+.6)^2})e^{i50k}$

integration is now made more difficult since it is a two dimensional stationary phase integral. For this reason it was necessary to restrict the initial condition to a wave packet around the feeder mode. Again the agreement is good, but not exact due to the higher order asymptotic terms omitted in the approximation, as well as the fact that again the asymptotic form is used for all times as opposed to just long times.

Subsequent order terms can be similarly computed, and at each order will alternate between corrections to the growth at $\bar{k}$ in the odd terms and feedback in the even terms. For example

$$a_3 \approx \frac{8\pi^2 iH(\bar{l}-\bar{k},\bar{k})H(\bar{k}-\bar{l},\bar{l})H(k-\bar{l},\bar{l})}{\sqrt{-\Delta\omega_{ll}(\bar{k},\bar{l})}\sqrt{-\Delta\omega_{ll}(k,\bar{l})\alpha}} a_0(\bar{l})a_0(\bar{k}-\bar{l})a_0(\bar{l}-\bar{k})a_0(k-\bar{l})\frac{e^{-i\Delta\omega(k,\bar{l})t}-1}{-i\Delta\omega(k,\bar{l})}$$
$$+\frac{8\pi^2 iH(-\bar{l},\bar{k})H(\bar{k}-\bar{l},\bar{l})H(k-\bar{k}+\bar{l},\bar{k}-\bar{l})}{\sqrt{(-\Delta\omega_{ll}(\bar{k},\bar{l}))}\sqrt{-\Delta\omega_{ll}(k,\bar{k}-\bar{l})\alpha}} a_0(\bar{l})a_0(\bar{k}-\bar{l})a_0(-\bar{l})a_0(k-\bar{k}+\bar{l})\frac{e^{-i\Delta\omega(k,\bar{k}-\bar{l})t}-1}{-i\Delta\omega(k,\bar{k}-\bar{l})} \quad (2.14)$$

Note the temporal terms represent an $O(t)$ growth in the limit $\Delta\omega \to 0$ or in other words as $k \to \bar{k}$. Thus this term represents a correction to the peak in a_1 of $O(\epsilon^3 t)$.

And in general, subsequent terms will generate an ordering of the form

$$\begin{aligned} A &\approx 1+\epsilon\sqrt{t}+\epsilon^3 t+\epsilon^5 t^{\frac{3}{2}}+\dots, \\ B &\approx 1+\epsilon^2\sqrt{t}+\epsilon^4 t+\epsilon^6 t^{\frac{3}{2}}+\dots, \\ C &\approx 1+\epsilon^2\sqrt{t}+\epsilon^4 t+\epsilon^6 t^{\frac{3}{2}}+\dots, \end{aligned} \tag{2.15}$$

where A, B, and C represent the amplitudes at $\bar{k}$,$\bar{l}$, and $\bar{k}-\bar{l}$ respectively. The mismatch in orders between the doubly resonant and feeder modes highlights the difference between this and the simple resonant case. Moreover this underlies the difficulty in obtaining a single system of equations in the spirit of the three-wave equations for the simple triad case.

2.2 Derivation of a Three Wave type System

There does not seem to be any clear time-scale suggested by (2.15). The initial growth of the doubly resonant peak is on a scale $O(\epsilon\sqrt{t})$ but then the subsequent terms suggest that the feedback occurs on the scale $O(\epsilon^2\sqrt{t})$, and in general there is a power series structure on this scale.The most successful analytic approach involves a direct slow-time analysis with a truncation of the expansion, keeping sufficiently many terms to get the feedback. The success of this method, of course, depends crucially on the nature of the truncated terms. Often in nonlinear oscillator problems such truncations do provide successful closures, but it is often not obvious *a priori* that such a truncation is justified.

2.2.1 Direct Multiple Scale Analysis

Using the previous analysis of the terms in the perturbation expansion of a, it is clear that the doubly resonant peak, and the two feeder modes, behave like:

$$a(\bar{k}+s,t) = a_0(\bar{k}+s)+\epsilon a_1(\bar{k}+s,t)+\epsilon^3 a_3(\bar{k}+s,t)+\dots,$$

$$
\begin{aligned}
a(\bar{l}+s,t) &= a_0(\bar{l}+s)+\epsilon^2 a_2(\bar{l}+s,t)+\dots\,, \\
a(\bar{k}-\bar{l}+s,t) &= a_0(\bar{k}-\bar{l}+s)+\epsilon^2 a_2(\bar{k}-\bar{l}+s,t)+\dots
\end{aligned}
$$

where s represents a new wavenumber variable corresponding to detuning from exact resonance. The perturbation expansion suggests that the effects of the double resonance are localized to regions around the three modes $\bar{k}$,$\bar{l}$, and $\bar{k}-\bar{l}$, so s is assumed small. How small is yet to be determined but one would expect a range of s on the order of the width of the peaks. For convenience, as in (2.15), let:

$$
\begin{aligned}
a(\bar{k}+s,t) &= A(s,t)\,, \\
a(\bar{l}+s,t) &= B(s,t)\,, \\
a(\bar{k}-\bar{l}+s,t) &= C(s,t)\,.
\end{aligned}
\tag{2.16}
$$

Without loss of generality the slow time-scale is chosen to be that of the initial growth of a_1. Let $T=\epsilon\sqrt{t}$, and let A,B,C be functions of s,t and T. This then means that (2.16) effectively becomes

$$
\begin{aligned}
A(s,t,T)+\epsilon\sqrt{t}A_T &= a_0(\bar{k}+s)+\epsilon a_1(\bar{k}+s,t)+\epsilon^3 a_3(\bar{k}+s,t)+\dots\,, \\
B(s,t,T)+\epsilon\sqrt{t}B_T &= a_0(\bar{l}+s)+\epsilon^2 a_2(\bar{l}+s,t)+\dots\,, \\
C(s,t,T)+\epsilon\sqrt{t}C_T &= a_0(\bar{k}-\bar{l}+s)+\epsilon^2 a_2(\bar{k}-\bar{l}+s,t)+\dots\,,
\end{aligned}
$$

where the additional slow variation terms are the result of a total derivative in time due to the PDE, and then an integration in the fast time only. Secular terms on the right are now balanced with the slow time variation. Where to truncate the right hand sides is in general not obvious, but clearly in order to capture both the growth and feedback, terms up to $O(\epsilon^2)$ must be kept and in fact a_3 should also be included in order to consistently have both time scales present in all equations. The validity of this truncation will be discussed later. Using (2.9), (2.12), and (2.14) the following system is obtained:

$$
\begin{aligned}
A_T(s) &= g(s)B(\tilde{r})C(s-\tilde{r})\int_0^1 e^{-i\Delta\omega(\bar{k}+s,\bar{l}+\tilde{r})\frac{T^2}{\epsilon^2}v^2}dv \\
&\quad +\epsilon T(F(s,\bar{l},T)B(0)\,|C(0)|^2\,C(s)+F(s,\bar{k}-\bar{l},T)C(0)\,|B(0)|^2\,B(s))\,, \\
B_T(s) &= \epsilon h(\bar{l}+s)B(0)C(0)C^*(s)\int_0^1 e^{-i\Delta\omega(\bar{l}+s,\bar{k})\frac{T^2}{\epsilon^2}v^2}dv\,, \qquad (2.17)\\
C_T(s) &= \epsilon h(\bar{k}-\bar{l}+s)B(0)C(0)B^*(s)\int_0^1 e^{-i\Delta\omega(\bar{k}-\bar{l}+s,\bar{k})\frac{T^2}{\epsilon^2}v^2}dv\,,
\end{aligned}
$$

where

$$
g(s)=\frac{2\sqrt{2\pi}e^{i\frac{\pi}{4}}H(\bar{k}+s-\bar{l}-\tilde{r},\bar{l}+\tilde{r})}{\sqrt{-\Delta\omega_{ll}(\bar{k}+s,\bar{l}+\tilde{r})}}\,,
$$

$$
h(l)=\frac{4\pi\sqrt{2\pi}e^{i\frac{\pi}{4}}H(l-\bar{k},\bar{k})H(\bar{k}-\bar{l},\bar{l})}{\sqrt{-\Delta\omega_{ll}(\bar{k}+s,\bar{l})}\tilde{v}|\alpha|}\,,
$$

$$
F(s,l,T)=\frac{h(l)H(\bar{k}+s,l)e^{i\frac{\pi}{4}}\sqrt{2\pi}}{\sqrt{-\Delta\omega_{ll}(\bar{k}+s,l)}}\frac{\epsilon^2}{T^2}\frac{e^{-i\Delta\omega(\bar{k}+s,l)\frac{T^2}{\epsilon^2}}-1}{-i\Delta\omega(\bar{k}+s,l)}\,,
$$

and $\tilde{r}$ is given by

$$
\omega'(\bar{l}+\tilde{r})=\omega'(\bar{k}+s-\bar{l}-\tilde{r})\,.
$$

As discussed earlier, the growth of the secular terms is confined to a narrow region around the three wavenumbers. It is now possible to quantify this by considering the Fresnel type integral terms in (2.17). In particular it is required that the argument of the exponential be $O(1)$, as this corresponds to the $\sqrt{t}$ growth which is balanced with the slow time. Secondly note that $\Delta\omega(\bar{k}-\bar{l}+s,\bar{k})\approx\alpha s$ for small s where α is as defined earlier (2.13). But $\Delta\omega(\bar{k}-\bar{l}+s,\bar{k})$ and $\Delta\omega(\bar{k}+s,\bar{l}+\tilde{r})$ will be quadratic in s, since by definition $\omega'(\bar{l})=\omega'(\bar{k}-\bar{l})$. Thus the limiting term will be:

$$
|\,\Delta\omega(\bar{k}+s,\bar{l}+\tilde{r})\frac{T^2}{\epsilon^2}|=O(1)\,,
$$

or

$$s = O(\frac{\epsilon^2}{T^2\alpha}) = O(\frac{1}{t\alpha}) .$$

Exact Resonance

In particular, exactly at resonance, i.e. at $s = 0$, (2.17) reduces to

$$\begin{aligned} A_T &= g(0)BC + \epsilon T(F(0,\bar{l},T)B\,|C|^2\,C + F(0,\bar{k}-\bar{l},T)C\,|B|^2\,B) , \\ B_T &= \epsilon h(\bar{l})BCC^* , \\ C_T &= \epsilon h(\bar{k}-\bar{l})BCB^* . \end{aligned} \tag{2.18}$$

There is a fixed point at $A = const$, $B = const$, $C = 0$ (or without loss of generality $A = const$, $C = const$, $B = 0$), the stability of this point depends crucially on the nature of h and thus H. This can be seen using a linear stability analysis but in fact the decoupling of the B and C equations enables this system to be integrated exactly. First introduce the standard complex decomposition

$$B = b(T)e^{i\theta_b(T)} \qquad C = c(T)e^{i\theta_c(T)} .$$

Then from (2.18) the last two equations may be combined

$$\frac{d}{dT}\left(\frac{b^2}{2Re(h(\bar{l}))} - \frac{c^2}{2Re(h(\bar{k}-\bar{l}))}\right) = 0 ,$$

then integrated

$$b^2 = \frac{Re(h(\bar{l}))}{Re(h(\bar{k}-\bar{l}))}(c^2 - c_0^2) + b_0^2 ,$$

where b_0, and c_0 are the initial values of b and c respectively. This yields a single

autonomous equation for c which can then be integrated to give

$$c^2 = \frac{-c_0^2 \kappa e^{-2\epsilon\kappa T}}{Re(h(\bar{k}-\bar{l}))b_0^2 - Re(h(\bar{l}))c_0^2 e^{-2\epsilon\kappa T}} , \tag{2.19}$$

and similarly

$$b^2 = \frac{b_0^2 \kappa e^{2\epsilon\kappa T}}{Re(h(\bar{l}))c_0^2 - Re(h(\bar{k}-\bar{l}))b_0^2 e^{2\epsilon\kappa T}} , \tag{2.20}$$

where $\kappa = Re(h(\bar{l}))c_0^2 - Re(h(\bar{k}-\bar{l}))b_0^2$. And the corresponding phase functions are

$$\theta_b = \theta_{b_0} + \frac{Im(h(\bar{l}))}{2Re(h(\bar{k}-\bar{l}))}\left(-2\epsilon\kappa T - \ln\frac{-Re(h(\bar{k}-\bar{l}))b_0^2 + Re(h(\bar{l}))c_0^2 e^{-2\epsilon\kappa T}}{\kappa}\right) ,$$

$$\theta_c = \theta_{c_0} + \frac{Im(h(\bar{k}-\bar{l}))}{2Re(h(\bar{l}))}\left(2\epsilon\kappa T - \ln\frac{-Re(h(\bar{l}))c_0^2 + Re(h(\bar{k}-\bar{l}))b_0^2 e^{2\epsilon\kappa T}}{-\kappa}\right) ,$$

These expressions can then be used in the first equation to determine A. But the essential information with respect to stability for the fixed point can now be deduced from (2.20) and (2.19). In particular if $Re(h(\bar{l}))$ and $Re(h(\bar{k}-\bar{l}))$ are both positive then b and c approach ∞ in finite T. Otherwise one of b or c will approach a constant while the other goes to zero. Specifically:

if $Re(h(\bar{l}))c_0^2 > Re(h(\bar{k}-\bar{l}))b_0^2$ then $c \to 0$ and

$$b \to \sqrt{b_0^2 - \frac{Re(h(\bar{l}))}{Re(h(\bar{k}-\bar{l}))}c_0^2} ,$$

if $Re(h(\bar{k}-\bar{l}))b_0^2 > Re(h(\bar{l}))c_0^2$ then $b \to 0$ and

$$c \to \sqrt{c_0^2 - \frac{Re(h(\bar{k}-\bar{l}))}{Re(h(\bar{l}))}b_0^2} ,$$

otherwise if $Re(h(\bar{k}-\bar{l}))b_0^2 = Re(h(\bar{l}))c_0^2 < 0$ as would be the case for the degenerate Wilton ripple situation where $\bar{l} = \bar{k} - \bar{l}$, and thus B and C are identical. In this case then both b and c go to zero algebraically in T. The variation in amplitude of the

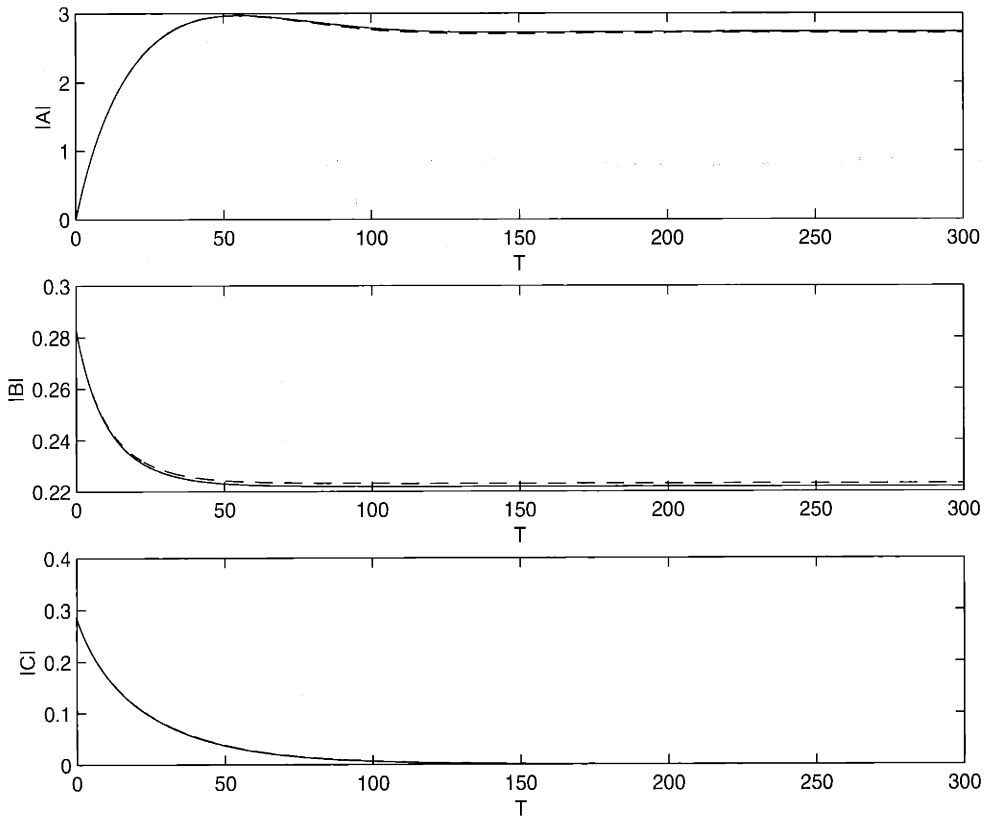

Figure 2-5: Evolution at s=0 for $\omega(k) = -\tanh(.116335k + 6.31965k^3)$ with $b_0 = c_0 = .28$, $H(k_1, k_2) = i(k_1 + k_2)$, $\epsilon = .1$. Dashed line corresponds to computation with terms for a_4 and a_5 also included.

feeder mode in this case takes the form

$$b^2 = \frac{b_0^2}{1 - 2b_0^2 \epsilon Re(h(\bar{l}))T} \tag{2.21}$$

This stability criterion, for example, shows that if $H(k_1, k_2) = (ik_1 + ik_2)^n$ corresponding to a nonlinearity of $\frac{d^n}{dx^n}u^2$, there is stability for all n odd, and a finite time "blow-up" for n even, as one would expect since odd derivatives allow for a conservation law in u^2 while even derivatives do not.

Figure 2-5 shows the result of numerically integrating (2.18) for a dispersion relation chosen so $\bar{k} = .9$, $\bar{l} = .25$ and a nonlinearity of $2uu_x$. In this case $h(\bar{l}) = -2.81(1+i)$ and $h(\bar{k} - \bar{l}) = -7.29(1+i)$. Thus the above stability criterion suggests

that the fixed point is stable and $c \to 0$ and

$$b \to .2217$$

agreeing with the numerical result. This dispersion will be studied in more detail in the next section. Actual numerical tests of the *full* equations for this case have also been run and indeed suggest a saturation, but the long times and highly oscillatory nature of the fast time structure make accurate numerical integration only possible up to values of $t = O(10^3)$ translating to $T \approx 5$. Regardless one cannot expect exact numerical agreement as (2.17) and thus (2.18) are based an asymptotic analysis and therefore valid only for long time. But the numerical results obtained, and presented in the next section, did indeed provide good evidence of saturation and this model certainly does provide qualitative information as to the mechanism behind it.

As for the validity of the truncation, although as discussed earlier it is difficult to justify rigorously, it is possible to consider the effect of including the next terms in the double resonance and feedback. The forms of a_4 and a_5 were deduced and added to (2.17) but provided no qualitative and only a small numerical change to the previous truncation as shown in Figure 2-5. This can be seen by the fact that all higher order terms will involve more and more factors of B and C which therefore will not affect the stability of the fixed point as one amplitude approaches zero. The dashed lines in Figure 2-5 give an example this and how the correction due to higher order terms is negligible in terms of the overall behavior.

Another key distinction between the system (2.17) and the classical three wave equations is that there is now a parameter related to detuning from resonance. This will allow for not only the amplitudes of the modes in the doubly resonant triad to be traced, but also modes nearby.

Non-Zero s

As shown above, a doubly resonant mode will grow on a scale of $O(\sqrt{t})$ whereas members of a non-doubly resonant triad will not exhibit any growth at all in the

continuous spectrum case. This then implies that there is a transition region in wavenumber space joining these two behaviors. Since the peaks become narrower as time goes on, if one traces a mode near to a double resonance then it should initially exhibit $O(\sqrt{t})$ growth, which will cease once the peak becomes sufficiently narrow. Figure 2-6 shows the same run as that in Figure 2-5 along with traces corresponding

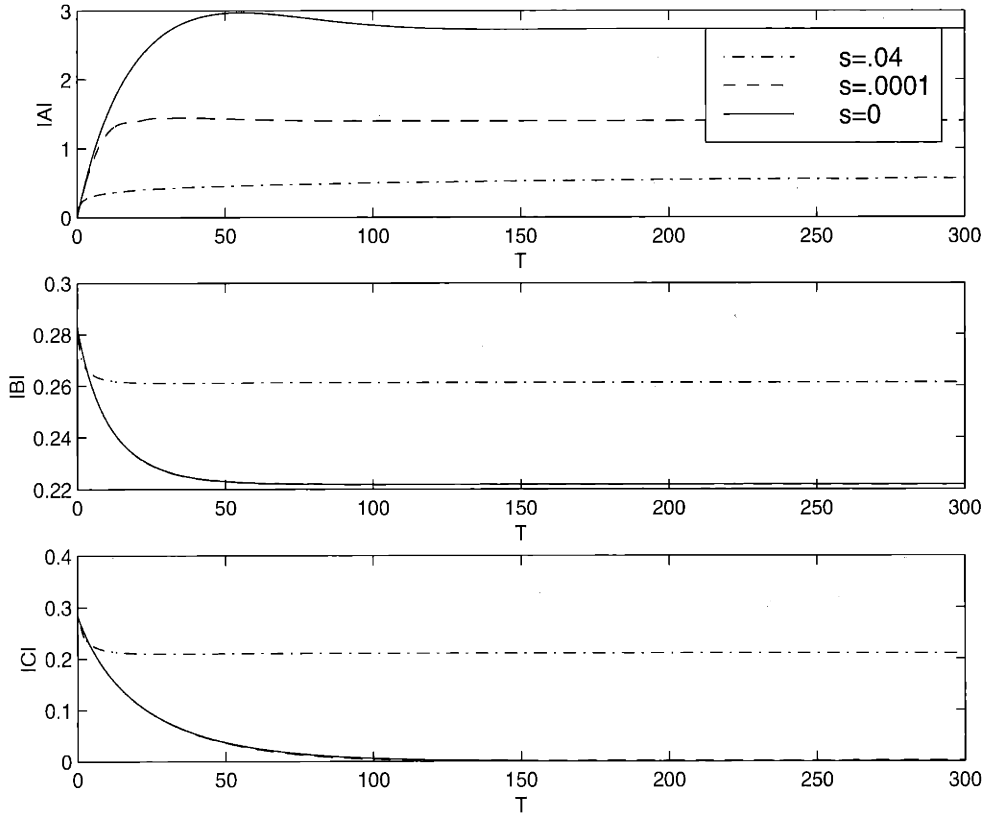

Figure 2-6: Evolution of model for various values of s. $\omega(k) = -\tanh(.116335k + 6.31965k^3)$ with $b_0 = c_0 = .28$, $H(k_1, k_2) = i(k_1 + k_2)$, $\epsilon = .1$.

to $s \neq 0$. It shows that as one moves away from the resonance, growth is indeed inhibited, leveling off at a far smaller value.

2.2.2 Real Space Interpretation

At this point, some comment should be made regarding the real space interpretation of the double resonances. The essential question is to what extent will these double resonances be manifested in real space. The answer lies in the fact that the magnitude

of the effect in real space depends on the area under the spectral distribution. To investigate this consider the real space analog of the double resonant peak found earlier

$$u_1 = \int a_1(k,t)e^{i(kx-\omega(k)t)}dk \ ,$$

where $a_1(k,t)$ is the first order correction found earlier. By using the asymptotic form of this (2.9) and assuming that observations are taken in a frame moving at some velocity U, i.e. $x = Ut$ then asymptotically, a saddle point type critical point is obtained when $U = \omega'(\bar{l})$ yielding a dominant contribution

$$u_1 = \frac{2\pi\sqrt{2\pi}H(\bar{k}-\bar{l},\bar{l})a_0(\bar{l})a_0(\bar{k}-\bar{l})}{\sqrt{-\Delta\omega_{ll}(\bar{k},\bar{l})|\alpha|}}\frac{e^{i(\bar{k}\omega'(\bar{l})t-\omega(\bar{k})t)}}{\sqrt{t}} \ . \tag{2.22}$$

The first noteworthy point is that unlike the typical case of a nonlinear wavetrain in a dispersive medium where the dominant contribution at a given wavenumber travels at the group velocity of that wavenumber, now due to the extra phase term in a_1, the real space effects of the double resonance will propagate at the group velocity of the feeder modes. In other words $U = \omega'(\bar{l})$ as opposed to $U = \omega'(\bar{k})$. Furthermore it should be noted that with the extra factor of t^{-1} coming from the stationary phase, the $\sqrt{t}$ growth in Fourier space does not translate to a growth in real space. So although the amplitude around the doubly resonant mode increases, the fact that the peak also narrows mitigates this effect. But still double resonances cannot be ignored since the analytic computations in Fourier space depend on the perturbation expansion being well ordered. In fact an interesting conclusion which can be drawn in the case of a continuous spectrum is that the dominant component to the solution will simply be the linear part for all times. This is in contrast with the discrete case where multi wave resonances do cause a disordering in the real space expansion. However, a main purpose of this discussion is to look at the effects caused by the weak nonlinearity and amongst these, double resonances will certainly play a large role. Moreover, besides the mathematical implications, the disorderedness of the perturbation expansion in Fourier space when double resonances are present has direct ramifications on areas

such as statistical treatments of turbulence ([6], [14]), a discussion of which will be given in Chapter 4.

2.3 Numerical Experiments

In order to verify and extend these analytic results, a number of numerical experiments were conducted. This was done by using a spectral decomposition in space and appropriate discretizations in time in order to maintain stability. A combination of MATLAB and Fortran77 was used for this work, along with Mathematica and Maple for some of the algebraic computations. Adding to the difficulty was the necessity of simulating a "continuous" spectrum, meaning a very high resolution was required in order to suitably resolve the region around the doubly resonant modes. Additionally it was necessary to accurately evolve the equations for a sufficiently long time for the asymptotic results to be applicable. In spite of these difficulties, results were obtained, a summary of which will be presented in this section. Various dispersion relations including those for internal waves and Rossby waves were analyzed but for simplicity, a pair of artificial "gravity-capillary" like dispersion relations will first be studied, designed so that only a single double resonance exists. This will serve to provide clear information on how the full system evolves and isolate the effects of the double resonance.

2.3.1 Artificial Dispersions

To begin, the following dispersion relations will be considered

$$\textbf{Disp. 1}\ \omega(k) = \tanh\left(\frac{k}{4} + \frac{25k^3}{8}\right),$$

$$\textbf{Disp. 2}\ \omega(k) = -\tanh\left(.116355k - 6.31965k^3\right),$$

For small wavenumbers these do resemble the dispersion for gravity-capillary

waves on a finite depth, but for reasons of ease of numerical simulation they were chosen so that the high wavenumbers have negligible velocities. They are indeed both odd in k and possess only a single double resonance. This is the main motivation for this choice of dispersions, as having a single double resonant point will allow for direct and clear comparison to the analytic analysis above. More physical dispersions, such as that for internal waves, often contain more than one double resonance and will be considered later in this section.

Disp. 1

It can easily be verified that this dispersion contains a double resonance at

$$\bar{k} = 1.02468, \qquad \bar{l} = \bar{m} = .5123 \, .$$

This therefore represents a simple example of a Wilton ripple type double resonance. Furthermore, for simplicity we choose a nonlinearity corresponding to $(u^2)_x$ or likewise $H(k_1, k_2) = i(k_1 + k_2)$. For this and all subsequent trials $\epsilon = .1$. Also, again in order to isolate the double resonant effects, an initial condition is chosen of the form

$$A(k, 0) = (e^{-50(k-.6)^2} + e^{-50(k+.6)^2})e^{i100k} \, .$$

A resolution of 2^{16} modes in k space was chosen, with bounding values of ± 2.3103. It should also be noted that the spectrum bound was chosen so that $\bar{k}, \bar{l}, \bar{m}$ are amongst the modes, exact up to the precision of the computation. The time stepping was done using an RK4 scheme with $dt = .01$ and all calculations were done in double precision. As mentioned above, these rather extreme measures are necessary due to the high precision required in order to simulate a "continuous" spectrum for relatively long lengths of time.

Figures 2-7 and 2-8 show the change in the spectral distribution at times of 500 and 1000 respectively. Note that ΔA represents the spectrum once the simple linear

propagation of the initial condition has been removed. In other words

$$\Delta A = A(k,t) - A(k,0)e^{-i\omega(k)t} .$$

It is clear that there is definitely a peak forming at $\bar{k}$ and even the feedback is visible around $\bar{l}$. Figures 2-9 and 2-10 give a closer look at the peaks, showing that the structure is also quite similar to that predicted earlier, as shown in Figure 2-1. The slight bulge in the tail around $k = 1.07$ may be due to the fact that the initial condition is slightly biased above $\bar{l}$, and indeed it was verified that if the initial condition is shifted to peak below $\bar{l}$ then this bulge disappears. The peak at $\bar{l}$ is slightly less well defined, given that its growth is on a slower time scale, but there is at least at this point qualitative similarity which in itself is noteworthy given that the asymptotic analysis relies on long times. The question of how these peaks grow is also of interest as it will provide a good comparison to the models posed earlier. Figure 2-11 shows how the doubly resonant peak grows as the amplitude at the feeder mode decays. For a more quantitative comparison to the direct model note that from (2.21)

$$-2b_0^2\epsilon Re(h(\bar{l}))T = \left(\frac{b_0^2}{|B|} - 1\right) .$$

Figure 2-12 shows that indeed the relation between T and the right hand side of this expression appears to be linear for sufficiently large T for the model to be valid. The slope of this line can then be compared to the known parameter values to give a check this model. Roughly speaking, the slope is .007, whereas $-2b_0^2\epsilon Re(h(\bar{l})) = .0067$. So the numerical results provide a fairly reasonable agreement with the direct model, at least for the admittedly limited range of T for which computation was feasible.

Disp. 2

Now consider a second dispersion relation, similar to the previous but now designed so that the double resonance is composed of three distinct modes. The dispersion

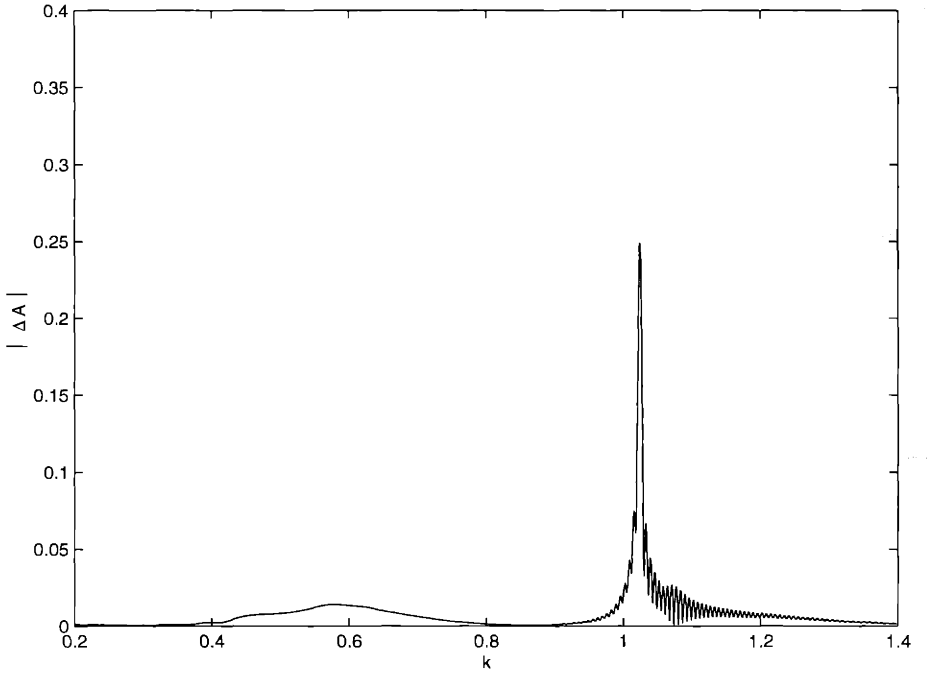

Figure 2-7: Spectral change at $t = 500$ for system with $\omega(k) = \tanh\left(\frac{k}{4} + \frac{25k^3}{8}\right)$.

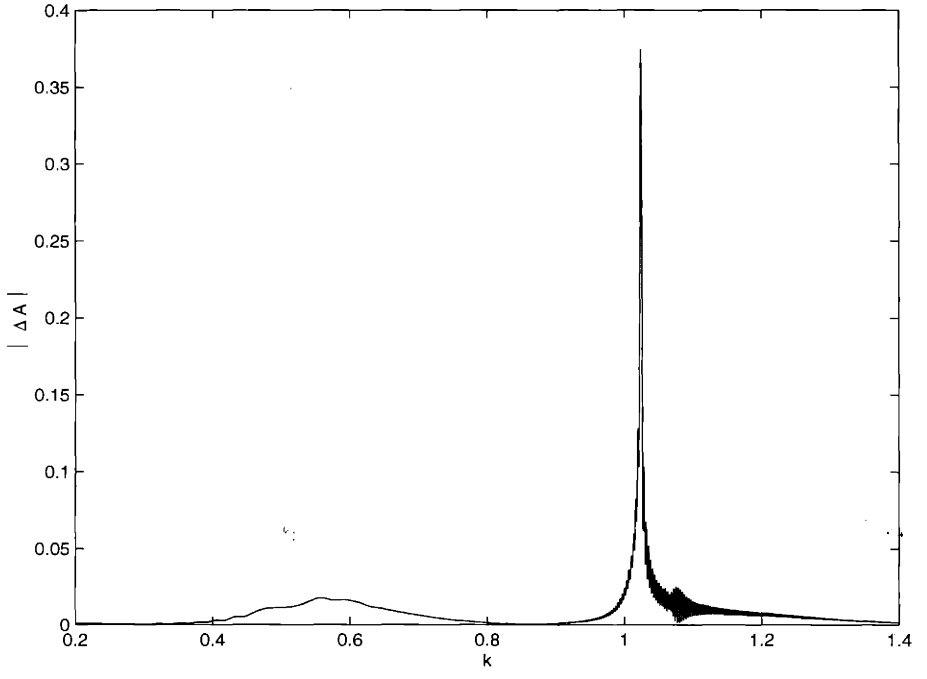

Figure 2-8: Spectral change at $t = 1000$ for system with $\omega(k) = \tanh\left(\frac{k}{4} + \frac{25k^3}{8}\right)$.

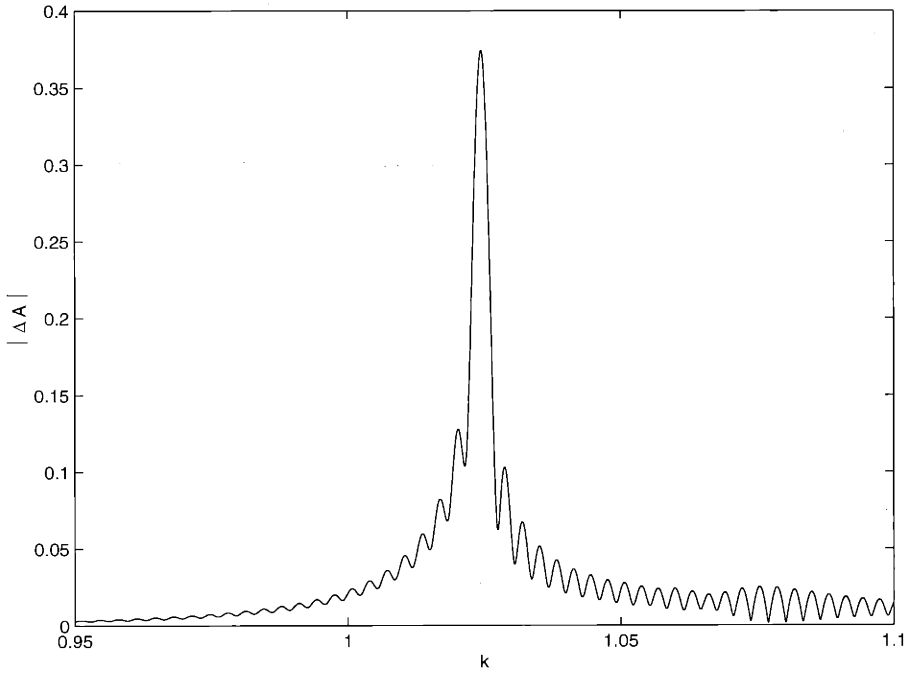

Figure 2-9: Double Resonance peak at $\bar{k} = 1.02468$. $t = 1000$.

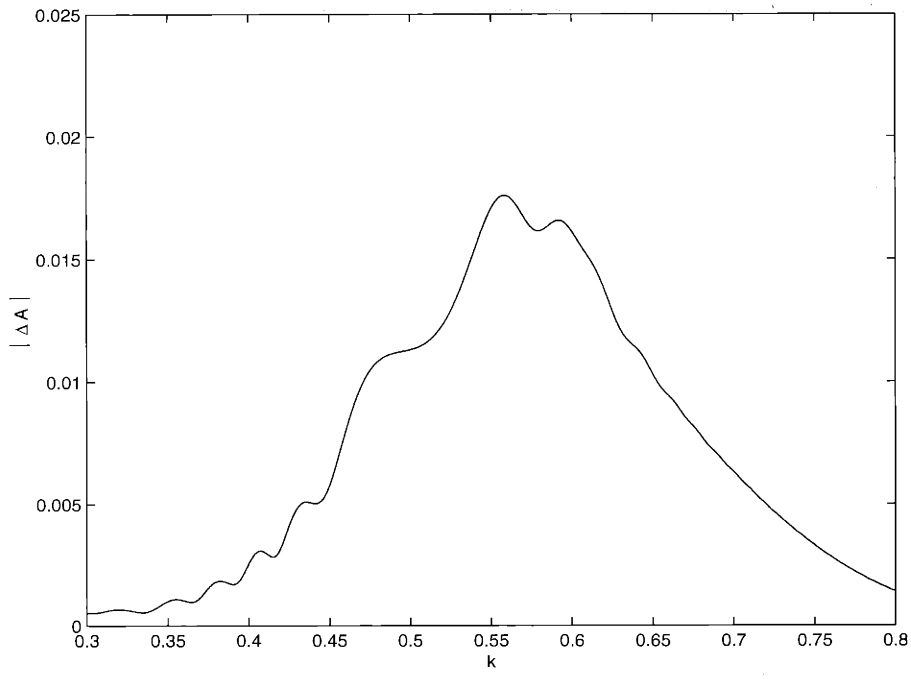

Figure 2-10: Feedback from Double Resonance at $\bar{l} = .5123$. $t = 1000$.

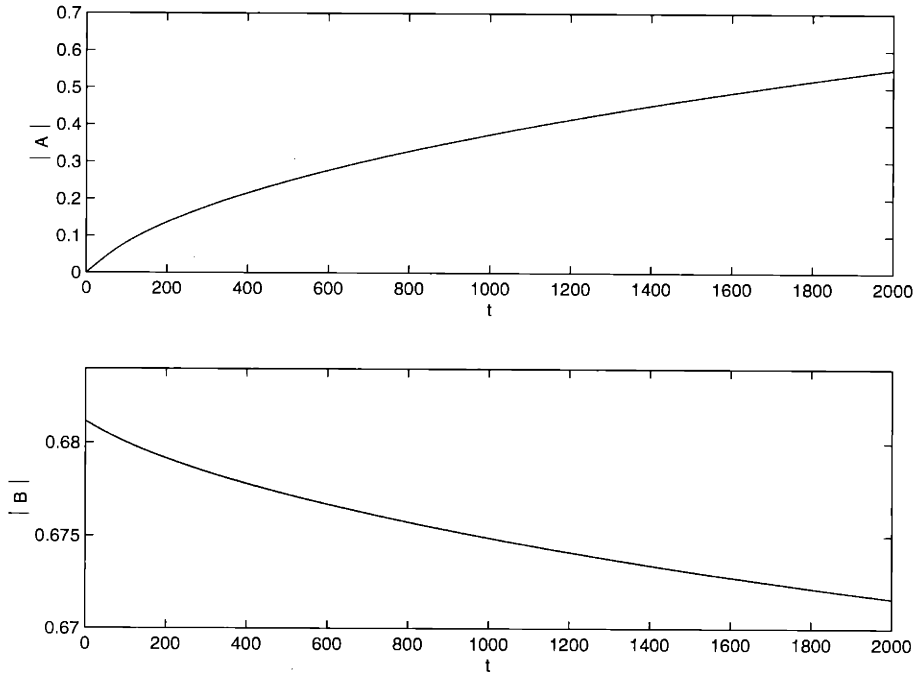

Figure 2-11: Trace of peak heights.

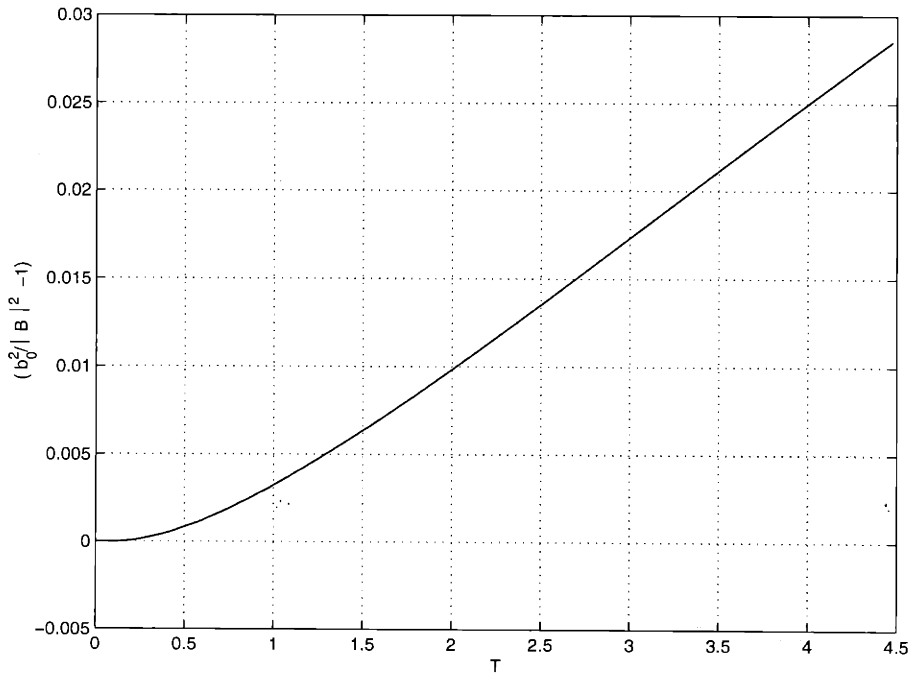

Figure 2-12: Comparison of $\frac{b_0}{|B|^2} - 1$ vs. T.

relation to be considered is

$$\omega(k) = -\tanh\left(.116355k - 6.31965k^3\right) ,$$

where the double resonance occurs for

$$\bar{k} = .9 \qquad \bar{l} = .25 \qquad \bar{m} = .65 .$$

Figure 2-13 shows the result of a run starting with

$$A_0(k) = 2\left(e^{-500(k-.65)^2} + e^{-500(k+.65)^2} + e^{-200(k-.25)^2} + e^{-200(k+.25)^2}\right) e^{i100k} .$$

Again the similarity to the direct model is clear. In this case $b_0 Re(h(\bar{k}-\bar{l})) > c_0 Re(h(\bar{l}))$ meaning that according to the previous discussion, the fixed point corresponds to $|B| \to const$, $|C| \to 0$, and this certainly appears to be the trend suggested by the numerical simulation. Again a more quantitative comparison can be made to the model. Note that based on (2.19) and (2.20),

$$\begin{aligned} 2\epsilon\kappa T &= \ln\left(\frac{1}{Re(h(\bar{k}-\bar{l}))b_0^2}\left[\frac{-c_0^2\kappa}{|C|^2} + Re(h(\bar{l}))c_0^2\right]\right) = \Delta_B \\ &= -\ln\left(\frac{1}{Re(h(\bar{l}))c_0^2}\left[\frac{b_0^2\kappa}{|B|^2} + Re(h(\bar{k}-\bar{l}))b_0^2\right]\right) = \Delta_C \end{aligned}$$

Figure 2-14 shows how these two possibilities compare to one another and vary with T. The striking similarity between Δ_B and Δ_C provides good evidence that the direct model does indeed capture the feedback mechanism and the interactions with the feeder modes. In fact the two curves only differ by at most 8% in an absolute sense. Furthermore the slope of the curves beyond the initial transient phase is roughly .08 while the value of $2\epsilon\kappa = .102$, again providing a further piece of evidence that the model has captured the basic energy transfer mechanism.

Based on these two trials, it is now clear that the direct slow time model agrees well with numerical simulations of the full nonlinear equations. This is not surprising,

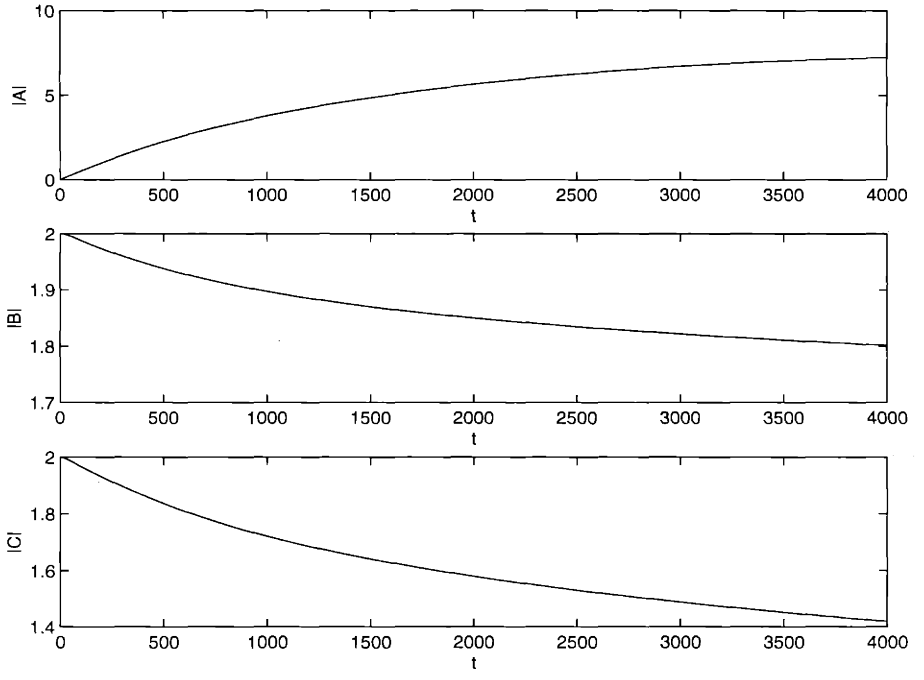

Figure 2-13: Trace of peak heights.

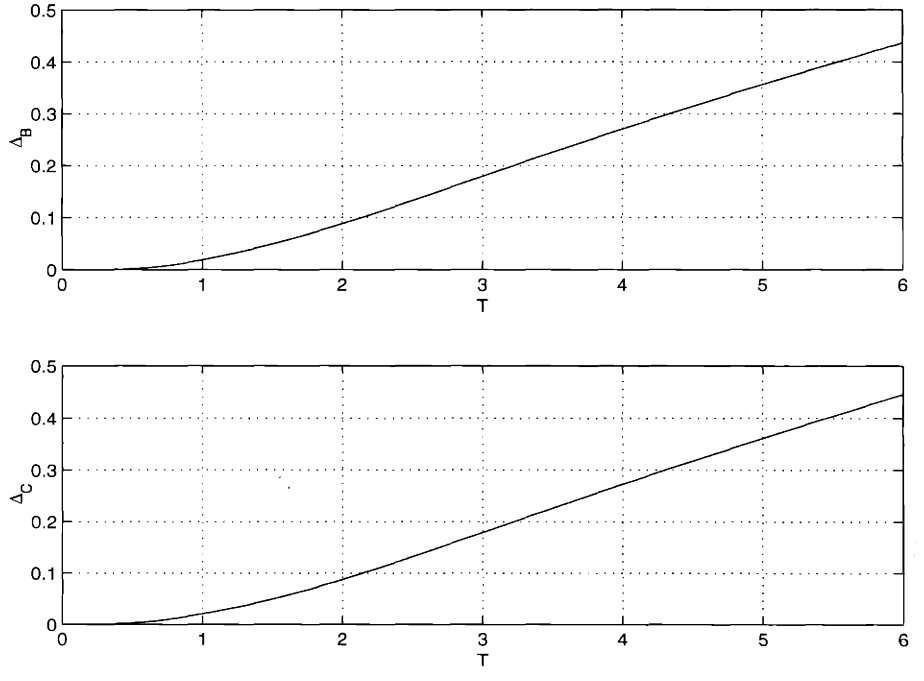

Figure 2-14: Δ_B, Δ_C vs. T

given that an essential component of the behavior appears to come from the modes around the doubly resonant modes which are captured in this model.

2.3.2 Gravity-Capillary Waves

Now a more physical dispersion is considered, namely that for capillary-gravity waves on deep water. As shown in Chapter 1, the dispersion relation for this case takes the form

$$\omega^2 = k + k^3 \,,$$

where without loss of generality, the coefficients were taken to be unity. For this dispersion a Wilton ripple type double resonance occurs for $\bar{k} = \sqrt{2}$ and $\bar{l} = \bar{k}/2$. Figures 2-15 and 2-16 show the results of a run made with an initial condition

$$A(k,0) = \left(e^{-50(k-.6)^2} + e^{-50(k+.6)^2}\right) e^{i100k}$$

and $\epsilon = .1$. Again, the double resonance is clear, as well as the feedback around $\bar{l}$. A more quantitative comparison is hampered by the limitations on the maximum computation time. Unlike the two previous dispersions, the group velocity in this case for high wave numbers becomes arbitrarily large. This then necessitates a large spatial domain in order to avoid the "wrap around" effect one encounters with the artificially periodic boundaries needed for a spectral approach. Consequently this limits the maximum time for which an accurate solution may be evolved using a reasonable amount of computation time. Nevertheless the traces show the energy exchange between the modes, which again is in qualitative agreement with the model.

General Initial Conditions

Thus far, the numerical results presented have involved situations where the initial conditions were chosen in such a way as to emphasize the effects of the double resonance in order to allow for clear comparison with the conclusions drawn from the asymptotics. Clearly, though, natural problems often involve much more general ini-

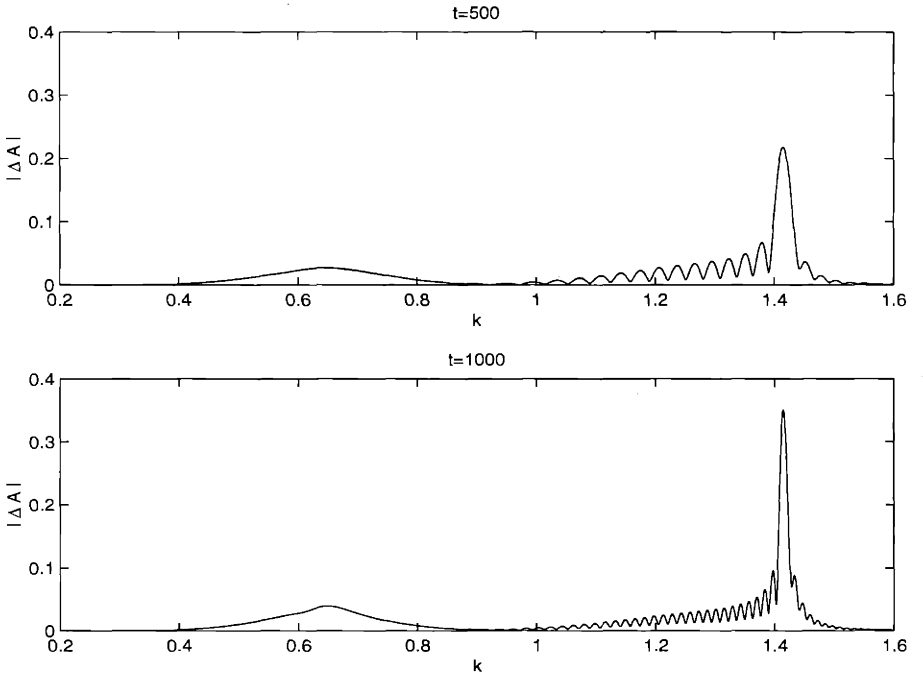

Figure 2-15: Double resonance peaks and feedback for Gravity-Capillary wave system.

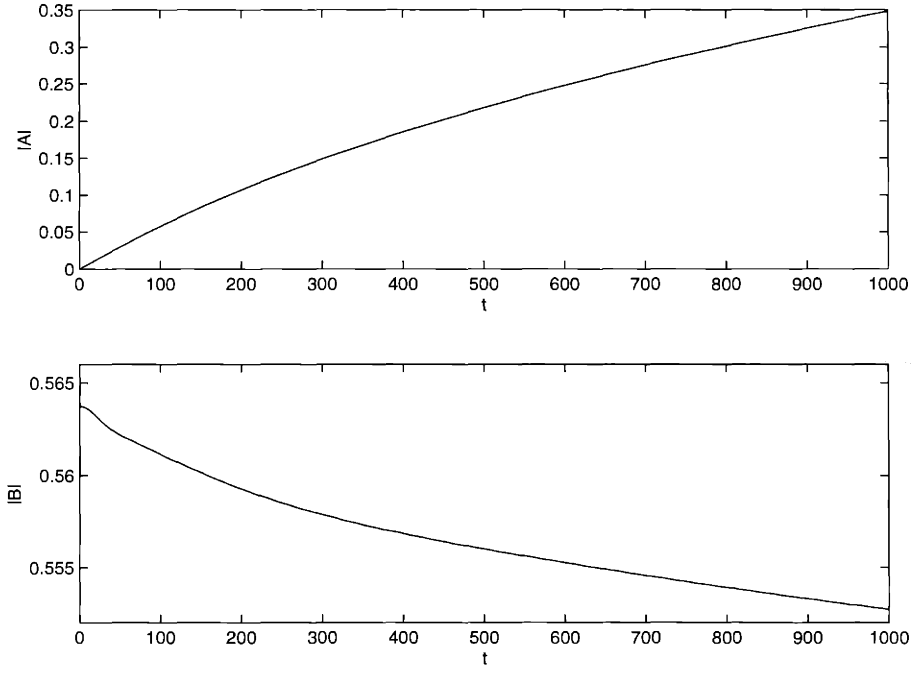

Figure 2-16: Trace of peak heights at $\bar{k}$ and $\bar{l}$ for Gravity-Capillary wave system.

tial conditions where the initial spectral distribution covers a much wider range. To investigate this, a second run was made with an initial condition of

$$A(k,0) = (e^{-.001(k-2.8)^8} + e^{-.001(k+2.8)^8})$$

As shown in Figure 2-17 this covers a much wider range of wavenumbers although not so wide as to necessitate too large a computational domain. Note that the modes near $k = 0$ were intentionally diminished in amplitude in order to eliminate trivial resonances caused by long-short wave interactions. By subtracting off the linear solution, Figure 2-18 shows the effects of the nonlinearity. It is clear that the double resonance still persists, but there are other effects present too arising from the simple resonances. The figure shows how these latter effects remain relatively constant in time, while the amplitude at the double resonance grows, as expected.

2.3.3 Internal Waves

Internal waves in a stratified fluid is another example of a physical situation where the dispersion relation admits double resonances. Eckart [12] first studied the problem of internal waves in the ocean, showing that to first order the evolution is governed by a Schrödinger type equation. In general, the equations for the two-dimensional motion of an inviscid incompressible stratified fluid are

$$u_x + v_y = 0 \ ,$$

$$\rho_t + u\rho_x + v\rho_y = 0 \ ,$$

$$\rho(u_t + uu_x + vu_y) = -p_x \ ,$$

$$\rho(v_t + uv_x + vv_y) = -p_y - g\rho \ ,$$

where (u, v) are the horizontal and vertical components of the velocity respectively, ρ the density, and p the pressure. Then, as noted in [18], given an initial steady state

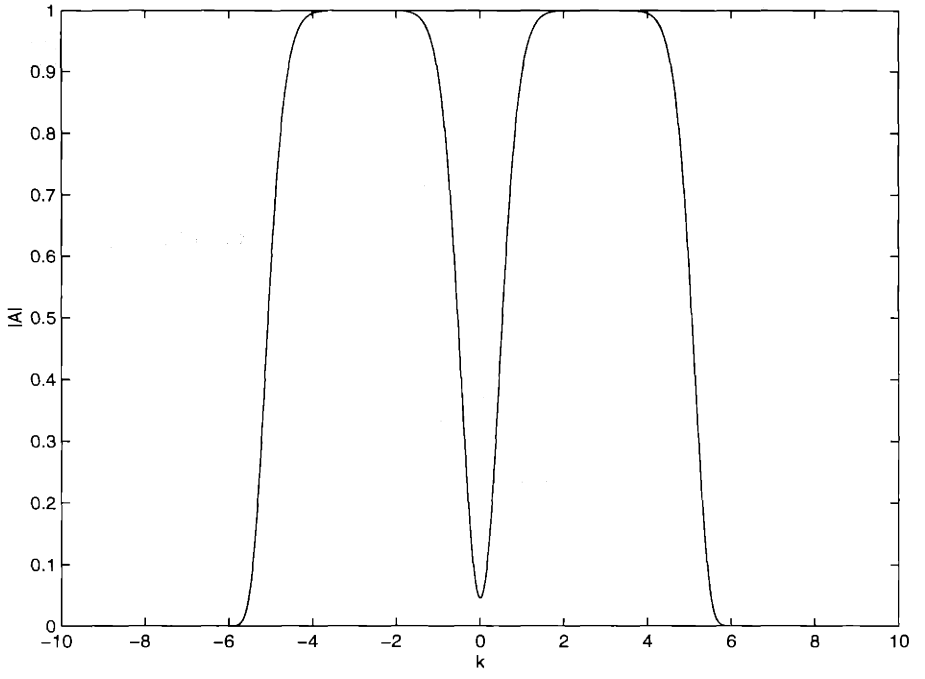

Figure 2-17: Initial Spectral distribution for gravity-capillary case using an initially wider range of wavenumbers.

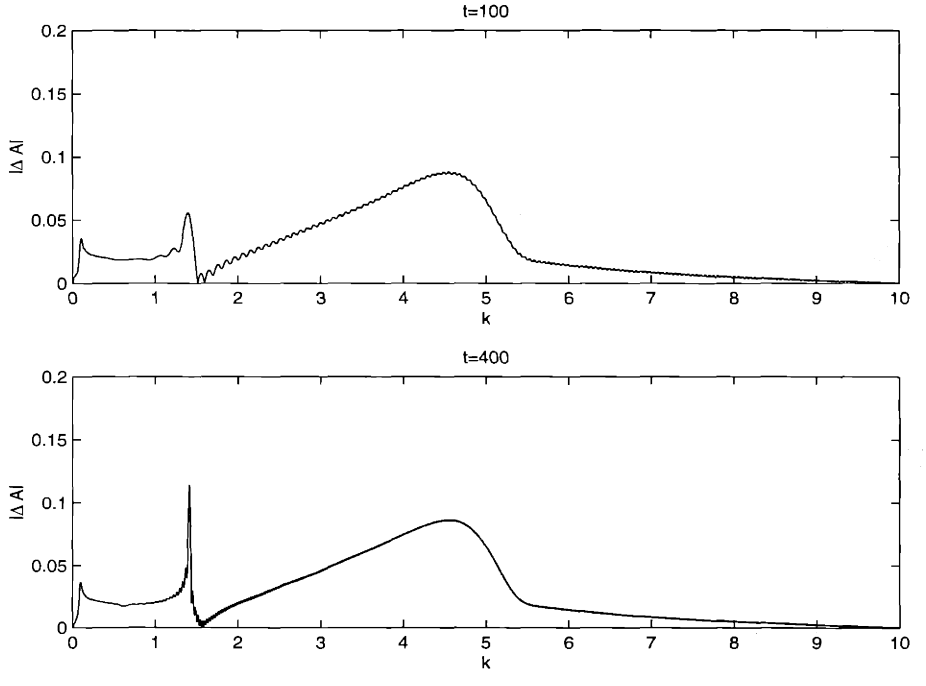

Figure 2-18: Change in spectral distribution due to nonlinear effects.

with

$$\bar{u} = \bar{v} = 0 \qquad \bar{\rho} = \rho_0[1 - \sigma f(y)]$$

take a perturbation of the form

$$u = \bar{u} + \epsilon\psi_y, \qquad v = \bar{v} - \epsilon\psi_x, \qquad \rho = \bar{\rho} + \epsilon\rho' \ .$$

Then upon using a Boussinesq approximation where the first order density variations are neglected in the inertial terms but kept in the buoyancy term, the following equations result for the perturbation stream and density functions

$$\nabla^2\psi_t - \rho_x + \epsilon J(\nabla^2\psi, \psi) = 0 \ , \tag{2.23}$$

$$\rho_t + N^2(y)\psi_x + \epsilon J(\rho, \psi) = 0 \ , \tag{2.24}$$

where $N^2(y) = f'(y)$ is the square of the Brunt-Väisälä frequency, and the Jacobian operator J is defined by

$$J(f, g) = f_x g_y - f_y g_x \ .$$

Separating the stream and density functions into vertical and normal mode components as follows $\psi = \hat{\psi}(y)e^{i(kx-\omega t)}$, $\rho = \hat{\rho}(y)e^{i(kx-\omega t)}$, the linearized system may then be decoupled to give

$$\left(\frac{d^2}{dy^2} - k^2 + \frac{N^2k^2}{\omega^2}\right)\hat{\psi} = 0 \ ,$$

$$\hat{\rho} = \frac{kN^2\hat{\psi}}{\omega} \ , \tag{2.25}$$

meaning that given boundaries on top($y = 0$) and bottom($y = -H$) so that

$$\hat{\psi}(0) = \hat{\psi}(-H) = 0 \ ,$$

the resulting eigenvalue problem can then be solved to give ω. At this point it is assumed that the stratification, characterized by N, is constant leading to simple

solutions

$$\hat{\psi}_n = \sin\left(\frac{n\pi y}{H}\right) ,$$

with

$$\omega_n^2 = \frac{k^2 N^2}{k^2 + \frac{n^2\pi^2}{H^2}} .$$

Turning to the fully nonlinear problem, take the solution to be an expansion around these linear eigenmodes, where the coefficients are allowed to modulate in space and time

$$\psi = \sum_{n=1}^{\infty} \psi_n(x,t) \sin\left(\frac{n\pi y}{H}\right) ,$$

$$\rho = \sum_{n=1}^{\infty} \rho_n(x,t) \sin\left(\frac{n\pi y}{H}\right) .$$

Plugging this into (2.23),(2.24) and eliminating the y structure by multiplying by the appropriate eigenfunction and integrating one obtains an infinite hierarchy of equations for the evolution of A_n and B_n, where

$$\psi_n(x,t) = \int A_n(k,t) e^{ikx} dk ,$$

$$\rho_n(x,t) = \int B_n(k,t) e^{ikx} dk ,$$

It is clear that without the nonlinear terms, the coefficients ψ_n and ρ_n are merely the normal modes listed above. The nonlinearity serves to couple the various vertical modes. In general this system will contain numerous double resonances, as was shown in Figure 1-1. For simplicity a truncation at $n = 3$ provides the minimum case where there is only a single double resonance corresponding to

$$\bar{k} = 8.0066, n = 1$$

$$\bar{l} = 4.435, n = 2$$

$$\bar{m} = 3.569, n = 3$$

where without loss of generality N will be taken to be unity. Although strictly speaking this system is not a scalar equation of the form (2.1), it will be seen that there is still room for qualitative comparison with the previous analytic analysis and resulting models. This system was simulated numerically with $\epsilon = .1$. The initial conditions were

$$\psi_1(x,0) = 0, \qquad \psi_2 = e^{-25x^2} \sin \bar{l}x, \qquad \psi_3 = e^{-25x^2} \sin \bar{m}x$$

and the initial conditions for ρ are computed from (2.25). These initial conditions were chosen in such a way that the modes in the doubly resonant triad were well represented. Figure 2-19 shows that indeed the structure of the doubly resonant peak grows and becomes narrower as time increases. The growth of the double resonance peak is indeed $O(\sqrt{t})$, as shown by Figure 2-20. Furthermore, note that one of the other two modes is asymptotically approaching zero, while the other approaches a nonzero value. Again it should be noted that further comparison would not be warranted, as the system is not strictly scalar any longer, so therefore the nonlinearity is not as clearly defined, but this example does illustrate the robust and fundamental nature of double resonances.

Higher Order Truncations

A clear limitation of the previous simulation is that the system was truncated at 3 modes in the vertical direction. Figure 2-21 shows the same simulation as above, only now using 5 modes in the truncation. The double resonance at $\bar{k} = 8.0066$ remains clear, but there are now other peaks nearby corresponding to other resonances. The introduction of more vertical modes now allows for more possible double resonant points, as illustrated in Figure 1-1. This again emphasizes the effects of double resonances, and moreover suggests that as more and more vertical modes are included then more and more double resonances will occur giving rise to possible couplings and triad-triad interactions.

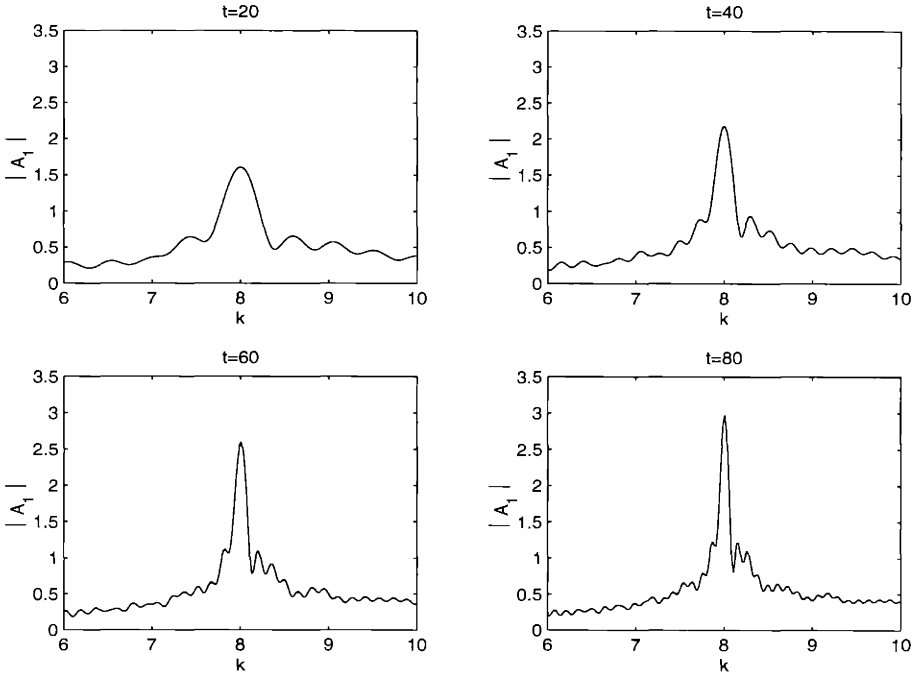

Figure 2-19: Double Resonance peaks for Internal Wave Simulation

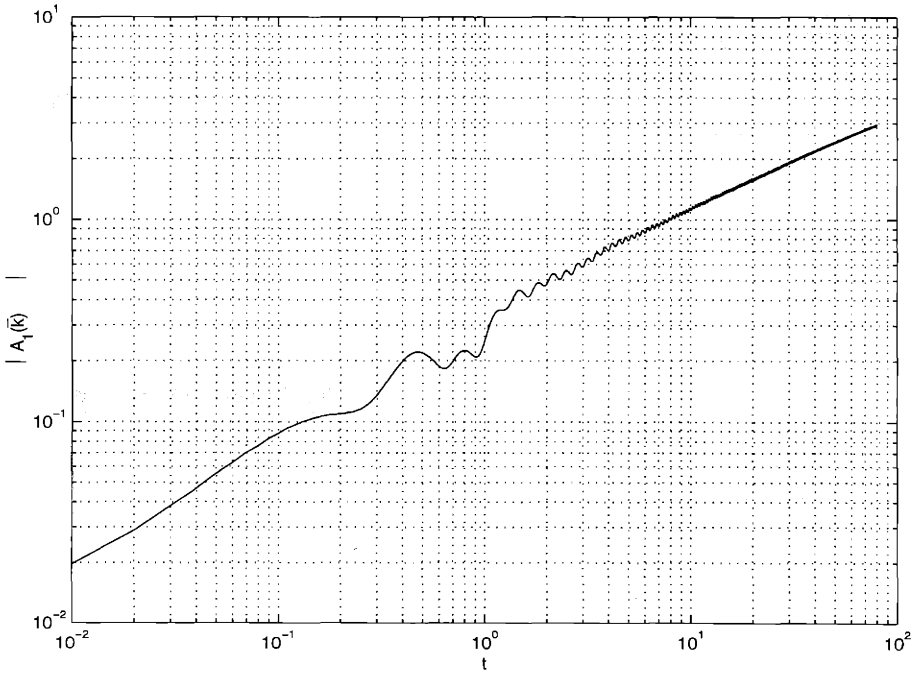

Figure 2-20: Log-Log plot of double resonant peak height showing $\sqrt{t}$ growth for internal wave system.

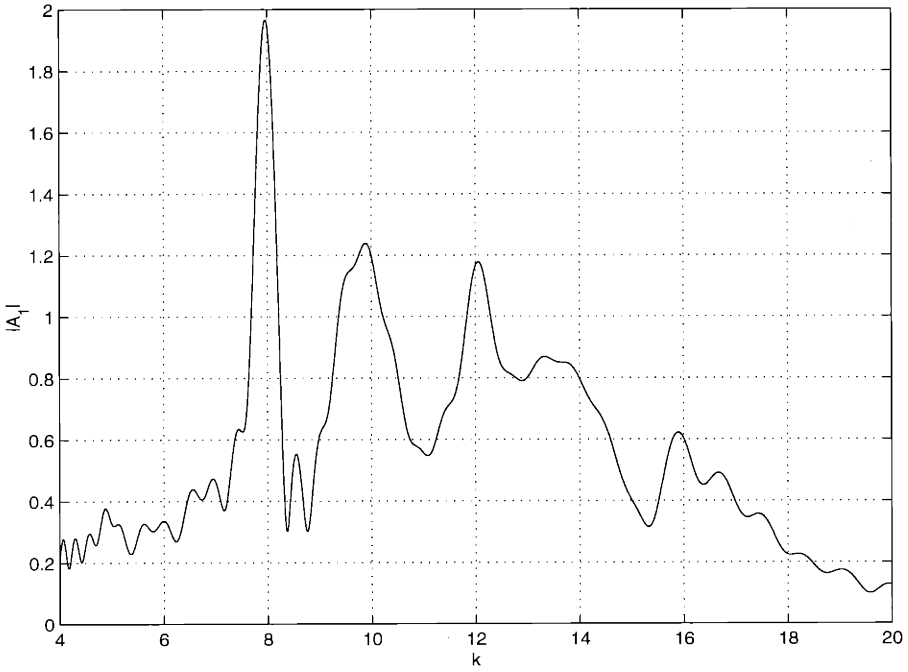

Figure 2-21: Spectral distribution A_1 at $t = 20$.

2.3.4 Rossby Waves

Another example of a physical regime which contains double resonances is that of Rossby waves. To begin, consider the equations for the two dimensional motion of a rotating fluid

$$\frac{d\mathbf{u}}{dt} + (\mathbf{u} \cdot \nabla)\mathbf{u} + f(\hat{k} \times \mathbf{u}) = -\nabla P \ ,$$

where $\mathbf{u} = (u, v)$ are the horizontal velocity components, f is the rotational frequency, the motion of the fluid being perpendicular to the rotation vector. Now by introducing a stream function $u = \psi_y, v = -\psi_x$, introducing the standard beta plane approximation ($f = f_0 + \beta y$) to allow for small variations in latitude and taking the curl of this equation, one obtains

$$\frac{d}{dt}\nabla^2\psi + \beta\psi_x = \epsilon J(\nabla^2\psi, \psi) \ , \tag{2.26}$$

where ϵ is a measure of the magnitude of the stream function. Again, for simplicity, a single layer is taken with a height of π. And just as in the internal wave case, the

boundary conditions restrict the vertical structure, again suggesting that the solution take the form of a sine series

$$\psi = \sum_{n=1}^{\infty} \psi_n(x,t) \sin ny \ .$$

Then taking the Fourier transform

$$\psi_n(x,t) = \int A_n(k,t) e^{ikx} dk \ ,$$

(2.26) becomes

$$\frac{d}{dt}(-k^2 - n^2)A_n + \beta ikA_n = \epsilon N.L.T. \ ,$$

where the nonlinear terms ($N.L.T.$) are given by substituting the expansion into the Jacobian term and then projecting onto the appropriate vertical eigenfunction. In particular it is clear that when $\epsilon = 0$, the linear solution is

$$A_n = e^{\frac{\beta ik}{n^2+k^2}t} \ ,$$

or in other words $\psi_n = e^{i(kx-\omega t)}$ where

$$\omega_n(k) = -\frac{\beta k}{n^2 + k^2} \ .$$

Truncating at 3 modes, there is a double resonance at

$$\bar{k} = 2.50829, n = 1$$

$$\bar{l} = 1.31225, n = 2$$

$$\bar{m} = 1.19604, n = 3$$

Figure 2-22 shows the results from a numerical simulation of the this system (with 3

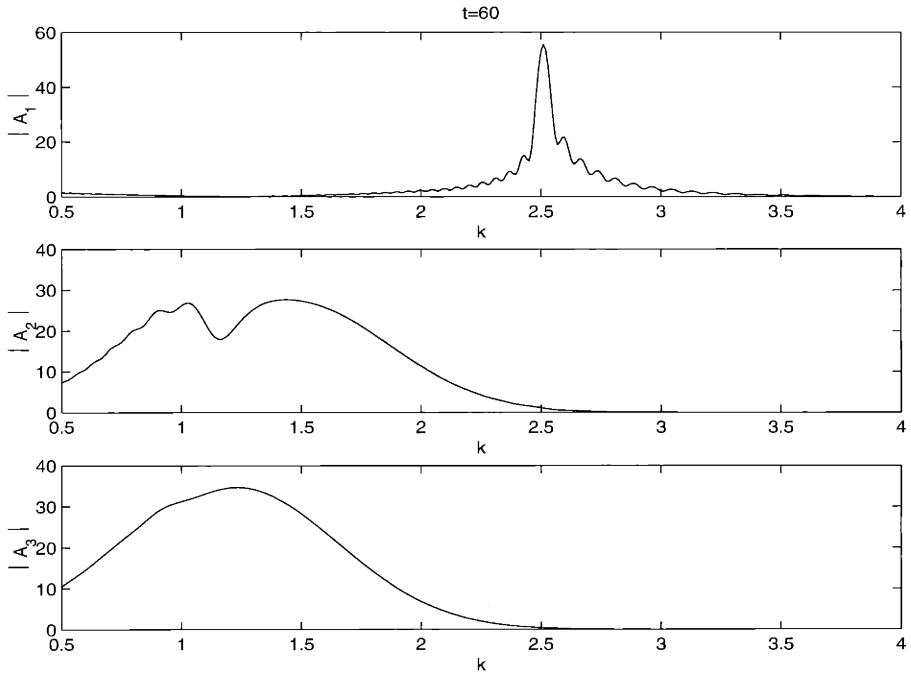

Figure 2-22: Spectral distribution at $t = 60$ for Rossby Wave system

vertical modes), with $\epsilon = .1$, $\beta = 10$. The initial conditions were

$$\psi_1(x,0) = 0 \qquad \psi_2(x,0) = \sin \bar{l}x e^{-.1x^2} \qquad \psi_3(x,0) = \sin \bar{m}x e^{-.1x^2} \ .$$

This gives a very clear illustration of how the energy is transferred from the feeder modes (in this case mostly $\bar{l}$) to the double resonance peak. Furthermore, the nearby structure is also in qualitative agreement with the asymptotics. Figure 2-23 shows the traces of the amplitudes of the peaks. Again the trends are clear, further computation was attempted, but was constrained by boundary effects in physical space due to the effects of a periodic rather than infinite domain.

Higher order truncations in the vertical structure were also attempted in this case. The results were identical in spirit to that of the internal wave case where simply more double resonant peaks became visible. The purpose of these simulations, and the three mode truncations was more to isolate and illustrate the effects of double resonances, and the results for higher order truncations can in some sense be thought of as a super position of these individual peaks. Of course there may also be a coupling for

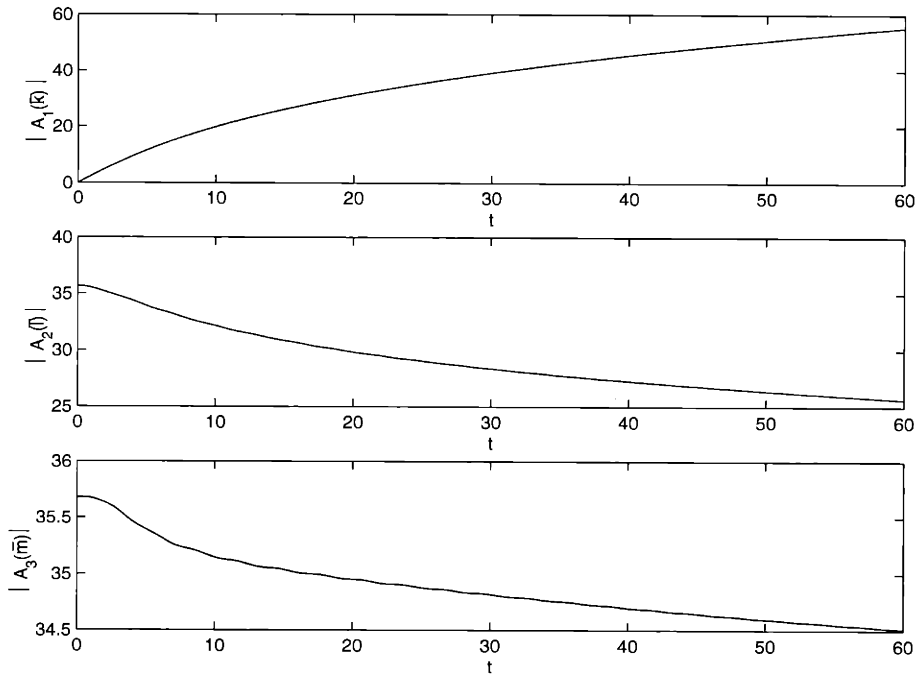

Figure 2-23: Amplitudes at $\bar{k}, \bar{l}, \bar{m}$ for Rossby Wave system

peaks which are sufficiently close to one another, and this will require further study.

Overall the numerical results appear to successfully verify the asymptotic results, and in the first two cases even give some quantitative agreement with the direct slow time model (2.17). What is clear from these trials is that in a continuous spectrum case, beyond the linear solution double resonances play a significant role in the spectral evolution. In the internal and Rossby wave cases, had more vertical modes been taken; there would simply be more such peaks, possibly even coupling with one another. This notion of coupled double resonances is interesting and certainly could arise, as for example is illustrated by Figure (1-1), the doubly resonant modes for various couplings can be quite close to one another. Although not the focus of the present study, this may provide an interesting avenue for future study.

2.4 Higher Order Nonlinearity

In many physical systems, quadratic nonlinearities giving rise to three wave interactions provide the dominant nonlinear effect. However, there are cases where triad

resonances do not exist. In these cases the dominant nonlinear effect becomes cubic or higher. An example of this is gravity waves on deep water, $\omega^2 = gk$, where no three wave resonances exist but four wave resonances do, corresponding to an effective cubic nonlinearity. This now motivates a more generalized version of the model equation introduced at the beginning of this chapter,

$$u_t + \mathcal{L}(u) = \epsilon \mathcal{N}_n(u) \ , \tag{2.27}$$

where $\mathcal{N}_n$ is an nth order nonlinear differential operator. Following similar analysis as before, in Fourier space this corresponds to:

$$A_t + i\omega(k)A = \epsilon \int H(k_1, k_2, ..., k_n)A(k_1)A(k_2)...A(k_n)\delta(k - \sum_{i=1}^{n} k_i)d^n\mathbf{k}, \tag{2.28}$$

where again ω is the linear dispersion relation, and now H is the interaction coefficient corresponding to the general nonlinearity. Again, the linear part can be eliminated:

$$a_t = \epsilon \int H(k_1, , k_2, ..., k_n)a(k_1)a(k_2)...a(k_n)e^{-i\Delta_n\omega(k,k_1,k_2,...,k_n)t}\delta(k - \sum_{i=1}^{n} k_i)d^n\mathbf{k} \ , \tag{2.29}$$

where $A(k,t) = a(k,t)e^{-i\omega(k)t}$ and $\Delta_n\omega(k, k_1, k_2, ..., k_n) = \sum_{i=1}^{n} \omega(k_i) - \omega(k)$ So now if one considers a perturbation series

$$a = a_0 + \epsilon a_1 + \epsilon^2 a_2 + ...$$

then to zeroth order, as before, a_0 is simply the initial spectral distribution. At first order (2.29) becomes,

$$a_{1_t} = \int H(k_1, k_2, ..., k_n)a_0(k_1)a_0(k_2)...a_0(k_n)e^{-i\Delta_n\omega(k,k_1,k_2,...,k_n)t}\delta(k - \sum_{i=1}^{n} k_i)d^n\mathbf{k} \ .$$

Again the dominant asymptotic contribution will come from the point of stationary phase, which once the delta function is removed from the integrand implies that *all*

the group velocities at each k_i must be equivalent,

$$\omega'(k_i) = \omega'(k_j) \qquad i,j = 1..n \ .$$

In general, should a solution, $\tilde{k}_i$, to these equations exist, the dominant contribution will be

$$a_{1_t} \approx C \frac{e^{-i\Delta_n \omega(k,\tilde{k}_1,\tilde{k}_2,...,\tilde{k}_n)t}}{t^{\frac{n-1}{2}}} \ ,$$

where C contains the constant factors. Then upon integration this gives

$$a_1 \approx C \int^t \frac{e^{-i\Delta_n \omega(k,\tilde{k}_1,\tilde{k}_2,...,\tilde{k}_n)s}}{s^{\frac{n-1}{2}}} ds \ .$$

Note the lower limit of integration is omitted since in this case there are now problems arising from the singularity at $s = 0$. The reason for this lies in the fact that the asymptotic analysis which gives the integrand is valid only for long times, and in fact near $s = 0$ is possibly not integrable.

There are now two possible cases. First if $n = 3$, then a substitution $s = e^v$ gives

$$a_1 \approx C \int^{\ln t} e^{-i\Delta_n \omega(k,\tilde{k}_1,\tilde{k}_2,...,\tilde{k}_n)e^v t} dv \ .$$

Second, if $n \geq 4$ then by a similar substitution as that used earlier, $s = v^{\frac{2}{3-n}} t$

$$a_1 \approx C t^{\frac{3-n}{2}} \int^1 e^{-i\Delta_n \omega(k,\tilde{k}_1,\tilde{k}_2,...,\tilde{k}_n)v^{\frac{2}{3-n}} t} dv \ ,$$

and therefore in both cases when there also is an n-wave resonance,

$$\Delta_n \omega(k, \tilde{k}_1, \tilde{k}_2, ..., \tilde{k}_n) = 0 \ ,$$

$$k = \sum_{i=1}^{n} \tilde{k}_i$$

this gives a leading order behavior

$$a_1 \approx O(t^{\frac{3-n}{2}}) \ .$$

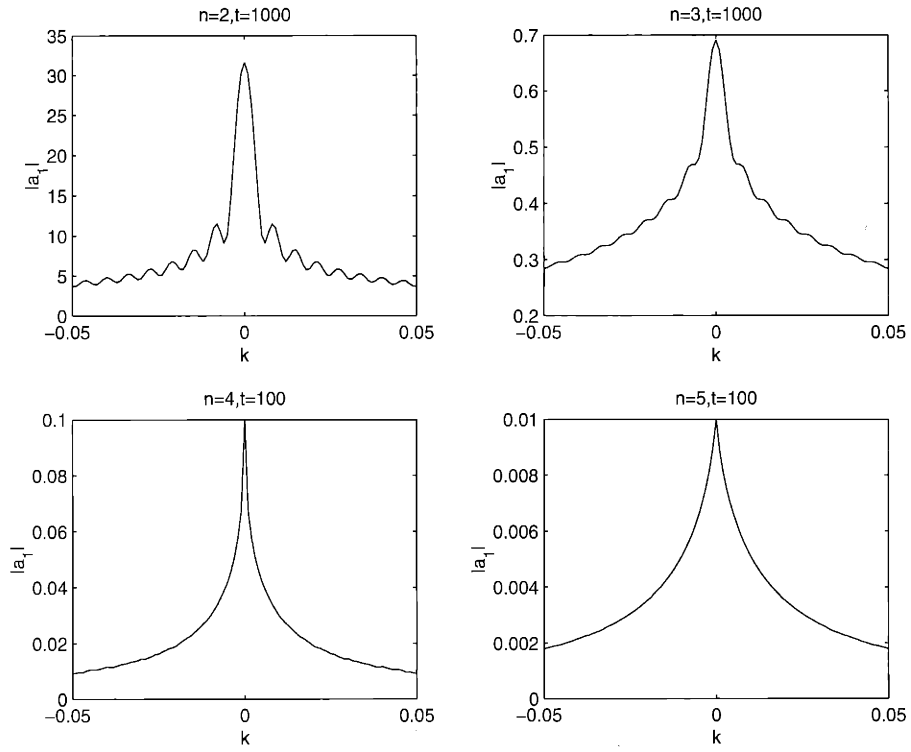

Figure 2-24: Peak structure for various degrees of nonlinearity. Without loss of generality $\bar{k} = 0$, $C = 1$ and $\Delta_n \omega = k$.

In general the structure around this resonant point will look the same as that for the $n = 2$ case, only now the width and height of the peak will scale accordingly. Figure 2-24 shows how the structure, and height of the peaks varies with the different nonlinearities. In particular, note that for $n > 3$ the ripple structure away from the peak disappears, and the peak itself takes on more of a cusp shape.

For $n > 2$ we expect no growth and thus no secularity of the terms. In fact in these cases, the $O(1)$ effects from the simple resonances may dominate and existing theory will be applicable. In other words the perturbation expansion will be well ordered. This emphasizes the uniqueness of the quadratic nonlinearity for continuous spectral distributions.

A readily available example of a higher order double resonance lies in the case of a higher order Wilton ripple type resonance. For example, Disp. 1 introduced earlier, possesses a solution

$$\omega(\bar{k}) = 3\omega\left(\frac{\bar{k}}{3}\right)$$

for $\bar{k} = 1.276$. This will trivially satisfy the group velocity criterion since the three

feeder modes are identical. Figure 2-25 shows a simulation using a cubic nonlinearity $(u^3)_x$ for this dispersion. Figure 2-26 shows a similar simulation using the gravity-capillary dispersion. Similarly Figure 2-27 is a simulation with a nonlinearity of $(u^4)_x$. In this case $\bar{k} = 1.49198$. Note that it is first of all clear that there is a distinct difference in the peak structure for the higher nonlinearities. In particular there is a confirmation of the smooth cusp like structure for $n = 4$ suggested by the analytical approximation above, and shown by a full numerical simulation in Figure 2-24. Moreover the $n = 4$ case also brings out the fact that there is also a resonance at $\bar{k} = 1.0246$, the resonant point for the quadratic nonlinearity. This represents a five wave resonance composed of three modes in the doubly resonant triad along with another copy of $\bar{l}$ and its conjugate. Lastly, note that these figures also bring out how higher the nonlinearities result in a weaker effect, as expected. To illustrate this further, Figure 2-28 shows a trace of the peak growth for various degrees of nonlinearity. Although there does appear to be growth (as opposed to decay for $n > 3$), it does suggest that the higher the nonlinearity, the slower the growth.

2.5 Higher Dimensional Equations

A second generalization of the model equation is to allow for higher dimensional dispersions. In other words we now consider our model equation in more than one spatial dimension

$$u_t + \mathcal{L}(u) = \epsilon \mathcal{N}(u), \tag{2.30}$$

where now $u = u(\mathbf{x}, t)$, $\mathbf{x}$ being an n dimensional vector. The analysis is again similar to before, only now the wave numbers are n-vectors as well.

$$a_t(\mathbf{k}, t) = \epsilon \int H(\mathbf{l}, \mathbf{k} - \mathbf{l}) a(\mathbf{l}) a(\mathbf{k} - \mathbf{l}) e^{-i\Delta\omega(\mathbf{k},\mathbf{l})t} d^n\mathbf{l}\,, \tag{2.31}$$

where $u(\mathbf{x}, t) = \int a(\mathbf{k}, t) e^{\mathbf{k}\cdot\mathbf{x} - i\omega(\mathbf{k})t} d^n\mathbf{k}$ and $\Delta\omega(\mathbf{k}, \mathbf{l}) = \omega(\mathbf{l}) + \omega(\mathbf{k} - \mathbf{l}) - \omega(\mathbf{k})$.

Again using a perturbation expansion, the zeroth order term will be constant

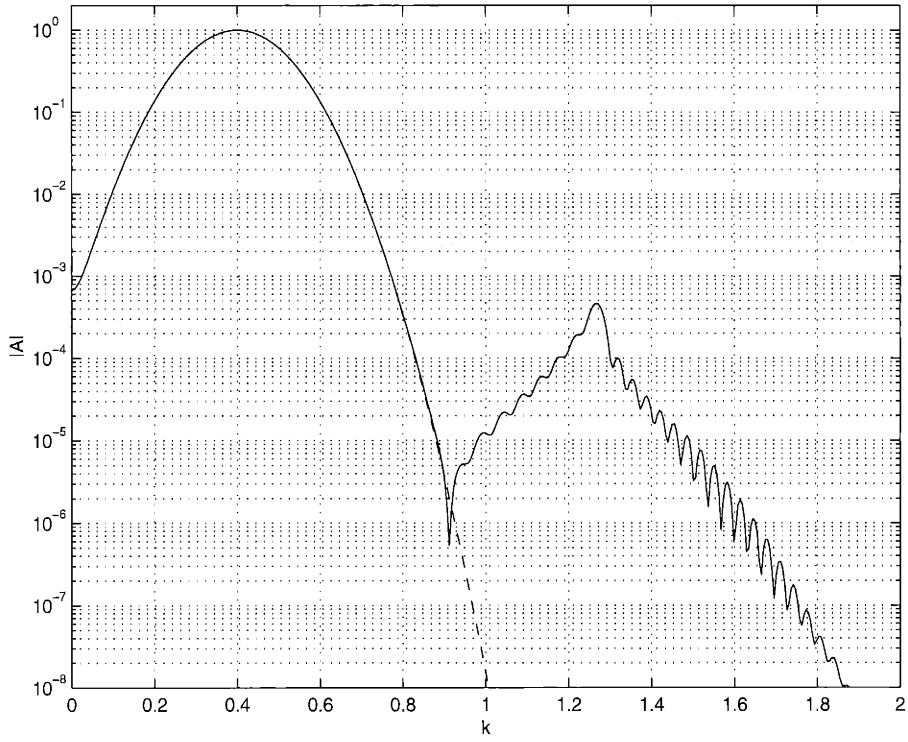

Figure 2-25: Spectral distribution for Disp. 1 at $t = 100$ for a cubic nonlinearity. Dashed line corresponds to initial spectral distribution. $\epsilon = .1$.

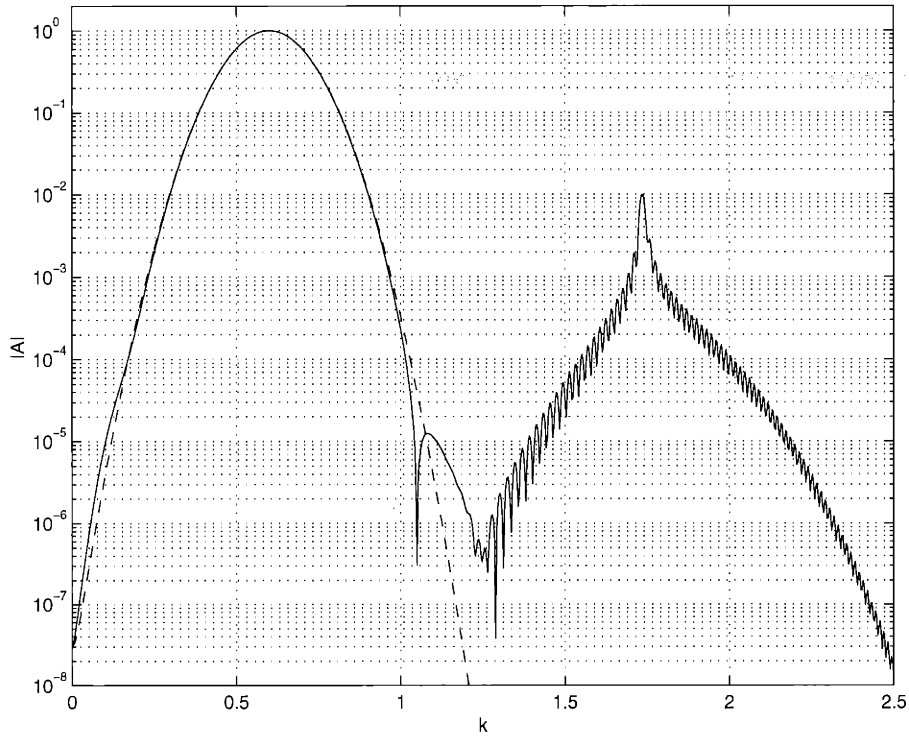

Figure 2-26: Spectral distribution for the gravity-capillary dispersion at $t = 500$ for a cubic nonlinearity. Dashed line corresponds to initial spectral distribution. $\epsilon = .1$.

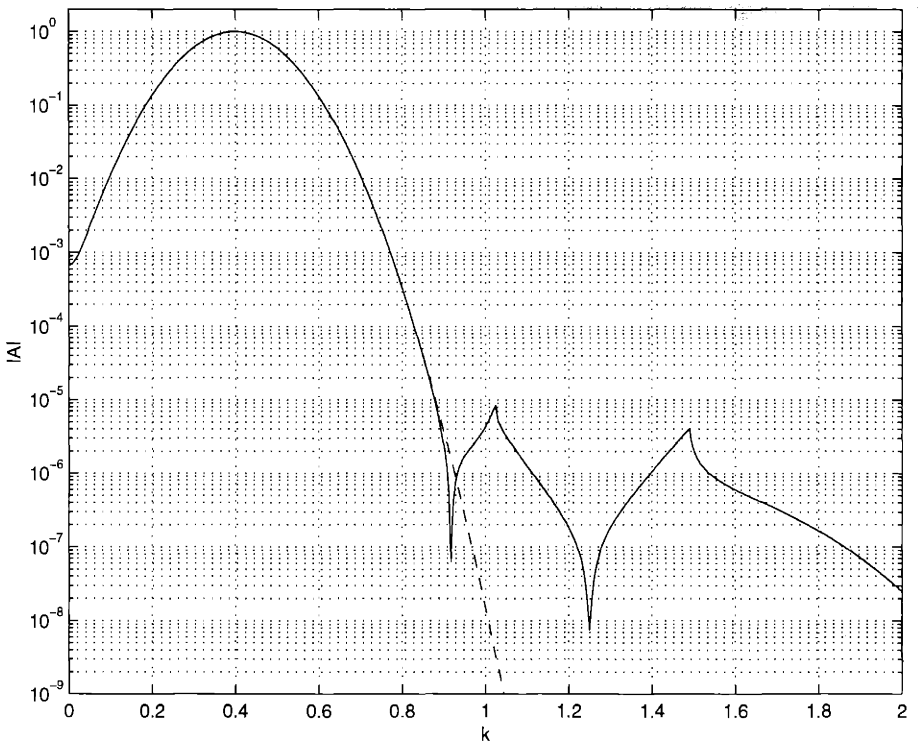

Figure 2-27: Spectral distribution for Disp. 1 at $t = 1000$ for a quadratic nonlinearity. Dashed line corresponds to initial spectral distribution. $\epsilon = .1$.

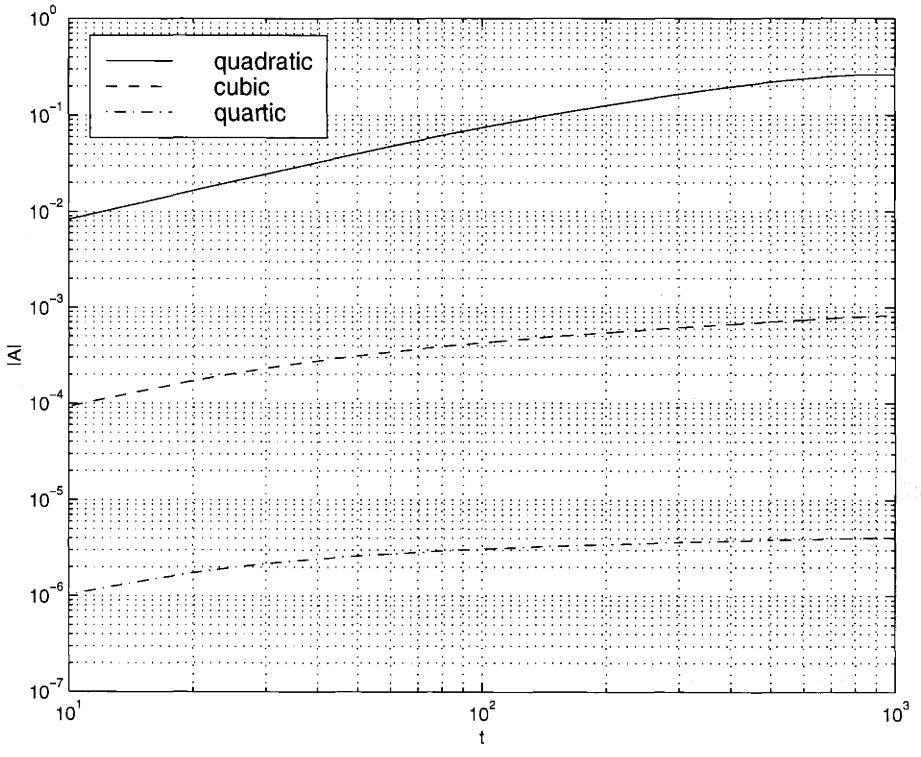

Figure 2-28: Trace of $|A(\bar{k})|$ for Disp.1 for three different nonlinearities $(u^2)_x$, $(u^3)_x$, and $(u^4)_x$.

while at first order

$$a_{1_t}(\mathbf{k},t) = \epsilon \int H(\mathbf{l},\mathbf{k}-\mathbf{l})a_0(\mathbf{l})a_0(\mathbf{k}-\mathbf{l})e^{-i\Delta\omega(\mathbf{k},\mathbf{l})t}d^n\mathbf{l}\,. \tag{2.32}$$

Now the stationary phase condition will take the form

$$\nabla_{\mathbf{l}}\Delta\omega(\mathbf{k},\tilde{\mathbf{l}}) = 0\,,$$

where $\nabla_{\mathbf{l}}$ corresponds to the gradient with respect to the components of $\mathbf{l}$. In other words the group velocities in each direction of the modes $\mathbf{l}$ and $\mathbf{k}-\mathbf{l}$ are equal. At vectors $\tilde{\mathbf{l}}$ where this is the case, the contribution will be

$$a_{1_t} \approx C\frac{e^{-i\Delta\omega(\mathbf{k},\tilde{\mathbf{l}})t}}{t^{\frac{n}{2}}}\,.$$

Then around a point where there is a triad resonance

$$\Delta\omega(\mathbf{k},\tilde{\mathbf{l}}) = 0\,,$$

the contribution to a_1 takes the form

$$a_1 \approx O(t^{\frac{2-n}{2}})\,.$$

Note that for $n \geq 2$ this system of double resonance relations is under determined. There are n equations from the group velocity relation, n equations from the wave number relation, and then 1 from the frequency relation giving $2n+1$ equations for $3n$ unknowns. This means that for higher dimensions there will in general be a continuum of doubly resonant points. On the other hand the asymptotics suggest that in higher dimensions the growth will be less pronounced as there will then be extra factors of $\frac{1}{\sqrt{t}}$ from each extra dimension. Does this mean that double resonances will only be "seen" in the 1-D case? To investigate this, Figure 2-29 shows the result

of a run using a 2-D version of Disp. 1.

$$\omega(\mathbf{k}) = \tanh(.25|\mathbf{k}| + 3.125|\mathbf{k}|) \ ,$$

with an initial condition

$$a_0(k,l) = (e^{-50(k-.6)^2} + e^{-50(k+.6)^2})e^{i50k} \ .$$

In this case the resolution must necessarily be lower (2^{10} modes in each direction) limiting the maximum computation time. But even with this constraint the figure brings out how at $l = 0$ the double resonance at $\bar{k} = 1.0246$ is clear. Moreover there is now a circle of doubly resonant points corresponding to the now isotropic nature of the dispersion relation. To obtain an idea of the growth of the peak, a comparison was made of this case to the 1D case with the same parameters. Figure 2-30 shows that indeed the growth of the doubly resonant mode is diminished when a second dimension is introduced. This then begs the question, how two dimensional does the system need to be for this effect to be felt? The answer lies in a careful study of the stationary phase analysis. In particular a truly one dimensional spectral distribution corresponds to, in the 2D case for instance, $a(\mathbf{k}) = a(k_1)\delta(k_2)$ where k_i are the components of the wavenumber vector. When this is substituted into (2.31) it reduces to (2.3) as would be expected. Stationary phase can only be applied in the second dimension provided the variation of the integrand is sufficiently small. Thus as the second dimension is introduced, the full extra factor of $\frac{1}{\sqrt{t}}$ is only present once there is enough structure in the second dimension to sufficiently broaden the delta function beyond the rapid oscillations of the rest of the integrand.

2.6 General Dimension and Nonlinearity

Having discussed the separate cases of higher order nonlinearity and higher dimensions, a combination of the two will be considered. Specifically the general case of an

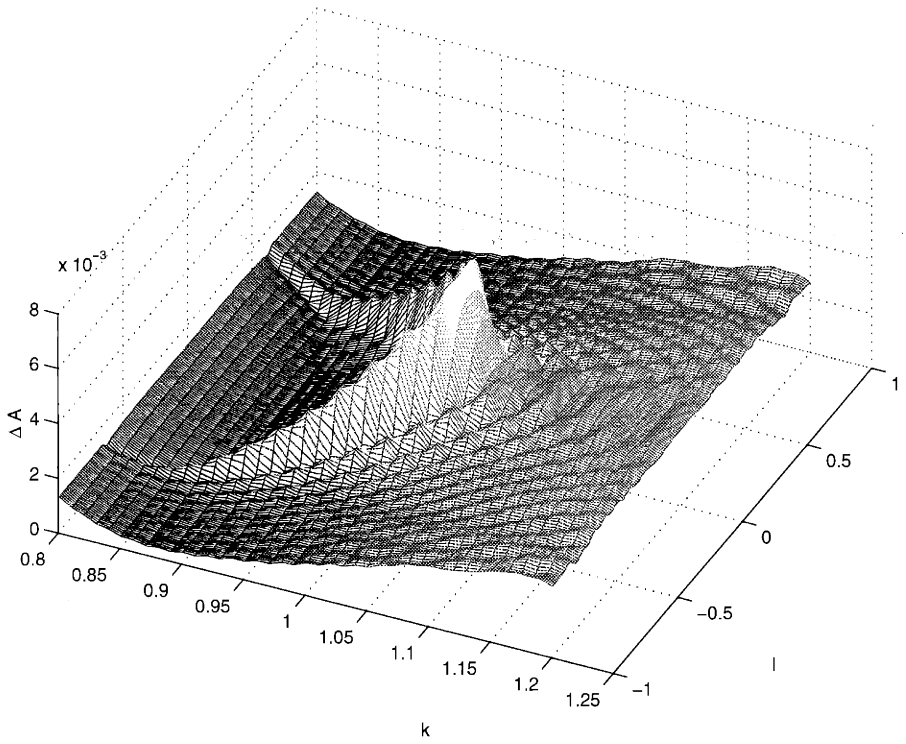

Figure 2-29: Spectral distribution for run using a 2-D dispersion relation at $t = 100$.

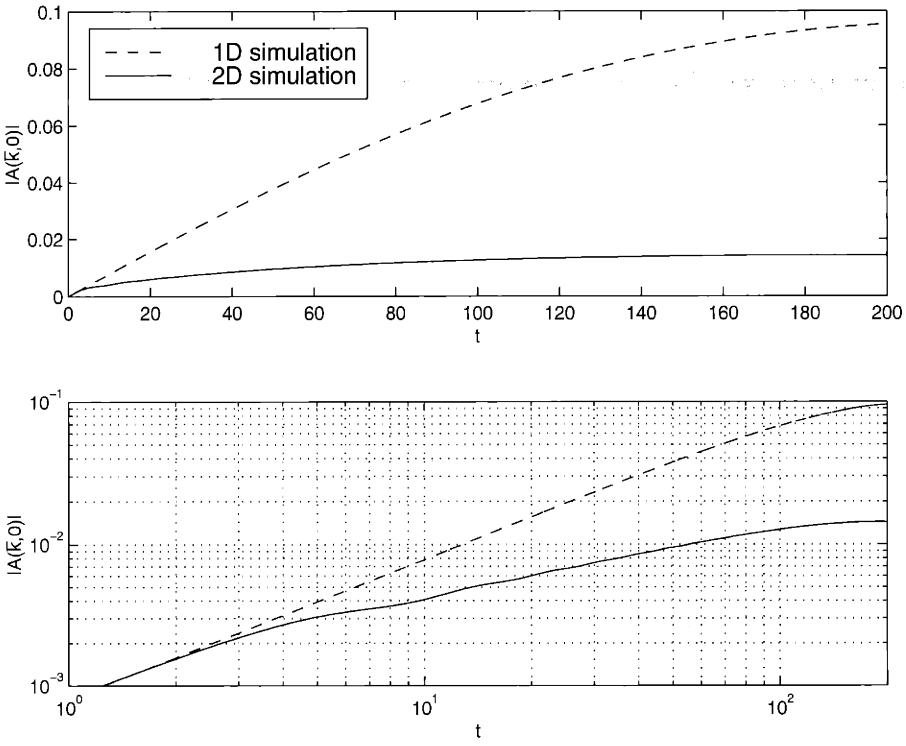

Figure 2-30: Comparison of peak height at $(\bar{k}, 0)$ for Disp.1

nth order nonlinearity in m dimensions. The model equation remains the same

$$u_t + \mathcal{L}(u) = \epsilon \mathcal{N}_n(u) \ , \tag{2.33}$$

only now $u = u(\mathbf{x}, t)$ where $\mathbf{x}$ is taken to be an m dimensional vector. This then corresponds in Fourier space to

$$a_t = \epsilon \int H(\mathbf{k}_1, , \mathbf{k}_2, ..., \mathbf{k}_n) a(\mathbf{k}_1) a(\mathbf{k}_2) ... a(\mathbf{k}_n) e^{-i\Delta_n \omega(\mathbf{k}, \mathbf{k}_1, \mathbf{k}_2, ..., \mathbf{k}_n)t} \delta(\mathbf{k} - \sum_{i=1}^{n} \mathbf{k}_i) d^m \mathbf{k}_\mathbf{i} \ . \tag{2.34}$$

The subsequent perturbation analysis is identical to the above discussions. The key factor in order to obtain an estimate of the leading order behavior, is the phase function

$$\Delta_n \omega(\mathbf{k}, \mathbf{k}_1, \mathbf{k}_2, ..., \mathbf{k}_{n-1}, \mathbf{k} - \sum_{i=1}^{n-1} \mathbf{k}_i) \ ,$$

where $\mathbf{k}_n$ has been chosen so that the delta function (wavenumber condition) has been automatically satisfied. This leaves n arbitrary vectors with m components, for a total of mn unknowns. The stationary phase integral is taken over $n-1$ of these vector components. The criterion for stationary phase is now

$$\nabla \omega(\mathbf{k}_j) = \nabla \omega(\mathbf{k} - \sum_{i=1}^{n-1} \mathbf{k}_i) \qquad\qquad j = 1...n-1 \ ,$$

meaning that all components of the group velocity for the now n feeder modes are equal. This when combined with the frequency criterion

$$\Delta_n \omega(\mathbf{k}, \mathbf{k}_1, \mathbf{k}_2, ..., \mathbf{k}_{n-1}, \mathbf{k} - \sum_{i=1}^{n-1} \mathbf{k}_i) = 0 \ ,$$

gives a total of $m(n-1)+1 = mn - m + 1$ equations. Meaning there are $m-1$ free parameters, *or* alternatively there are $m-1$ more equations which could be chosen for the wavenumbers to satisfy. This second option leads to an interesting possibility. Specifically one can then begin to satisfy some higher order stationary phase criteria involving the second derivatives of the phase functions. With both the constant and

linear terms of the expansion of the phase now rendered zero by the above conditions the next term in the expansion involves the Hessian matrix A where

$$A_{ij} = \frac{d}{dk_i dk_j}\Delta_n\omega(\mathbf{k}, \mathbf{k}_1, \mathbf{k}_2, ..., \mathbf{k}_{n-1}, \mathbf{k} - \sum_{i=1}^{n-1}\mathbf{k}_i) \qquad i, j = 1..m(n-1) \ ,$$

the derivatives being taken over each of the m components of the $n-1$ vectors involved in the integration. Typically if this matrix is non-singular, then the resulting stationary phase integral will contribute a factor of $\frac{1}{\sqrt{t}}$ for each component of the integral, meaning that with only the wavenumber, frequency and group velocity conditions satisfied,

$$a_{1_t} \approx O(\frac{1}{t^{\frac{m(n-1)}{2}}}) \ ,$$

so that to leading order

$$a_1 \approx O(t^{\frac{m-mn+2}{2}}) \ .$$

A degeneracy will occur if $\mathrm{Det}(A) = 0$ and for each dimension for which this matrix is rank deficient, the corresponding contribution to the stationary phase integral is now $\frac{1}{\sqrt[3]{t}}$ [22]. This then means that if the $m-1$ free parameters are used to render the rank of A to be $m(n-1)-(m-1) = mn-2m+1$ then the corresponding leading order behavior will now be

$$a_{1_t} \approx O(\frac{1}{t^{\frac{mn-2m+1}{2}+\frac{m-1}{3}}}) \ ,$$

so that

$$a_1 \approx O(t^{\frac{2m}{3}-\frac{mn}{2}+\frac{5}{6}}) \ .$$

In particular, of interest are any possible values of $n \geq 2$ and $m \geq 1$ where this exponent is positive since regardless of dimension or nonlinearity, simple resonances will have an $O(1)$ contribution. Table 2.1 shows some possible values of this exponent, and in particular along with the doubly resonant triad case $(m, n) = (1, 2)$ that has been investigated, a positive exponent is encountered for $(m, n) = (2, 2)$. This corresponds to a case where there is a quadratic nonlinearity in two dimensions. And

m	n	$\frac{2m}{3} - \frac{mn}{2} + \frac{5}{6}$
1	2	$\frac{1}{2}$
2	2	$\frac{1}{6}$
3	2	$-\frac{1}{6}$
1	3	0
2	3	$-\frac{5}{6}$
3	3	$-\frac{5}{3}$

Table 2.1: Leading order exponents for various dimensions m and nonlinearities n.

in particular when there are modes $\bar{\mathbf{k}}$ and $\bar{\mathbf{l}}$ such that

$$\omega(\bar{\mathbf{l}}) + \omega(\bar{\mathbf{k}} - \bar{\mathbf{l}}) - \omega(\bar{\mathbf{k}}) = 0 \,,$$

$$\nabla\omega(\bar{\mathbf{l}}) = \nabla\omega(\bar{\mathbf{k}} - \bar{\mathbf{l}})$$

$$\Big(\omega_{11}(\bar{\mathbf{l}}) + \omega_{11}(\bar{\mathbf{k}} - \bar{\mathbf{l}})\Big)\Big(\omega_{22}(\bar{\mathbf{l}}) + \omega_{22}(\bar{\mathbf{k}} - \bar{\mathbf{l}})\Big) - \Big(\omega_{12}(\bar{\mathbf{l}}) + \omega_{12}(\bar{\mathbf{k}} - \bar{\mathbf{l}})\Big)^2 = 0$$

which compose four equations for the four unknown components. The numerical subscripts represent derivatives with respect to the particular component of the vector. Examples of dispersion relations containing points satisfying these conditions although not overly abundant, are also not difficult to find. One such example, in some ways a generalized version of the artificial dispersions introduced earlier, is

$$\omega(\mathbf{k}) = \tanh\left(.4k_1 + .5k_2 + .7k_1^3 + .6k_2^3\right)$$

This has a generalized double resonance at $\bar{\mathbf{k}} = (1.25874, .400524)$, $\bar{\mathbf{l}} = \frac{\bar{\mathbf{k}}}{2}$. Figure 2-31 shows the result of a run using this dispersion relation, a nonlinearity of $(u^2)_x$, and initial condition of

$$A(\mathbf{k}, 0) = e^{-50(k_1-.6)^2}e^{-50(k_2-.2)^2} + e{-}50(k_1 + .6)^2e^{-50(k_2+.2)^2} \,.$$

In particular the figure gives a clear picture of a 2 dimensional version of a doubly resonant peak. Indeed it is located at $\bar{\mathbf{k}}$ and Figure 2-32 shows how this peak grows

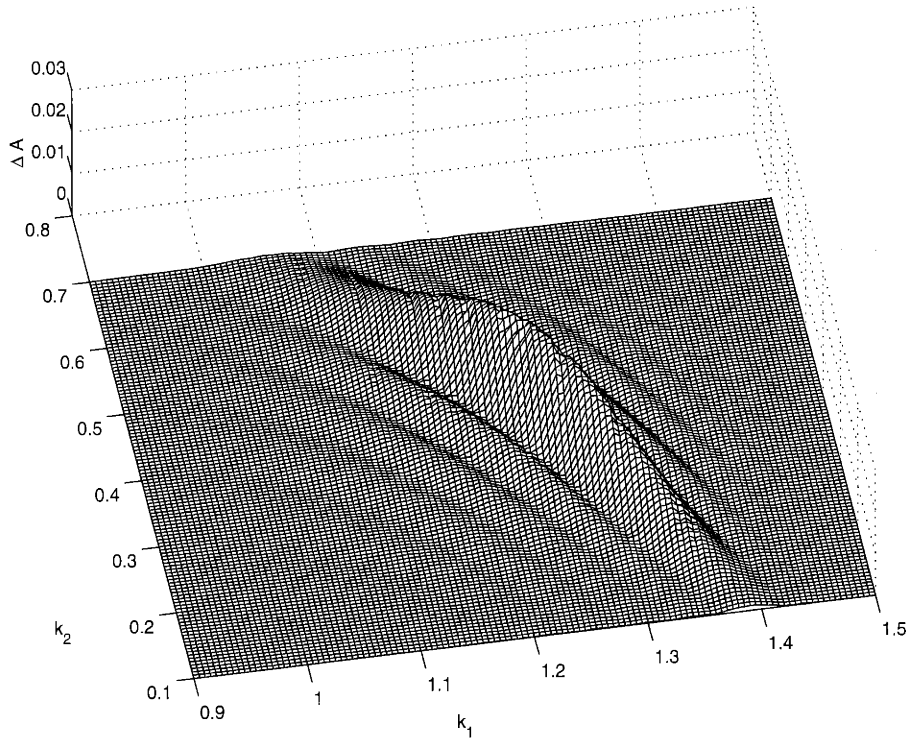

Figure 2-31: Spectral distribution near doubly resonant mode for generalized double resonance at $t = 200$.

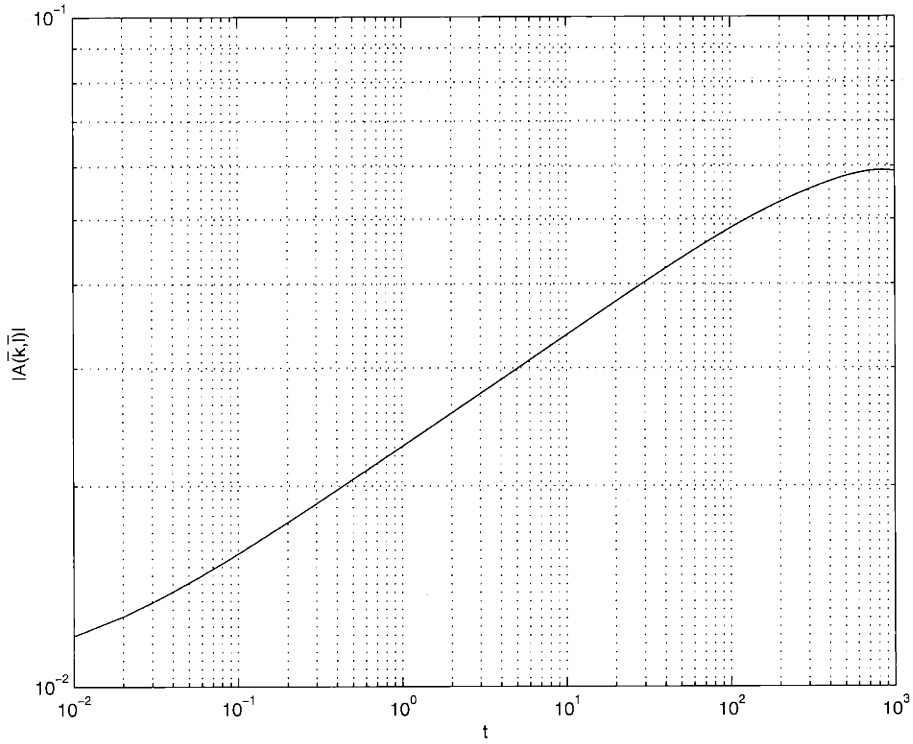

Figure 2-32: Growth of doubly resonant peak for 2D simulation.

in time, and indeed the growth is slowed to roughly $O(\sqrt[6]{t})$.

The results presented in this chapter provide clear evidence that the three wave problem behaves in a very different fashion when the spectral distribution is continuous as opposed to discrete. In particular, without the additional resonance criteria, no modal growth will occur. But when a double resonance does occur, the governing equations for the three modes (2.17) are similar to the classical three wave system (1.15). Key differences being a time scale for growth of $\epsilon\sqrt{t}$ as opposed to ϵt and the inclusion of a parameter for modes away from exact resonance. The effects of double resonances appear to be robust, occurring for a wide range of dispersions, and each time with a qualitatively similar peak structure around the doubly resonant mode. The following chapter will attempt to investigate further the differences between the continuous and discrete cases, attempting to find a link between the two.

Chapter 3

The Three Wave Problem: Discrete Spectrum

As it was shown in the previous chapter, there is clearly a dramatic difference in the evolution of a three wave system when the spectrum is assumed continuous as opposed to discrete. Is there a middle-ground? This chapter will attempt to investigate this question. Perhaps a modification of the traditional discrete three wave system will serve to bridge the gap between these two cases.

Recall from Chapter 1, a multiple scales analysis yields a system of the form

$$\begin{aligned}
\mu A_T + \mu C_g(\bar{k}) A_X - i\frac{\mu^2}{2}\frac{d^2\omega(\bar{k})}{dk^2} A_{XX} + O(\mu^3) &= \epsilon\gamma_1 BC + O(\epsilon^2, \epsilon\mu)\ , \\
\mu B_T + \mu C_g(\bar{l}) B_X - i\frac{\mu^2}{2}\frac{d^2\omega(\bar{l})}{dk^2} B_{XX} + O(\mu^3) &= \epsilon\gamma_2 AC^* + O(\epsilon^2, \epsilon\mu)\ , \quad (3.1) \\
\mu C_T + \mu C_g(\bar{m}) C_X - i\frac{\mu^2}{2}\frac{d^2\omega(\bar{m})}{dk^2} C_{XX} + O(\mu^3) &= \epsilon\gamma_3 AB^* + O(\epsilon^2, \epsilon\mu)\ ,
\end{aligned}$$

where μ represents the spatial scaling parameter for the long space coordinate X and long time T, while ϵ is a measure of the nonlinearity. It is understood that A, B, C represent the Fourier amplitudes at the wavenumbers of the members of the triad k_1, k_2, k_3 respectively. Traditionally the $O(\mu^2)$ terms are dropped and a balance is struck between the $O(\mu)$ and $O(\epsilon)$ terms. In this case solutions are well known. A brief discussion of these will first be given.

3.1 The Classical Three Wave Problem

For a simple triad resonance, it has been shown that the evolution equations for the amplitude of the three modes involve taking (3.1) where the higher order terms of $O(\mu^2)$ are dropped. This system has been well studied, a comprehensive summary is presented by Craik [10]. A re-scaling of the dependent variables reduces the system to the more canonical form

$$\begin{aligned} A_T + c_1 A_X &= s_1 BC \,, \\ B_T + c_2 B_X &= s_2 AC^* \,, \\ C_T + c_3 C_X &= s_3 AB^* \,, \end{aligned} \tag{3.2}$$

where $s_1, s_2, s_3 = \pm 1$, and where the wavenumbers satisfy the conditions for a simple three wave resonance

$$k_1 = k_2 + k_3 \qquad \omega(k_1) = \omega(k_2) + \omega(k_3)$$

Solutions of this system are well known. In the spatially independent case, conservation laws can be derived and the system integrated to give solutions in terms of Jacobi Elliptic functions. The spatially dependent case is more complicated but has been shown to be integrable via the Inverse Scattering Technique [16]. For s_j of all the same sign, the solutions become singular in finite time, but for s_j of differing signs, the solutions remain bounded. But it should be pointed out that *a priori* it is assumed in the Inverse Scattering argument that the group velocities are all distinct, and in fact the argument depends on this fact. This is illustrated by the form of the solutions and specifically they will be singular should any two of c_1, c_2, c_3 be equal. To investigate this breakdown we note that supposing that, say, $c_2 = c_3$, (3.2) becomes

$$\begin{aligned} A_T + c_1 A_X &= s_1 BC \\ B_T + c_2 B_X &= s_2 AC^* \\ C_T + c_2 C_X &= s_3 AB^* \end{aligned} \tag{3.3}$$

In the following section a new system of equations is proposed, a more generalized system which will hopefully provide some connection between the effects seen in the continuous and discrete analysis.

3.2 A More Generalized Three Wave System

As discussed in the previous section, it appears that in the case where two of the three group velocities are equal, (3.2) exhibits dramatically different behavior. A loose justification of this can be seen by noting that if a Galilean transformation is made such that $X \to X - c_2 T$ then the spatial dependence of the second two equations is lost. This suggests that in these two equations the higher order derivative terms may be significant and should not have been dropped. In other words, consider the more generalized system

$$\begin{aligned} A_T + c_1 A_X &= \gamma_1 BC \\ B_T + c_2 B_X + i d_2 B_{XX} &= \gamma_2 AC^* \\ C_T + c_2 C_X + i d_3 C_{XX} &= \gamma_3 AB^* \end{aligned} \tag{3.4}$$

It is hoped that the addition of second order terms will serve to bring about similar effects to those seen in the continuous treatment. Comparison with (1.15), the full system derived earlier, shows that the constants can be thought of as representing the appropriate derivatives of the dispersion relation, or interaction coefficients, along with the scaling parameters.

To obtain a general solution of (3.4) via techniques such as Inverse Scattering is now likely somewhat optimistic, but numerical simulation along with some analytic analysis where possible does give some good insight into this system and the effect of

the additional terms. To begin, it is first helpful to consider a slightly simplified case where it assumed that $B = C$. Physically, this is analogous to the case of Wilton's ripples, where two of the modes are exactly the same. In other words $\bar{l} = \bar{m} = \bar{k}/2$.

3.2.1 The Wilton's ripple case

Assuming modes B and C are identical, (3.4) now reduces to a system of the form

$$\begin{aligned} A_T + c_1 A_X &= \gamma_1 B^2 \\ B_T + c_2 B_X + i d_2 B_{XX} &= \gamma_2 A B^* \end{aligned}$$

Without loss of generality, a Galilean transformation can be made to eliminate c_1, and leave us with the system

$$\begin{aligned} A_T &= \gamma_1 B^2 \\ B_T + c_2 B_X + i d_2 B_{XX} &= \gamma_2 A B^* \end{aligned} \tag{3.5}$$

Which can be quickly reduced to a single equation by eliminating A

$$\left(\frac{B_T + c_2 B_X + i d_2 B_{XX}}{B^*} \right)_T = \gamma_1 \gamma_2 B^2 \tag{3.6}$$

Using a combination of analytic and numerical techniques, this system will now be analyzed with emphasis on the effect of the presence of the d_2 term.

Normal Mode Solutions and their Stability

To begin, it is instructive to consider the presence of normal mode solutions. i.e. solutions of the form

$$B = B_0 e^{i(kx - \omega t)}$$

Substituting this into (3.6) it can be shown that such solutions exist provided

$$\omega = \frac{(d_2k^2 - c_2k) \pm \sqrt{(d_2k^2 - c_2k)^2 - 2\gamma_1\gamma_2}}{2}$$

In particular it is interesting to consider the possibility that ω be complex. In other words the solution will exhibit unbounded growth. This "instability" is only possible if $\gamma_1\gamma_2 > 0$, which remains consistent with previous analysis of the three wave system where explosive growth has been found to occur when all interaction coefficients are of the same sign. Assuming that $\gamma_1\gamma_2 > 0$ and also without loss of generality that $c_2 > 0$, it is clear that if $d_2 = 0$ then explosive growth occurs for

$$-\frac{\sqrt{2\gamma_1\gamma_2}}{c_2} < k < \frac{\sqrt{2\gamma_1\gamma_2}}{c_2}$$

The next order correction to this for d_2 nonzero but small is

$$-\frac{\sqrt{2\gamma_1\gamma_2}}{c_2} + \frac{2\gamma_1\gamma_2 d_2}{c_2^3} + O(d_2^2) < k < \frac{\sqrt{2\gamma_1\gamma_2}}{c_2} + \frac{2\gamma_1\gamma_2 d_2}{c_2^3} + O(d_2^2)$$

which shows that this window of instability is shifted by the presence of d_2 giving some insight as to the effect of this added term.

Perturbation around known non-periodic Wilton Ripple Solution

To further grasp the impact of the higher order dispersive term suppose it is now imposed that $d_2 = O(\epsilon)$. In other words (3.6) takes the form:

$$\left(\frac{B_T + c_2B_X + i\epsilon d_2 B_{XX}}{B^*}\right)_T = \gamma_1\gamma_2 B^2 \tag{3.7}$$

Then applying an analysis similar to that of Whitham [20], by introducing a fast phase coordinate θ, and slow time and space coordinates $\tau = \epsilon T, \chi = \epsilon X$ such that

$$\theta_T = -\omega(\chi, \tau) \qquad \theta_X = k(\chi, \tau)\ ,$$

then by introducing an expansion

$$B = B_0(\theta, \chi, \tau) + \epsilon B_1(\theta, \chi, \tau)$$

to zeroth order in ϵ, (3.7) reduces to:

$$(\omega^2 - c_2\omega k)(B_0 B_{0_{\theta\theta}} - B_{0_\theta}^2) = |B|^4 \ ,$$

for which there is a solution [10]

$$B_0 = \alpha(\chi, \tau)\mathrm{sech}\theta$$

with a corresponding dispersion relation

$$\omega^2 - c_2\omega k + \alpha^2 = 0 \ .$$

In order to determine the slow time and space variation of θ as well as the effect of the extra dispersive term, the next order must be considered. At this order the solution can be shown to be

$$B_1 = i\frac{d_2\omega k^2}{\alpha}\tanh\theta\mathrm{sech}\theta$$

with

$$\omega_\tau + c_2\omega_\chi = 0 \ .$$

At the next order, a further secularity condition gives an equation for the evolution of α

$$-\alpha_{\tau\tau} - c_2\alpha_{\chi\tau} + \frac{\alpha_\tau^2}{\alpha} + c_2\frac{\alpha_\chi\alpha_\tau}{\alpha} = 0 \ .$$

These results give more insight into how the added dispersive term effects this solution. Not surprisingly the first order correction depends on the value of d_2, but what is somewhat surprising is that it does not enter into the slow time and space evolution of the phase or amplitude of the zeroth order solution. This suggests that although the added dispersive term leads to higher order corrections in the solution,

the more global evolution of the phase and amplitude, at least to leading order, remain unaffected.

Craik [11] gives a more general class of "multiple-lump" solutions to the zeroth order system around which one may perturb and carry out a similar analysis. Although such analysis may be more general than that presented above, there is qualitatively no difference in the effect of the added dispersive term. This is not entirely unexpected as away from the lumps themselves the system becomes approximately linear.

Perturbation in Weakly Nonlinear case

A second regime which allows some analytic analysis is one closer to that of the three wave system (1.15). In particular one must be aware of the relative sizes of the coefficients. Note that when compared to the this system the coefficients in (3.4) c_1 and c_2 are $O(1)$, d_2 and d_3 are $O(\mu)$ and γ_1, γ_2 and γ_3 are $O(\frac{\epsilon}{\mu})$. This suggests that if the scaling parameter is chosen so that $\mu = O(\sqrt{\epsilon})$ then the effects of the nonlinearity will be balanced by the second order dispersive terms.

Under this scaling, (3.5) now becomes

$$A_T = \epsilon\gamma_1 B^2 \tag{3.8}$$

$$B_T + c_2 B_X + i\epsilon^2 d_2 B_{XX} = \epsilon\gamma_2 A B^* \tag{3.9}$$

where all coefficients are now assumed to be $O(1)$. For simplicity a coordinate change

$$s = T - \frac{X}{c_2}$$

$$r = \frac{X}{c_2}$$

is made so that (3.8) now becomes

$$\begin{aligned} A_s &= \epsilon\gamma_1 B^2 \\ B_r + i\epsilon^2 \frac{d_2}{c_2^2}(B_{ss} - 2B_{sr} + B_{rr}) &= \epsilon\gamma_2 AB^* \end{aligned} \tag{3.10}$$

Eliminating A as before yields

$$\left(\frac{B_r + i\epsilon^2 \frac{d_2}{c_2^2}(B_{ss} - 2B_{sr} + B_{rr})}{B^*} \right)_s = \epsilon^2 \gamma_1 \gamma_2 B^2 \tag{3.11}$$

Now introducing the perturbation expansion

$$A(r,s) = A_0(r,s) + \epsilon^2 A_1(r,s) + ...$$

$$B(r,s) = B_0(r,s) + \epsilon^2 B_1(r,s) + ...$$

it is clear that at $O(1)$

$$A_{0_s} = 0 \qquad \Rightarrow \qquad A_0 = A_0(r) = A_0(\frac{X}{c_2})$$

$$B_{0_r} = 0 \qquad \Rightarrow \qquad B_0 = B_0(s) = B_0(T - \frac{X}{c_2})$$

Introducing a slow time coordinate $\tau = \epsilon^2 t$ so that $B_0 = B_0(\tau, s)$ and then at $O(\epsilon^2)$ of (3.11)

$$\frac{d^2}{drds}\left(\frac{B_1}{B_0^*}\right) + \left(\frac{B_{0_\tau}}{B_0^*}\right)_s = -\frac{id_2}{c_2^2}\left(\frac{B_{0_{ss}}}{B_0^*}\right)_s + \gamma_1\gamma_2 B_0^2$$

This can be immediately integrated in r since B_0 is independent of this coordinate. On doing so, this indicates that B_1 will grow linearly in r. In order to avoid this secularity, we obtain the following relation for the slow evolution of B_0:

$$\left(\frac{B_{0_\tau}}{B_0^*}\right)_s = -\frac{id_2}{c_2^2}\left(\frac{B_{0_{ss}}}{B_0^*}\right)_s + \gamma_1\gamma_2 B_0^2 \,. \tag{3.12}$$

In general this is a nonlinear PDE governing the slow evolution of the amplitude function, which as opposed to the strongly nonlinear case above, does indeed contain a dependence on d_2. Although in general not obviously integrable, some information

can be obtained by considering the stability of normal mode solutions in the same way as is done on equations such as the Nonlinear Schrödinger Equation [10].

It can be shown that $B_0 = Be^{i(\mu s+(\frac{d_2}{c_2^2}\mu^2+\frac{B^2}{2\mu}))}$ solves (3.12). Then linearizing around this solution by substituting $B_0 = (B+b_+e^{i(\lambda s+\sigma\tau)}+b_-e^{-i(\lambda s+\sigma^*\tau)})e^{i(\mu s+(\frac{d_2}{c_2^2}\mu^2+\frac{B^2}{2\mu}))}$ into (3.12) and keeping all terms linear in b_+ and b_-. σ remains real provided that

$$\Delta = \frac{d^2}{c^4}\mu^2\lambda^6 - (8\frac{d^2}{c^4}\mu^4 - \gamma_1\gamma_2B^2\frac{d}{c^2}\mu)\lambda^4 + 16\frac{d^2}{c^4}\mu^6\lambda^2 + 4\gamma_1^2\gamma_2^2B^4\mu^2 - 16\gamma_1\gamma_2B^2\mu^5\frac{d}{c^2} > 0 \tag{3.13}$$

This then gives a stability criterion for all values of λ for a given normal mode solution with wavenumber μ. In particular for a given μ one can predict which modes will exhibit the most growth.

Figure 3-1 shows an example of the stability region. One noteworthy point is

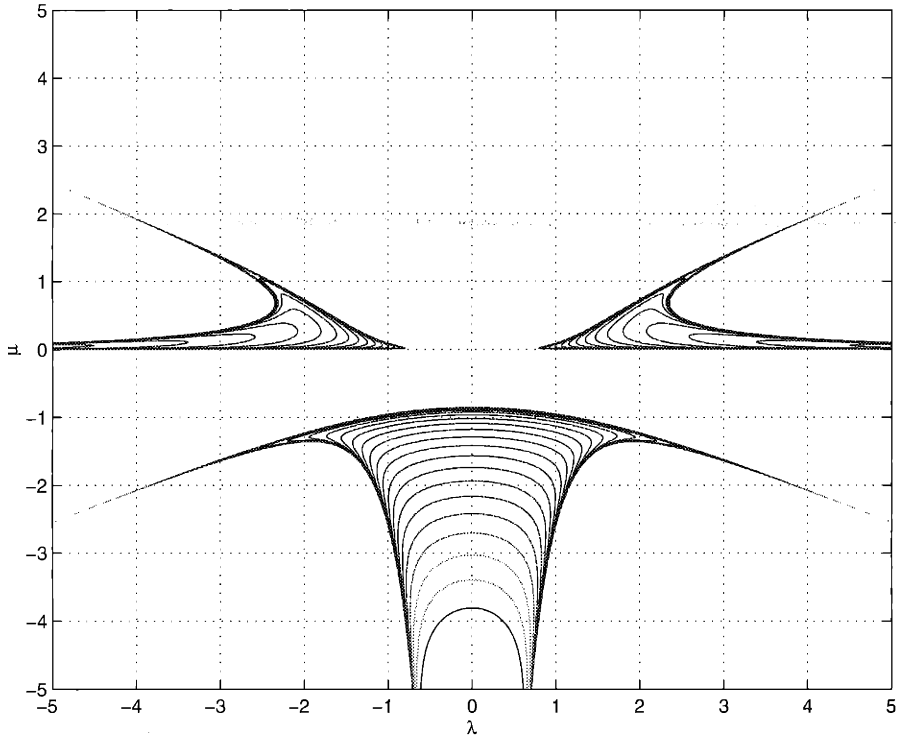

Figure 3-1: Normal mode stability for Wilton's ripple with $B = 1$, $d_2 = .1$,$\gamma_1\gamma_2 = -1$ and $c_2 = .5$. Contours indicate region of instability.

that for a range of values of μ, the region of instability includes arbitrarily small values of λ. This suggests that the normal modes are unstable to perturbations from

modes arbitrarily close to that of the underlying wave train. This is analogous to the Benjamin-Fier instability [3] where growth of sideband modes render a wave train on deep water unstable.

To illustrate this further Figure 3-2 shows the spectral evolution of B after a numerical simulation of the full system (3.6). Clearly there is a sideband growth, the peaks corresponding to a detuning of roughly $\lambda = 1.5$. To compare to the analytic prediction, Figure 3-3 shows the value of Δ in this parameter regime, indicating that maximum growth occurs at the minimum at $\lambda \approx 2$, giving reasonable agreement to the numerical simulation.

3.2.2 The General Case

Having now investigated the case of the Wilton's ripple, where $B = C$, the focus now will turn to the full system (3.4)

$$\begin{aligned} A_T + c_1 A_X &= \gamma_1 BC \\ B_T + c_2 B_X + i d_2 B_{XX} &= \gamma_2 AC^* \\ C_T + c_2 C_X + i d_3 C_{XX} &= \gamma_3 AB^* \end{aligned}$$

again, with the key question being the effect of the higher order dispersive terms. To begin, a similar analysis to the Wilton's ripple can be made in the weakly nonlinear regime where d_2, d_3 are small.

Weakly Nonlinear case

Consider (3.4) in the following scaling regime

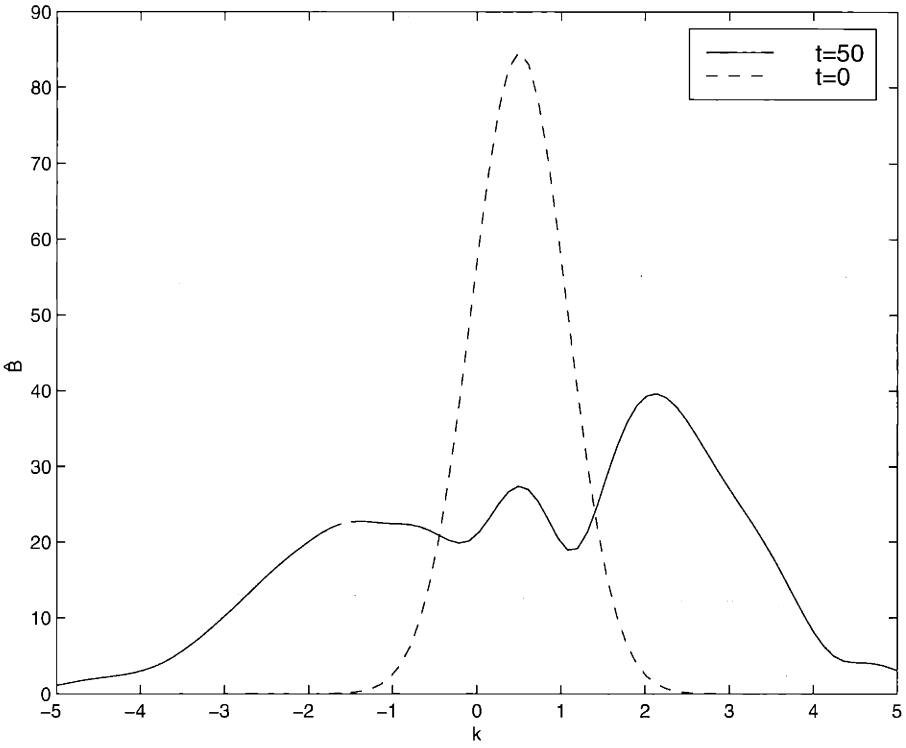

Figure 3-2: Fourier transform of full numerical simulation of Wilton's ripple with $\mu = .5$, $d_2 = .01$, $c_2 = .5$ $\gamma_1\gamma_2 = -1$.

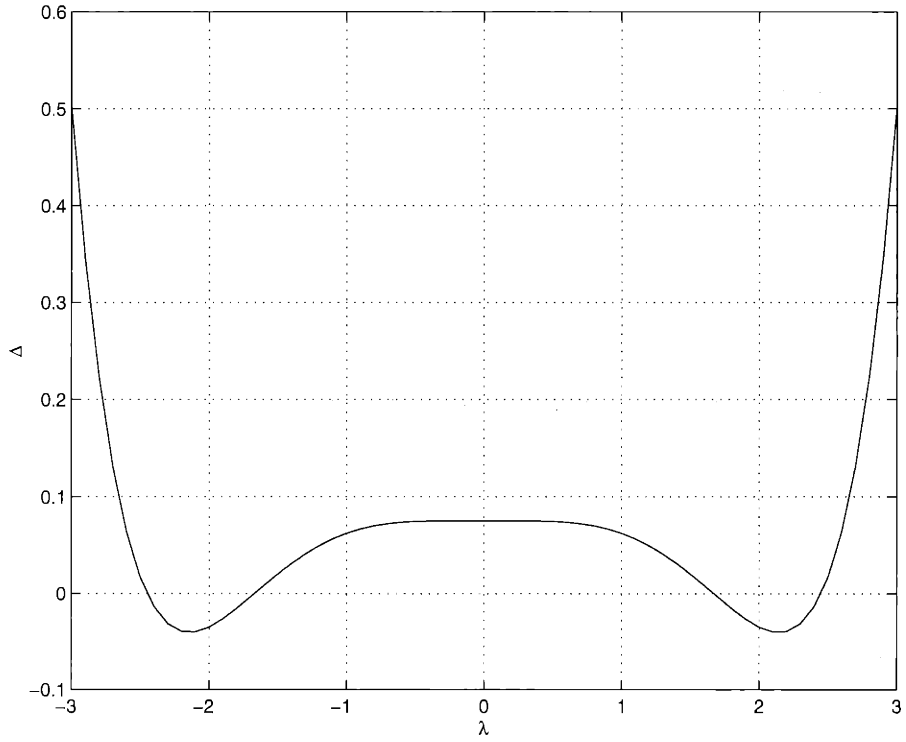

Figure 3-3: Stability criterion for Wilton's ripple numerical simulation. $\Delta < 0$ corresponds to modal growth.

$$
\begin{aligned}
A_T + c_1 A_X &= \epsilon\gamma_1 BC \,, \\
B_T + c_2 B_X + i\epsilon^2 d_2 B_{XX} &= \epsilon\gamma_2 AC^* \,, \\
C_T + c_2 C_X + i\epsilon^2 d_3 C_{XX} &= \epsilon\gamma_3 AB^* \,.
\end{aligned} \tag{3.14}
$$

Then by applying the same transformation as above

$$
s = T - \frac{X}{c_2} \,,
$$

$$
r = \frac{X}{c_2} \,,
$$

a similar analysis as in the Wilton ripple case may be conducted. Only now rather than being able to reduce to a single equation for B, a system of coupled equations for B and C is obtained. Each of which has zeroth order solutions

$$
B_0 = B_0(s) \qquad C_0 = C_0(s) \,,
$$

and again by allowing a slow time τ variation of these functions and computing the secularity condition at the next order the following evolution equations are obtained

$$
\begin{aligned}
\left(\frac{B_{0_\tau}}{C_0^*}\right)_s &= -\frac{id_2}{c_2^2}\left(\frac{B_{0_{ss}}}{C_0^*}\right)_s + \gamma_1\gamma_2 B_0 C_0 \,, \\
\left(\frac{C_{0_\tau}}{B_0^*}\right)_s &= -\frac{id_3}{c_2^2}\left(\frac{C_{0_{ss}}}{B_0^*}\right)_s + \gamma_1\gamma_3 B_0 C_0 \,.
\end{aligned}
$$

These equations, not surprisingly, have a similar structure to the Wilton's ripple case, only now with a coupling between the two feeder modes. And although in both cases similar to the NLS, it is not immediately clear that these equations are integrable analytically. A similar normal mode stability analysis was conducted as for the previous case, yielding qualitatively similar results.

Run	c_1	c_2	c_3	d_2	d_3	γ_1	γ_2	γ_3
1	0	-.5	-.8	0	0	.1	-.1	-.1
2	0	-.5	-.5	0	0	.1	-.1	-.1
3	0	-.5	-.5	.1	.2	.1	-.1	-.1
4	0	-.5	-.5	.1	.1	.1	-.1	-.1
5	0	-.5	-.5	0	0	1	-1	-1
6	0	-.5	-.5	.1	.1	1	-1	-1

Table 3.1: Coefficients for numerical runs.

Other Regimes

Although for more general parameter regimes, (3.4) is not as tractable analytically, numerical simulations can give insight into the nature of the solutions and in particular the effect of the dispersive terms.

A number of runs were conducted, and for ease of comparison all with an initial condition

$$A(X,0) = 0$$

$$B(X,0) = C(X,0) = .5e^{-.8ix}e^{-.01x^2}$$

The parameters used in the runs are summarized in Table 3.1

To begin Figure 3-4 shows the result of a run where the group velocities are distinct and the extra dispersive terms are not present. In other words this is a simulation of the regular three wave equations with a weak nonlinearity. This example shows how the initial condition in B and C basically propagates at the prescribed group velocities, after initially interacting and transferring energy to A. In A, the peak at zero remains there as $c_1 = 0$. Conversely the left hand peak in A is not permanent, merely a result of B and C not having completely separated at this point, and thus still providing some transient forcing to A. Figure 3-5 shows the effect of setting the group velocities equal. Now the second peak in A does not disappear and will remain coupled to B and C. This underlies why the analytical solution breaks down in this case. Now there is a significant part of A moving at the group velocities of the other two modes. It is this peak that represents the analogy to the doubly resonant peak

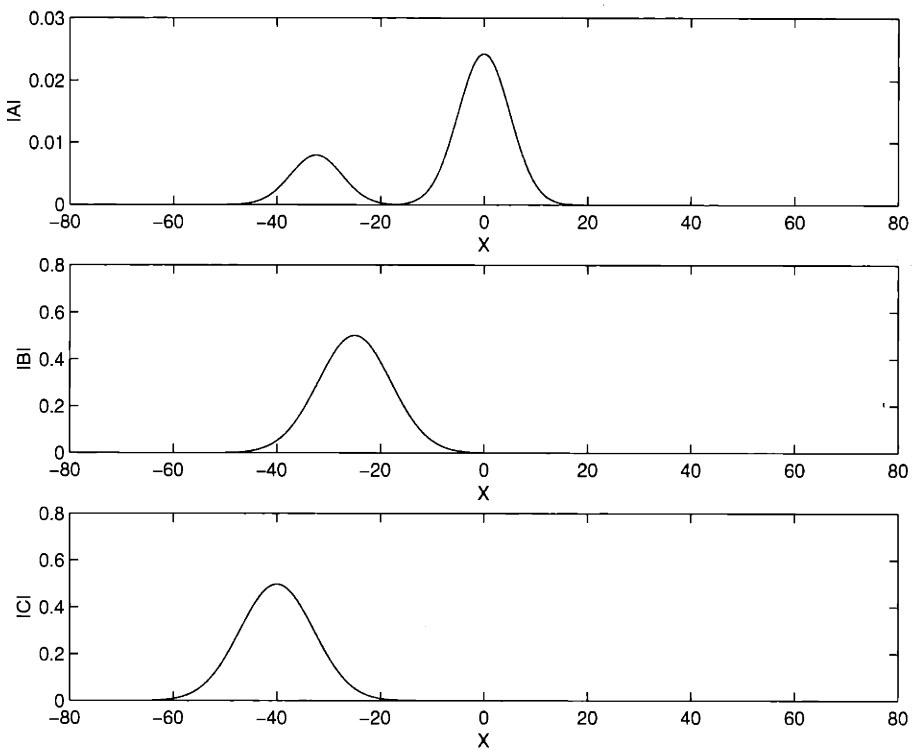

Figure 3-4: 3 Wave simulation for Run 1 at $t = 50$.

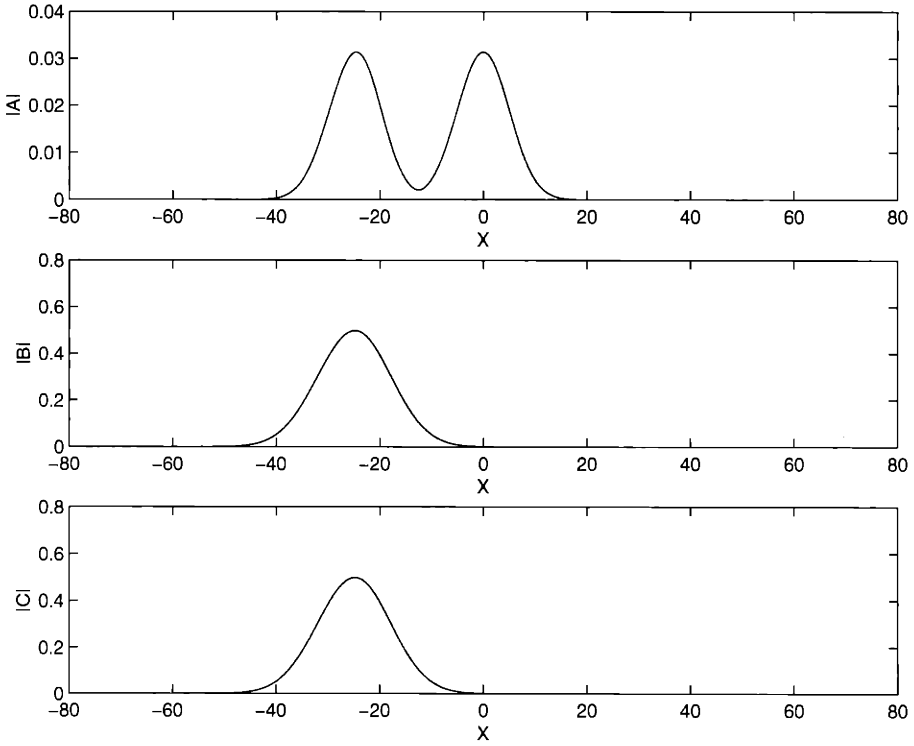

Figure 3-5: 3 Wave simulation for Run 2 at $t = 50$.

found in the previous chapter. As was shown in 2.22, it too was characterized by moving not at the group velocity of the mode $\bar{k}$ but of the feeder modes $\bar{l}, \bar{m}$. Now consider what happens when the coefficients of the higher order dispersive terms are nonzero. The third run, shown in Figure 3-6, uses the same parameters as Run 2 only now with nonzero and distinct d_2 and d_3. In this case the group velocities of the B and C peaks are now $c_2 + 2d_2k$ and $c_2 + 2d_3k$ respectively where k is the underlying wavenumber of the wave packet. So as is borne out by the numerical simulation, the peaks in B and C begin to separate, and thus the second peak in A will disappear as it did in Run 1. If the coefficients are not distinct, then as shown in Figure 3-7 the group velocities of B and C are now back to being equivalent and thus the second peak in A will persist. The difference now is the fact that the added terms also produce dispersion within the wave packet. This is not expected to occur in the classical three wave case where the group velocities are independent of k. Consequently there is a gradual spreading of the wave packet which does not occur, for example, in Run 2; borne out by the slight decrease in height of this peak in Run 4. Thus far the runs have involved a relatively weak nonlinearity in order to bring out the effects of the added dispersive term without too much inter modal coupling. Figures 3-8 and 3-9 show that the nonlinearity mainly accentuates this dispersion by more readily facilitating energy transfer in to other modes which then move at different speeds.

Overall the main effects of the added dispersive terms appear to be to modify the group velocity of wave packets and create dispersion within them. It has been shown that there is a link between this case and the continuous case since when the two feeder modes represented by B and C have the same group velocity, a wave packet is produced in A which also moves at this velocity. This is analogous to the behavior of the doubly resonant peak in the continuous case. Where this analogy fails is in how the peak grows. A system such as this will always produce an initial growth in A of $O(T = \mu t)$ and thus it depends very much and somewhat arbitrarily on what scaling is chosen for the slow time variable. And for instance when the balance $\mu^2 = \epsilon$ is taken this implies $T = \sqrt{\epsilon}t$ whereas the continuous analysis suggests a time scale of $T = \epsilon^2 t$. This again reinforces how important the neighboring modes are in the

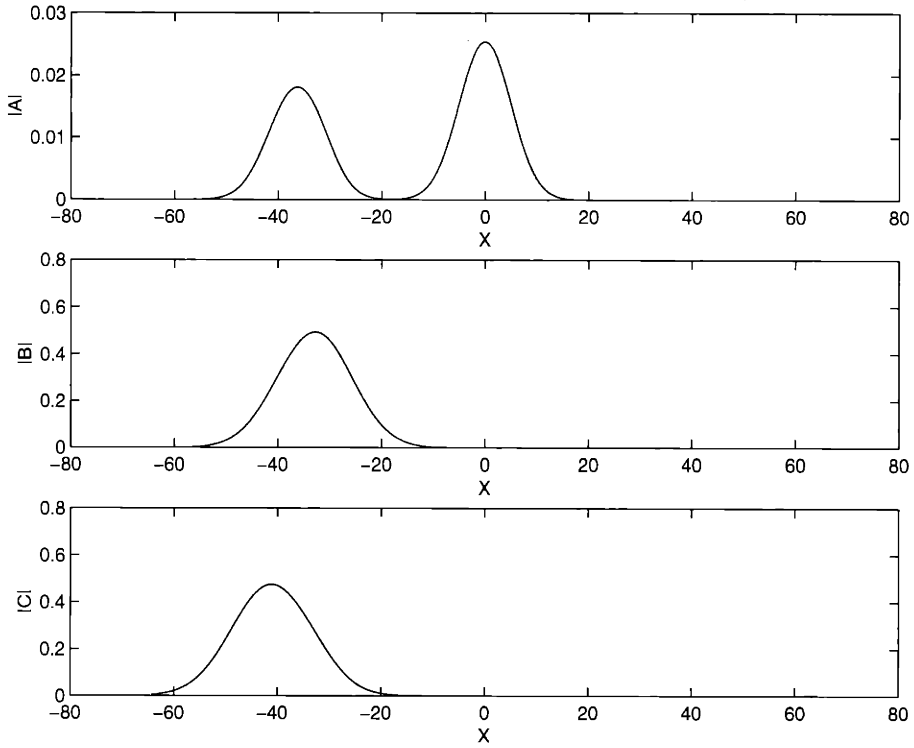

Figure 3-6: 3 Wave simulation for Run 3 at $t = 50$.

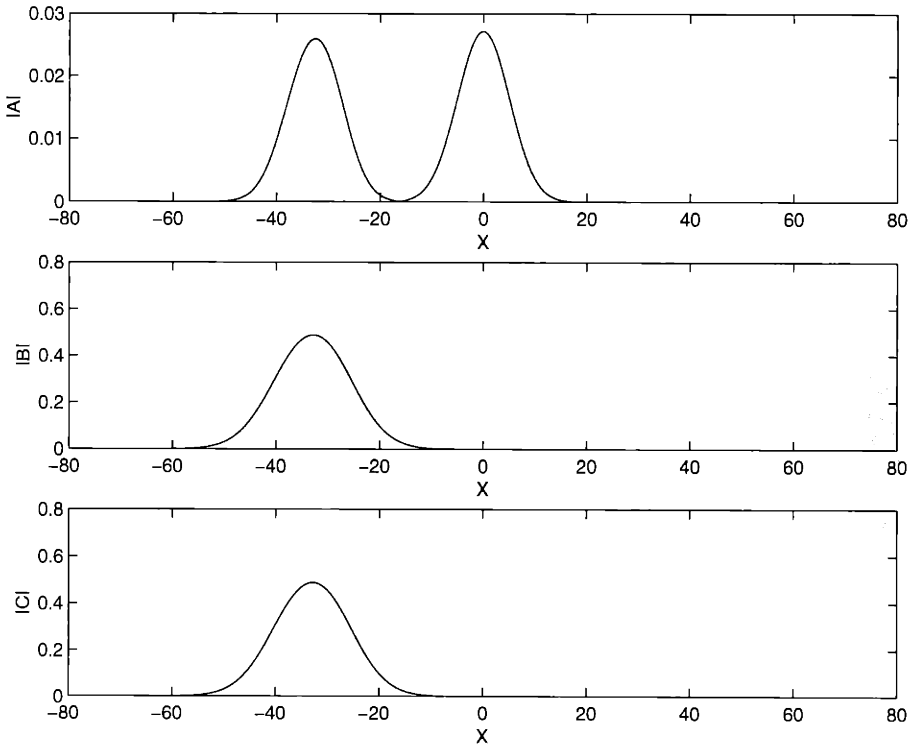

Figure 3-7: 3 Wave simulation for Run 4 at $t = 50$.

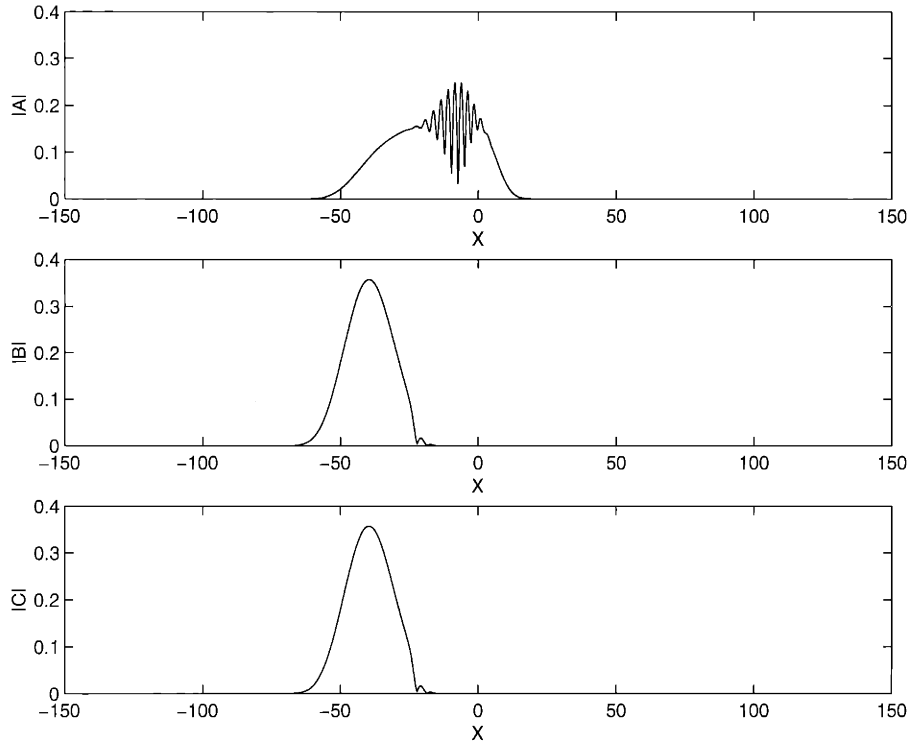

Figure 3-8: 3 Wave simulation for Run 5 at $t = 80$.

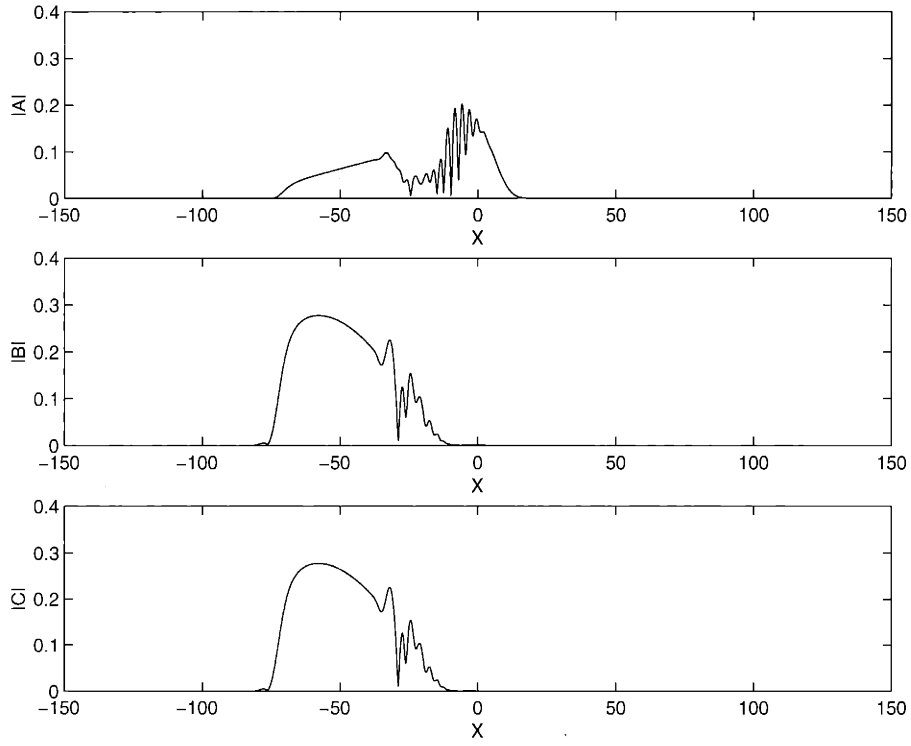

Figure 3-9: 3 Wave simulation for Run 6 at $t = 80$.

spectral evolution in the continuous case, an effect which is inevitably lost in any discrete treatment.

Chapter 4

Random Waves

The statistical description of weakly nonlinear wave interactions in a homogeneous media is a regime where the presence of double resonances may dramatically affect the evolution. Essentially the problem involves determining the evolution of certain statistical quantities of a flow (such as all mean values) given their initial values. This type of approach is important, for instance, in weak turbulence theories [23] where the spatial correlations of the velocity field translate directly to the distribution of eddies and direction of energy exchange. This yields theoretical predictions for the spectrum of the statistical steady state and thus ultimately insight into the physical mechanisms behind turbulence. Present theories rely explicitly on there being no double resonances present in the interactions, as is noted in [6]. This chapter will investigate the modifications necessary to account for double resonances, and the implications thereof. First a review of previous theory will be given.

4.1 Random Wave Theory: Simple Resonances

Due to the fundamental nature of this problem and its relevance to turbulence, it has been well studied. Hasselmann, [14] approached this problem under the assumption that the correlations obey a Gaussian property allowing four point correlations to be reduced to products of two point correlations. Benney and Saffman [6] then demonstrated that this assumption is not necessary, the same closure may be obtained

in a more general fashion. A brief summary of the analysis is as follows, based on both this and the subsequent work of Benney and Newell [5].

As discussed earlier, starting with our model equation introduced in Chapter 1 for the velocity $u(x,t)$,

$$u_t + \mathcal{L}(u) = \epsilon \mathcal{N}(u) \ , \tag{4.1}$$

where $\mathcal{L}$ is a linear differential operator, $\mathcal{N}$ is a nonlinear and for our purposes assumed quadratic, differential operator, and ϵ is a small parameter governing the weak nonlinearity. In Fourier space this corresponds to:

$$A_t + i\omega(k)A = \epsilon \int H(l, k-l)A(l)A(k-l)dl \ , \tag{4.2}$$

where A is the Fourier transform of u, ω corresponds to the linear dispersion relation given by $\mathcal{L}$, and H is an interaction coefficient corresponding to the derivatives in $\mathcal{N}$. There is no loss in generality in taking H to be symmetric in its arguments. The linear time dependence is then separated by taking,

$$A(k,t) = a(k,t)e^{-i\omega(k)t}$$

so that (4.2) becomes

$$\frac{da_l}{dt} = \epsilon \int H_{mn} a_m a_n e^{i\omega_{l,mn}t} \delta_{l,mn} dk_{mn} \ , \tag{4.3}$$

where as in [5], the following condensed notation is used:

$$a_l = a(l,t) \qquad H_{mn} = H(m,n) \qquad dk_{mn} = dmdn$$

$$\delta_{l,mn} = \delta(l-m-n) \qquad \omega_{l,mn} = \omega(l) - \omega(m) - \omega(n) \ ,$$

and the limits of integration on all wavenumber variables is understood to be $-\infty$ to

∞. Then assuming a regular perturbation expansion of the form

$$a_l = \sum_{n=0}^{\infty} \epsilon^n a_{nl} \ ,$$

and substituting into (4.3) and matching orders of ϵ, one finds that

$$a_{0l} = a_0(l) \qquad \text{(time independent)} \ , \tag{4.4}$$

$$a_{1l} = \int H_{mn} a_{0m} a_{0n} \Delta(\omega_{l,mn}) \delta_{l,mn} dk_{mn} \ , \tag{4.5}$$

$$a_{2l} = 2 \int H_{mn} H_{pq} a_{0m} a_{0p} a_{0q} E(\omega_{l,mpq}; \omega_{l,mn}) \delta_{l,mn} \delta_{n,pq} dk_{mnpq} \ , \tag{4.6}$$

where

$$\Delta(x) = \frac{e^{ixt} - 1}{ix}, \qquad E(x,y) = \int_0^t \Delta(x-y) e^{iyt} dt,$$

4.1.1 Spatial Correlations

It will be assumed that u, the solution to (4.1), is a stationary random function. Furthermore, it should be noted that although [5] treats the more general non-zero mean case, for the purposes of this discussion a zero mean value will be assumed as in [6]. In other words,

$$< u(x,t) >= 0 \ ,$$

where $< .. >$ represents a spatial average. The 2 point correlation takes the form

$$< u(x,t) u(x+r,t) >= R^{(2)}(r,t) = \int \int a_m a_n e^{-i\omega_{mn} t} e^{i(m+n)x} e^{imr} dk_{mn} \ . \tag{4.7}$$

The assumption of spatial homogeneity implies that the above correlation should be independent of x and merely depend on r. In other words it should have a Fourier transform of the form

$$< u(x,t) u(x+r,t) >= \int q^{(2)}(m,t) e^{imr} dk_m \ . \tag{4.8}$$

Comparison of (4.7) and (4.8) implies then that notationally one can represent the mean of the spectral distributions as follows

$$< a(m,t)a(n,t) >= q^{(2)}(m,t)\delta(m+n) \ . \tag{4.9}$$

Note that the fact ω is odd is used to eliminate the temporal phase term in (4.7).

Similarly the third order correlation is

$$\begin{aligned} < u(x,t)u(x+r,t)u(x+r',t) > \ &= \ R^{(3)}(r,r',t) \\ &= \int\int\int a_m a_n a_p e^{-i\omega_{mnp}t} e^{i(m+n+p)x} e^{i(mr+nr')} dk_{mnp} \ , \end{aligned} \tag{4.10}$$

and again using , the Fourier transform of this

$$R^{(3)}(r,r',t) = \int\int q^{(3)}(m,n,t) e^{-i\omega_{mnp}t} e^{i(mr+nr')} dk_{mn} \ . \tag{4.11}$$

Thus one can make the identification

$$< a_m a_n a_p >= \delta(m+n+p) q^{(3)}(m,n,t) \ . \tag{4.12}$$

The fourth order correlation is not quite so simply represented. Although a zero mean value has been assumed, there still is the possibility of pairs of points remaining correlated even as their relative separation goes to infinity. This then means that cumulant terms must be introduced in order to insure the existence of a Fourier transform,

$$\begin{aligned} & < u(x,t)u(x+r,t)u(x+r',t)u(x+r'') > - < u(x,t)u(x+r,t) >< u(x+r',t)u(x+r'') > - \\ & < u(x,t)u(x+r') >< u(x+r,t)u(x+r'') > - < u(x,t)u(x+r'') >< u(x+r,t)u(x+r') > \\ = \ & R^{(4)}(r,r',r'',t) \\ = \ & \int\int\int\int q^{(4)}(m,n,p,t)\delta(m+n+p+s) e^{-i\omega_{mnps}t} e^{i(mr+nr'pr'')} dk_{mnps} \ , \end{aligned} \tag{4.13}$$

meaning that spectrally one can represent this correlation as

$$< a_m a_n a_p a_s > \;=\; \delta(m+n+p+s)q^{(4)}(m,n,p,t) + \delta(m+n)\delta(p+s)q^{(2)}(m,t)q^{(2)}(p,t) + \delta(m+p)\delta(n+s)q^{(2)}(m,t)q^{(2)}(n,t) + \delta(m+s)\delta(n+p)q^{(2)}(m,t)q^{(2)}(n,t)\ . \tag{4.14}$$

4.1.2 Asymptotic Analysis

An essential component of the subsequent analysis involves the asymptotic behavior of the temporal dependence of the terms in the expansion of a. For simplicity of the following perturbation analysis, the required asymptotic terms will now be stated, derivations of which are given in [5].

$$\Delta(x) \approx \pi\delta(x) + iP\left(\frac{1}{x}\right) \tag{4.15}$$

$$E(x;0) \approx \left(\pi\delta(x) + P\left(\frac{1}{x}\right)\right)\left(t - i\frac{\partial}{\partial x}\right) \tag{4.16}$$

$$\Delta(x)\Delta(-x) \approx 2\pi t\delta(x) + 2P\left(\frac{1}{x}\right)\frac{\partial}{\partial x} \tag{4.17}$$

where P represents a principle value integral.

Thus, for example, in the large t limit one can use (4.15) to deduce that to leading order

$$\int h(x)\Delta(x)dx \approx \pi h(0) + iP\int \frac{h(x)}{x}dx\ .$$

4.1.3 Perturbation Analysis

In order to study the effect of the weak nonlinearity, introduce a perturbation expansion

$$q^{(2)} = q_0^{(2)} + \epsilon q_1^{(2)} + \epsilon^2 q_2^{(2)} + ... \tag{4.18}$$

and likewise for the higher order correlations. Now using the above expressions for the various orders of a, these correlations may be computed and then using the asymptotic properties of the temporal functions, secular terms may be identified and balanced

by a slow time variation.

To zeroth order,

$$q_0^{(2)}(m,t)\delta(n+m) =< a_0(m,t)a_0(n,t) > ,$$

and since a_0 is time independent this term will likewise be constant in time and thus will not affect the well-orderedness of the perturbation expansion.

At the next order

$$q_1^{(2)}(m,t)\delta(n+m) =< a_1(n,t)a_0(m,t) + a_0(n,t)a_1(m,t) > \ .$$

Using (4.4) and (4.5), along with the symmetry of these two terms

$$q_1^{(2)}(m,t)\delta(n+m) = 2\int\int H_{pq} < a_{0_{mpq}} > \Delta(\omega_{n,pq})\delta_{n,pq}dk_{pq} ,$$

and on using (4.12) and (4.15)

$$\begin{aligned} q_1^{(2)}(m,t)\delta(n+m) &= 2\int\int H_{pq}\left(\pi\delta(\omega_{n,pq}) + iP\left(\frac{1}{\omega_{n,pq}}\right)\right) q_0^{(3)}(m,p,t)\delta(m+p+q)\delta_{n,pq}dk_{pq} \\ &= 2\delta(m+n)\int\int H_{pq}\left(\pi\delta(\omega_{n,pq}) + iP\left(\frac{1}{\omega_{n,pq}}\right)\right) q_0^{(3)}(m,p,t)\delta_{n,pq}dk_{pq} \end{aligned} \qquad (4.19)$$

At this point a note should be made regarding the criteria for well-orderedness of this expansion. Since the primary concern is with the real space behavior of the solution, the criterion for uniformity of the perturbation expansion will be that all the *real space* cumulants remain well ordered. In particular, since Δ remains $O(1)$ for long time, (4.19) shows that $q_1^{(2)}$ remains bounded. Moreover, the δ functions will render the real space equivalent (inverse transform) of this term also $O(1)$ in time so there is no secularity at this order.

Secular terms in fact do not arise until $O(\epsilon^2)$ where

$$q_2^{(2)}(m,t)\delta(n+m) =< a_2(n,t)a_0(m,t) + a_0(n,t)a_2(m,t) + a_1(n,t)a_1(m,t) > \ .$$

Using (4.4),(4.5), and (4.6) along with the asymptotic forms, it is readily shown that

$$q_2^{(2)}(m,t)\delta(n+m) = 4t\delta(n+m)\mathcal{P}_{mn}\int\int\left(\pi\delta(\omega_{m,pq}) + iP\left(\frac{1}{\omega_{m,pq}}\right)\right)H_{pq-m-p}q_0^{(2)}(m,t)q_0^{(2)}(p,t)\delta_{m,pq}dk_{pq}$$
$$+4\pi\int\int\delta(\omega_{m,pq})H_{mn-m-n}q_0^{(2)}(p,t)q_0^{(2)}(q,t)\delta_{m,pq}dk_{pq} + O(1)\ ,$$

where $\mathcal{P}_{mn}$ represents a permutation over wavenumbers m and n. It is evident that to leading order there is linear growth in time, giving rise to secularity and thus potentially eliminating the well-orderedness of the expansion beyond some time. To avoid this a long time scale $T = \epsilon^2 t$ is introduced. Then allowing $q^{(2)} = q^{(2)}(m,t,T)$ it can now be seen that this secularity may be eliminated as long as

$$\begin{aligned}\frac{dq_0^{(2)}}{dT} &= 4\mathcal{P}_{mn}\int\int\left(\pi\delta(\omega_{m,pq}) + iP\left(\frac{1}{\omega_{m,pq}}\right)\right)H_{pq-m-p}q_0^{(2)}(m)q_0^{(2)}(p)\delta_{m,pq}dk_{pq} + \\ &\quad 4\pi\int\int\delta(\omega_{m,pq})H_{mn-m-n}q_0^{(2)}(p)q_0^{(2)}(q)\delta_{m,pq}dk_{pq}\ , \qquad (4.20)\end{aligned}$$

This is the closure obtained in [14] and [6] and it represents the slow time energy exchange within the zero order energy spectrum. But again it should be emphasized that this result was carried out under the assumption of there being no doubly resonant modes present. The next section will investigate the modifications to this closure caused by the presence of double resonances.

4.2 Random Wave Theory: Double Resonances

Relaxing the restriction that there be no double resonances changes the analysis significantly. The key difference arises in the asymptotic analysis where terms similar to those derived in Chapter 2 will arise in the spectral functions. These terms will embody the spectral growth brought about by the double resonances, terms which will also affect the real space hierarchy of the perturbation expansion. To begin, the asymptotic terms derived above will now be recomputed under the assumption that double resonances are present.

4.2.1 Revised Asymptotic Analysis

The following is a more general summary of the leading order behavior of some of the temporal terms, allowing for double resonances.The additional terms are the result of a stationary phase analysis, and not surprisingly bear distinct similarity to the terms in the system (2.17) derived in Chapter 2.

$$\Delta(f(x)) \approx \frac{2\sqrt{2\pi}e^{i\frac{\pi}{4}}}{\sqrt{f''(x)}}\sqrt{t}\hat{\delta}(f(x))\delta(f'(x)) + \pi\delta(f(x)) + iP\left(\frac{1}{f(x)}\right) \tag{4.21}$$

$$E(g(x);0) \approx \frac{4\sqrt{2\pi}e^{i\frac{\pi}{4}}}{3\sqrt{g''(x)}}t^{\frac{3}{2}}\hat{\hat{\delta}}(g(x))\delta(g'(x)) + \left(\pi\delta(g(x)) + P\left(\frac{1}{g(x)}\right)\right)\left(t - ig'(x)\frac{\partial}{\partial x}\right) \tag{4.22}$$

$$\Delta(f(x))\Delta(-f(x)) \approx \frac{4\sqrt{2\pi}}{3\sqrt{f''(x)}}t^{\frac{3}{2}}\left(\hat{\hat{\delta}}(f(x)) + \hat{\hat{\delta}}(-f(x))\right)\delta(f'(x)) + 2\pi t\delta(x) + 2P\left(\frac{1}{x}\right)\frac{\partial}{\partial x}, \tag{4.23}$$

where

$$\hat{\delta}(f(x)) = \int_0^1 e^{if(x)v^2t}dv$$

$$\hat{\hat{\delta}}(f(x)) = \int_0^1\int_0^1 e^{if(x)v^2u^{\frac{2}{3}}t}dudv$$

4.2.2 Perturbation Analysis

Again introduce a perturbation expansion for the spectral representations of the correlation functions, (4.18). At zeroth order the correlations remain bounded as there are no temporal terms present.

At first order, using (4.4), (4.5),(4.12) and now (4.21), the second order correlation is

$$\begin{aligned} q_1^{(2)}(m,t)\delta(n+m) &= 2\mathcal{P}_{mn}\delta(m+n)\int\int H_{pq}\left(\frac{2\sqrt{2\pi}e^{i\frac{\pi}{4}}}{\sqrt{\omega''(p)+\omega''(q)}}\sqrt{t}\hat{\delta}(\omega_{n,pq})\delta(\omega'(p)-\omega'(q))\right. \\ &+ \left.\pi\delta(\omega_{n,pq}) + iP\left(\frac{1}{\omega_{n,pq}}\right)\right) q_0^{(3)}(m,p,t)\delta_{n,pq}dk_{pq} \end{aligned}$$

The additional term represents the double resonance, and as was discussed in Chapter

2, it will exhibit $O(\sqrt{t})$ growth around modes corresponding to $n = \bar{k}$,$p = \bar{l}$, and $q = \bar{k} - \bar{l}$. This means that around $n = \bar{k}$ the expansion in Fourier space will be disordered. In particular the integrations can be carried out to give

$$q_1^{(2)}(m,t)\delta(m+n) = \delta(m+n)\mathcal{P}_{mn}\left(\sum_{\tilde{p}} \frac{2\sqrt{2\pi}e^{-i\frac{\pi}{4}}H_{\tilde{p}n-\tilde{p}}}{\sqrt{\omega''(\tilde{p})+\omega''(n-\tilde{p})}}\sqrt{t}\hat{\delta}(\omega_{n,\tilde{p}n-\tilde{p}})q_0^{(3)}(m,\tilde{p},t)\right.$$
$$\left. + \pi\int H_{pn-p}q_0^{(3)}(m,p)\delta(\omega_{n,pn-p})dk_p + i\int P\left(\frac{1}{\omega_{n,pn-p}}\right)q_0^{(3)}(m,p)dk_p\right) . \quad (4.24)$$

where $\tilde{p}$ corresponds to wavenumbers such that

$$\omega'(\tilde{p}) = \omega(n-\tilde{p})$$

This shows that near a double resonance (i.e. where $\hat{\delta}$ is $O(1)$) the dominant contribution of $O(\sqrt{t})$ will come from the double resonance, but otherwise the simple resonance terms will dominate with an $O(1)$ contribution. This is analogous to the situation found in Chapter 2 where the disorderedness of the expansion is restricted to a band of wavenumbers around the double resonance. And also analogous to the discussion of double resonances in a continuous spectrum, higher order terms must be investigated before a closure can be proposed. These will include the next order term in the second order correlation as well as the leading terms in the third order correlation. The latter is required since unlike in the simple resonance case, (4.24) shows that the coefficients of q_0^3 will be secular near a double resonance and thus this term must be present in any closure.

For the second order correlation at $O(\epsilon^2)$, using (4.4),(4.5), and (4.6) along with (4.23) and (4.22)

$$q_2^{(2)}(m,t)\delta(m+n) = \delta(m+n)\Bigg(-4t^{\frac{3}{2}}\mathcal{P}_{mn}\sum_{\tilde{p}} K\hat{\tilde{\delta}}(\omega_{n,\tilde{p}n-\tilde{p}})H_{\tilde{p}n-\tilde{p}-\tilde{p}n}q_0^{(2)}(m,t)q_0^{(2)}(\tilde{p},t)$$

$$+2t^{\frac{3}{2}}\sum_{\tilde{p}} K(\hat{\tilde{\delta}}(\omega_{n,\tilde{p}n-\tilde{p}}) + i\hat{\tilde{\delta}}(-\omega_{n,\tilde{p}n-\tilde{p}}))H_{\tilde{p}n-\tilde{p}-\tilde{p}\tilde{p}-n}q_0^{(2)}(\tilde{p},t)q_0^{(2)}(n-\tilde{p},t)$$

$$+4t\mathcal{P}_{mn}\int\left(\pi\delta(\omega_{n,pn-p}) + iP\left(\frac{1}{\omega_{n,pn-p}}\right)\right)H_{pn-p-pn}q_0^{(2)}(m,t)q_0^{(2)}(p,t)dk_p$$

$$+4t\int \pi\delta(\omega_{n,pn-p})H_{pn-p-pp-n}q_0^{(2)}(p,t)q_0^{(2)}(n-p,t)dk_p\Bigg) + O(\sqrt{t})\ , \qquad (4.25)$$

where

$$K = \frac{4}{3}\frac{\sqrt{2\pi}e^{\frac{-i\pi}{4}}}{\sqrt{\omega''(\tilde{p})+\omega''(n-\tilde{p})}}\ .$$

The last two terms in this expression represent the contribution from the simple resonance seen earlier. The first two terms correspond to the additional terms arising from the doubly resonant terms. So again, as has been thematic of double resonances throughout this investigation, the time scales are modified around doubly resonant points.

Turning to the triple correlation, at $O(\epsilon)$

$$q_1^{(3)}(m,n,t)\delta(m+n+p) = \mathcal{P}_{mnp}\int H_{rs} < a_{0_{nprs}} > \Delta(\omega_{m,rs})\delta_{m,rs}dk_{rs}\ ,$$

and then using (4.14) and applying the δ functions, the leading order term will be

$$q_1^{(3)}(m,n,t)\delta(m+n+p) \;=\; 2\delta(m+n+p)\mathcal{P}_{mnp}\Bigg(H_{-n-p}\Delta(\omega_{m,-n-p})q^{(2)}(n,t)q^{(2)}(p,t)$$

$$+\sum_{\tilde{r}}\frac{2\sqrt{2\pi}e^{-i\frac{\pi}{4}}H_{\tilde{r}n-\tilde{r}}}{\sqrt{\omega''(\tilde{r})+\omega''(n-\tilde{r})}}\sqrt{t}\hat{\delta}(\omega_{n,\tilde{r}n-\tilde{r}})q_0^{(4)}(m,p,\tilde{r},t) + O(1)\Bigg) \qquad (4.26)$$

It can be easily shown that asymptotically

$$\Delta(0) \approx t\ ,$$

meaning that this term will be $O(\epsilon t)$ around any simply resonant point. Thus in this

case it is not merely doubly resonant terms contributing at leading order. A similar term would have been present in $q_1^{(2)}$ had the assertion of zero mean velocity not been made. Similar terms can be derived for subsequent terms in the expansion and for higher order correlations, but it will be seen that (4.24), (4.25), and (4.26) will suffice to provide a closure.

4.2.3 Discussion of Ordering and a Closure

First it should be noted that in the absence of double resonances (4.24), (4.25), (4.26), and in general all terms in the hierarchy will reduce to the simple resonance case where the previously derived closures [5] will apply. Thus this discussion will focus on the case where the modes are members of a doubly resonant triad. Adopting the convention of Chapter 2, let A, B, C represent the amplitudes at modes $\bar{k}$, $\bar{l}$ and $\bar{k}-\bar{l}$ respectively, the first being a doubly resonant mode, and the latter two being the feeder modes. In order to gain a better idea of the ordering, the secular terms of (4.24), (4.25), and (4.26) can be represented as follows

$$\begin{aligned}
< AA^* > &\propto \epsilon\sqrt{t}(< AB^*C^* > + < A^*BC >) \\
&\quad +\epsilon^2 t^{\frac{3}{2}}(< AA^* >< BB^* > + < AA^* >< CC^* > + < BB^* >< CC^* >) + O(\epsilon^2\sqrt{t}) \\
< BB^* > &\propto \epsilon^2 t(< AA^* >< BB^* > + < AA^* >< CC^* > + < BB^* >< CC^* >) + O(\epsilon^2) \\
< CC^* > &\propto \epsilon^2 t(< AA^* >< BB^* > + < AA^* >< CC^* > + < BB^* >< CC^* >) + O(\epsilon^2) \\
< AB^*C^* > &\propto \epsilon t(< AA^* >< BB^* > + < AA^* >< CC^* > + < BB^* >< CC^* >) + O(\epsilon\sqrt{t})
\end{aligned}$$

where for example $< AA^* >$ corresponds to the second order correlation $q^{(2)}(\bar{k},t)$ and similarly for the other terms. All the coefficient terms have been set to unity for ease of discussion. Also it is to be understood that the terms on the left hand side represent the exact values while those on the right represent the zeroth order terms, $q_0^{(2)}, q_0^{(3)}$. Likewise the terms on the left can be thought of as being a slow time variation of the zeroth order terms as would be the usual procedure in order to eliminate secularity. As was seen in Chapter 2, the presence of doubly resonant modes creates a multitude

of time scales and also an asymmetry for the evolution of A compared with B and C. Not surprisingly, these characteristics appear to be manifested in this hierarchy as well, making closure somewhat difficult. Regardless, a consistent closure can be made by noting first that $< AB^*C^* >$, and likewise $< A^*BC >$, will depend on a time scale $\tau = \epsilon t$. But it is evident that the second order correlations will vary at slower scales $\epsilon^2 t$ and $\epsilon^2 t^{\frac{3}{2}}$. Thus assuming that the second order correlations are constant in τ, the third order correlations may be eliminated and the hierarchy reduces to,

$$
\begin{aligned}
< AA^* > &\propto \epsilon^2 t^{\frac{3}{2}}(< AA^* >< BB^* > + < AA^* >< CC^* > + < BB^* >< CC^* >) + O(\epsilon^2\sqrt{t}) \\
< BB^* > &\propto \epsilon^2 t(< AA^* >< BB^* > + < AA^* >< CC^* > + < BB^* >< CC^* >) + O(\epsilon^2) \\
< CC^* > &\propto \epsilon^2 t(< AA^* >< BB^* > + < AA^* >< CC^* > + < BB^* >< CC^* >) + O(\epsilon^2)
\end{aligned}
$$

which is a closed system for the two point correlations. Analogous to the three wave system for double resonances (2.17), there is a mismatch between the time scales for the doubly resonant mode and the feeder modes. So, for instance, if a time scale $T = \epsilon^2 t$ is chosen, as in [6], then an appropriate factor will be required for the A equation. But otherwise this closure is similar to the simply resonant closure (4.20), again with the characteristic double resonance effects of a slight mismatch in time scales and asymmetry between A, B, and C. In general, this closure may be stated as

$$
\begin{aligned}
\frac{dq_0^{(2)}(m)}{dT} = \Bigg(& -4\frac{\sqrt{T}}{\epsilon}\mathcal{P}_{mn}\sum_{\tilde{p}} K\hat{\tilde{\delta}}(\omega_{n,\tilde{p}n-\tilde{p}})H_{\tilde{p}n-\tilde{p}-\tilde{p}n}q_0^{(2)}(m)q_0^{(2)}(\tilde{p}) \\
& + \mathcal{P}_{mn}\frac{\sqrt{T}}{\epsilon}\sum_{\tilde{p}}\frac{2\sqrt{2\pi}e^{-i\frac{\pi}{4}}H_{\tilde{p}n-\tilde{p}}}{\sqrt{\omega''(\tilde{p})+\omega''(n-\tilde{p})}}\hat{\delta}(\omega_{n,\tilde{p}n-\tilde{p}})\mathcal{P}_{m\tilde{p}}\left(H_{-\tilde{p}-m-\tilde{p}}\Delta(\omega_{m,-\tilde{p}-m-\tilde{p}})q^{(2)}(m)q^{(2)}(-m-\tilde{p})\right) \\
& + 2\frac{\sqrt{T}}{\epsilon}\sum_{\tilde{p}} K(\hat{\tilde{\delta}}(\omega_{n,\tilde{p}n-\tilde{p}}) + i\hat{\tilde{\delta}}(-\omega_{n,\tilde{p}n-\tilde{p}}))H_{\tilde{p}n-\tilde{p}-\tilde{p}\tilde{p}-n}q_0^{(2)}(\tilde{p})q_0^{(2)}(n-\tilde{p}) \\
& + 4\mathcal{P}_{mn}\int\left(\pi\delta(\omega_{n,pn-p}) + iP\left(\frac{1}{\omega_{n,pn-p}}\right)\right)H_{pn-p-pn}q_0^{(2)}(m)q_0^{(2)}(p)dk_p \\
& + 4\int\pi\delta(\omega_{n,pn-p})H_{pn-p-pp-n}q_0^{(2)}(p)q_0^{(2)}(n-p)dk_p\Bigg),
\end{aligned}
$$

This closure contains both scales and is applicable to both simple and double resonant triads. For example a simply resonant point would not correspond to a wavenumber $\tilde{p}$, meaning that only the final two terms, the terms from (4.20), would remain. Moreover analogous to the modified three wave system (2.17) discussed in Chapter 2, the nature of the delta functions in the double resonance terms will provide the transition between the simple and doubly resonant regimes.

4.2.4 Justification of Closure

Now one must address the question of the validity of this closure and consider the terms which have been truncated. In particular the next order term in the expansion for $< AB^*C^* >$ will contain a fourth order correlation produced by a double resonance as shown in (4.26). Heuristically the ordering is

$$< AB^*C^* > \propto \epsilon t(< AA^* >< BB^* > + < AA^* >< CC^* > + < BB^* >< CC^* >)$$

$$+\epsilon\sqrt{t} < BCB^*C^* > +...$$

The question then arises, if the time scale $\epsilon^2 t$ is to be included as it was in the above closure, then so should the $\epsilon\sqrt{t}$ term. Indeed that is case but if the hierarchy for this term is investigated, it can be seen that

$$< BCB^*C^* > \propto \epsilon t(< AB^*C^* > + < A^*BC >)(< BB^* > + < CC^* >) + O(1) .$$

The key point to notice is that there is no $\epsilon\sqrt{t}$ term in this expression, due to the fact that A is not amongst the original modes. Therefore the dominant behavior is due to simple, rather than double resonances. And more importantly the terms involving 5 point correlations will be $O(1)$ meaning that the closure can be made at this point without having to include 5 point and higher correlations. Therefore this term may be coupled with the expression for the three point correlations to form a secondary closure with the assumption that the two point correlations vary on a slower time scale remaining valid.

4.3 Future Areas of Study

Alas, not all the various aspects of this problem could be studied and numerous avenues of investigation remain. The main focus of this study was to investigate from a mainly mathematical standpoint the differences that arise between simple and double resonances. Physical evidence of this phenomenon and experimental verification of the modified equations and time scales would be of great interest. This could come from not only studies of water waves, but undoubtedly there exist regimes in other areas such as nonlinear optics where such resonances may arise.

A key aspect of this study was to understand the effects of a continuous spectrum and it's distinctions to the discrete treatment of the three wave problem. Although Chapter 3 represents an attempt to bridge the gap between these two, certainly there is much room for more study of this. In particular the effects of introducing boundaries and how varying the size of the domain may produce varying degrees of "continuity" in the spectrum and may yield interesting insight

Furthermore, as noted in Chapter 2, many physical systems contain situations where there are numerous doubly resonant points. Thus a more generalized theory treating possible coupling of doubly resonant triads would be required before accurate modelling of such cases could be performed.

However, possibly the most immediately relevant implication of this work lies in the study of wave turbulence. The modification to the perturbation expansion hierarchy cannot be ignored and thus additions to the existing theory would be required in order to adequately model systems containing such resonances. The closure given in Chapter 4 may serve as a starting point for such a theory, but a more complete theory, allowing for non-zero mean for example, has yet to be derived and would involve an even more detailed asymptotic analysis.

Bibliography

[1] M.J. Ablowitz and P.A. Clarkson. *Solitons, Nonlinear Evolution Equations and Inverse Scattering*, volume 149 of *London Mathematical Society Lecture Note Series*. Cambridge University Press, 1991.

[2] J.A. Armstrong, N. Bloembergen, J. Ducuing, and P.S. Pershan. Interactions between light waves in a nonlinear dielectric. *Phys. Rev.*, 127:1918–1939, 1962.

[3] T.B. Benjamin and J.F. Feir. The disintegration of wavetrains on deep water. *J. Fluid Mech.*, 27:417–430, 1967.

[4] D.J. Benney. Non-linear gravity wave interactions. *J. Fluid Mech.*, 14:577–584, 1962.

[5] D.J. Benney and A.C. Newell. Sequential time closures for interacting random waves. *J. of Math. and Phys.*, 46:363–393, 1967.

[6] D.J. Benney and P.G. Saffman. Nonlinear interactions of random waves in a dispersive medium. *Proceedings of the Royal Society A*, 289:301–320, 1966.

[7] N. Bloembergen. *Non-linear optics.* Gordon and Breach, New York, 1965.

[8] F. P. Bretherton. Resonant interactions between waves. the case of discrete oscillations. *J. Fluid Mech.*, 20:457–479, 1964.

[9] K.M. Case and S.C. Chiu. Three-wave resonant interactions of gravity-capilliary waves. *Physics of Fluids*, 20:742–745, 1977.

[10] A.D.D. Craik. *Wave interactions and fluid flows.* Cambridge University Press, 1985.

[11] A.D.D. Craik. Exact solutions of the non-conservative equations for three-wave and second harmonic resonance. *Proc. Roy. Soc. Lond. A*, 406:1–12, 1986.

[12] Carl Eckart. Internal waves in the ocean. *Physics of Fluids*, 4:791–799, 1961.

[13] C.S. Gardner, J.M. Greene, M.D. Kruskal, and R.M. Miura. Method for solving the korteweg-de vries equation. *Phys. Rev. Lett.*, 19:1095–1097, 1967.

[14] K. Hasselmann. On the non-linear energy transfer in a gravity-wave spctrum, part i. *J. Fluid Mech.*, 12:481–500, 1962.

[15] A. Jurkus and Robson P.N. Saturation effects in a travelling-wave parametric amplifier. *Proc. I. E. E*, 107b:119–122, 1960.

[16] D.J. Kaup, A. Reiman, and A. Bers. Space-time evolution of nonlinear three-wave interactions. i. interaction in a homogeneous medium. *Rev. Modern Phys.*, 51:275–309, 1979.

[17] D.J. Korteweg and G. de Vries. On the change of form of long waves advancing in a rectangular canal, and on a new type of long stationary waves. *Philos. Mag. Ser. 5*, 39:422–443, 1895.

[18] A.K. Liu and D.J. Benney. The evolution of nonlinear wave trains in stratified shear flows. *Studies in Applied Mathematics*, 64:247–269, 1981.

[19] O.M. Phillips. On the dynamics of unsteady gravity waves of finite amplitude. part 1. the elemetary interactions. *J. Fluid Mech.*, 9:193–217, 1960.

[20] G.B. Whitham. *Linear and nonlinear waves.* New York, Wiley, 1974.

[21] J.R. Wilton. On ripples. *Philos. Mag. Ser. 6*, 29:688–700, 1915.

[22] R. Roderick Wong. *Asymptotic approximations of integrals.* Boston : Academic Press, 1989.

[23] V. Zakharov, V. L'vov, and G. Falkovich. *Kolmogorov Spectra of Turbulence, Wave Turbulence.* Springer-Verlag, New York, 1992.

[24] V.E. Zakharov and V.I. Karpman. On the nonlinear theory of the damping of plasma waves. *Soviet Physics JETP*, 16:351–357, 1962.